APPLICATION OF DRILLING MUD WATSE AS RAW MATERIAL IN CERAMIC TILE AND BUILDING BRICK MAKING

Chompunut Sawaengpol

A Thesis Submitted in Partial Fulfillment of the Requirements for the Degree of Master of Engineering in Geotechnology

Suranaree University of Technology

Academic Year 2016

การประยุกต์ใช้น้ำโคลนเจาะที่เป็นของเสียเป็นวัตถุดิบในการทำกระเบื้องเซรามิกและอิฐก่อสร้าง

นางสาวชมพูนุท แสวงผล

วิทยานิพนธ์นี้เป็นส่วนหนึ่งของการศึกษาตามหลักสูตรปริญญาวิศวกรรมศาสตรมหาบัณฑิต

สาขาวิชาเทคโนโลยีธรณี

มหาวิทยาลัยเทคโนโลยีสุรนารี

ปีการศึกษา 2559

APPLICATION OF DRILLING MUD WASTE AS RAW MATERIAL IN CERAMIC TILE AND BUILDING BRICK MAKING

Suranaree University of Technology has approved this thesis submitted in partial fulfillment of the requirements for a Master's Degree.

Thesis Examining Committee

____

(Prof. Dr. Kittitep Fuenkajorn)

Chairperson

____

(Asst. Prof. Dr. Akkhapun Wannakomol)

Member (Thesis Advisor)

____

(Asst. Prof. Dr. Sirirat Tubsungnoen Rattanachan)

Member

____

(Assoc. Prof. Kriangkrai Trisarn)

Member

____

(Asst. Prof. Dr. Bantita Terakulsatit)

Member

____

(Prof. Dr. Sukit Limpijumnong)

Vice Rector for Academic Affairs and Innovation

____

(Assoc. Prof. Flt. Lt. Dr. Kontorn Chamniprasart)

Dean of Institute of Engineering

ชมพูนุท แสวงผล : การประยุกต์ใช้น้ำโคลนเจาะที่เป็นของเสียเป็นวัตถุดิบในการทำกระเบื้องเซรามิกและอิฐก่อสร้าง (APPLICATION OF DRILLING MUD WASTE AS RAW MATERIAL IN CERAMIC TILE AND BUILDING BRICK MAKING) อาจารย์ที่ปรึกษา : ผู้ช่วยศาสตราจารย์ ดร.อัมพรรค์ วรรณโกมล, 130 หน้า

วัตถุประสงค์หลักของการวิจัยในครั้งนี้คือการศึกษาความเป็นไปได้ในการใช้น้ำโคลนเจาะซึ่งเป็นของเสียในกระบวนการเจาะเป็นวัตถุดิบในการทำกระเบื้องเซรามิคและอิฐก่อสร้าง น้ำโคลนเจาะที่ผสมด้วยน้ำจากหลุมเจาะปิโตรเลียมของแอ่งฝาง แอ่งลำปาง แอ่งแม่ทา และแอ่งพิษณุโลก ได้ถูกรวบรวม ทำให้แห้งและบดและวิเคราะห์ส่วนประกอบทางเคมีด้วยเทคนิคเอกซ์เรย์ฟลูออเรสเซนซ์และเอกซ์เรย์ดิฟแฟรคชันน้ำโคลนเสียที่ถูกทำให้แห้งและบดเป็นผงแล้วถูกนำมาขึ้นรูปให้เป็นตัวอย่างเซรามิก แล้วเผาที่อุณหภูมิ 800 900 1000 1100 1150 และ 1200 องศาเซลเซียส ตัวอย่างเซรามิกเหล่านี้ถูกนำไปทดสอบตามเกณฑ์มาตรฐาน ISO 10545-3: 1995 (Ceramic Tiles - part 3) และ TIS 2398 part 3-2553 เพื่อทำการวัดค่าร้อยละของการดูดซึมน้ำ ค่าความพรุนปรากฏ ค่าความหนาแน่นสัมพัทธ์ปรากฏค่าความหนาแน่นรวมและค่าการต้านทานแรงอัด น้ำโคลนเจาะที่เป็นของเสียเฉพาะจากหลุมเจาะของแอ่งพิษณุโลกถูกนำมาทำตัวอย่างอิฐก่อสร้างและผ่านการเผาที่อุณหภูมิ 1000 องศาเซลเซียส จากนั้นนำมาทำการทดสอบหาค่าร้อยละการดูดซึมน้ำและค่าการต้านทานแรงอัดตามเกณฑ์มาตรฐาน ASTM C67-11 และมอก.77-2545 การวิเคราะห์เอกซ์เรย์ฟลูออเรสเซนซ์และการวิเคราะห์เอกซ์เรย์ดิฟแฟรคชันบ่งชี้ว่าน้ำโคลนเจาะที่ผสมด้วยน้ำที่เป็นของเสียแล้วเหล่านี้ส่วนใหญ่ประกอบด้วยแร่ควอทซ์และแร่เคโอลิไนท์ผลการทดสอบในห้องปฏิบัติการแสดงให้เห็นว่าค่าร้อยละการดูดซึมน้ำ ค่าความพรุนปรากฏ ค่าความหนาแน่นสัมพัทธ์ปรากฏค่าความหนาแน่นรวมและค่าการต้านทานแรงอัดของตัวอย่างกระเบื้องเซรามิกนั้นเป็นไปตามเกณฑ์ของมอก.2508-2555 ตัวอย่างที่เผาที่อุณหภูมิ 800 ถึง 1000 องศาเซลเซียสสามารถจัดให้อยู่ในกลุ่ม BIII ของมาตรฐานกระเบื้องเซรามิกตัวอย่างที่เผาที่อุณหภูมิ 1100 องศาเซลเซียสสามารถจัดให้อยู่ในกลุ่ม BII_a ยกเว้นตัวอย่าง M และ P_2 ซึ่งถูกจัดอยู่ในกลุ่ม BII_b ตัวอย่างที่เผาที่อุณหภูมิ 1150 และ 1200 องศาเซลเซียส สามารถจัดให้อยู่ในกลุ่ม BI_b และสามารถนำมาใช้เป็นวัตถุดิบในการผลิตกระเบื้องปูพื้นได้เนื่องจากมีกำลังรับแรงอัดเฉลี่ยต่ำสุดมากกว่า 230 กิโลกรัมต่อตารางเซนติเมตร ค่าร้อยละ

การดูดซึมน้ำและค่าการต้านทานแรงอัดของตัวอย่างที่ทำเป็นอิฐก่อสร้างก็เป็นไปตามมาตรฐานและถูกจัดให้อยู่ในกลุ่มอิฐก่อสร้างเกรด A ตามเกณฑ์มาตรฐานที่ใช้อ้างอิง

สาขาวิชาเทคโนโลยีธรณี ลายมือชื่อนักศึกษา________

ปีการศึกษา 2559 ลายมือชื่ออาจารย์ที่ปรึกษา________

ลายมือชื่ออาจารย์ที่ปรึกษาร่วม________

CHOMPUNUT SAWAENGPOL : APPLICATION OF DRILLING MUD WASTE AS RAW MATERIAL IN CERAMIC TILE AND BUILDING BRICK MAKING. THESIS ADVISOR : ASST. PROF. AKKHAPUN WANNAKOMOL, Ph.D., 130 PP.

WATER BASED DRILLING MUD WASTE/ CERAMIC TILE/BUILDING BRICK

The main objective of this research is to study the possibility of using water based drilling mud waste as a raw material for ceramic tile and building brick making. The water based drilling mud wastes from petroleum drill holes of Fang, Lampang, Mae Tha and Phitsanulok basin had been collected, dried, ground, and analyzed theirs chemical composition by X-ray fluorescence and X-ray diffraction analysis. Dried and ground drilling mud waste powders were molded to ceramic tile samples and were then fired at 800, 900, 1,000, 1,100, 1,150 and 1,200°C. They were tested according to the ISO 10545-3: 1995 (Ceramic Tiles - part 3) and the TIS 2398 Part 3-2553 standard to determine water absorption percent, apparent porosity, apparent relative density, bulk density and compressive strength. Dried and ground drilling mud waste powders only drilling mud wastes from petroleum drill holes of Phitsanulok basin were made building brick samples and fired at 1,000°C, and were then tested water absorption and compressive strength according to the ASTM C67-11 and the TIS 77-2545 standard. X-ray fluorescence and X-ray diffraction analysis indicated that these drilling mud wastes were mainly composed of quartz and kaolinite. The results of laboratory tests showed that the water absorption, apparent porosity, relative density, bulk density and compressive strength of the ceramic tile

samples could be acceptable to the standard TIS 2508-2555. The sample fired at 800 to 1,000°C could be classified as Group BIII of ceramic tile standard. The sample fired at 1,100°C could be classified as Group BII_a, except sample M and P_2 which are classified as Group BII_b. The sample fired at 1,150 to 1,200°C could be classified as Group BI_b and could be used as raw material for making the floor tile due to the average compressive strength of more than 230 kilograms per square centimeter according to the reference standard. In addition to water absorption percent and the compressive strength of building brick samples could be met the acceptable limits and was classified into grade A brick according to the reference standard.

School of Geotechnology — Student's Signature ______________

Academic Year 2016 — Advisor's Signature ______________

Co-Advisor's Signature ______________

ACKNOWLEDGEMENTS

The author wishes to acknowledge the support from the Suranaree University of Technology (SUT) who has provided funding for this research.

Grateful thanks and appreciation are given to Asst. Prof. Dr. Akkhapun Wannakomol, thesis advisor, and Asst. Prof. Dr. Sirirat Tubsungnoen Rattanachan, co-thesis advisor, who lets the author work independently, but gave a critical review of this research. Many thank are also extended to Prof. Dr. Kittitep Fuenkajorn, Assoc. Prof. Kriangkrai Trisarn and Asst. Prof. Dr. Bantita Teerakulsatit who served on the thesis committee and commented on the manuscript.

Finally, I most gratefully acknowledge my parents and friends for all their supported throughout the period of this research.

Chompunut Sawaengpol

TABLE OF CONTENTS

Page

TABLE OF CONTENTS (Continued)

Page

TABLE OF CONTENTS (Continued)

Page

TABLE OF CONTENTS (Continued)

Page

LIST OF TABLES

Table **Page**

LIST OF FIGURES

LIST OF FIGURES (Continued)

Figure **Page**

LIST OF FIGURES (Continued)

Figure **Page**

LIST OF FIGURES (Continued)

Figure **Page**

CHAPTER I

INTRODUCTION

1.1 Rationale and background

In petroleum well drilling industry, drilling mud is used in a large amount resulting in large volumes of drilling mud waste. Drilling mud wastes are generated both from onshore and offshore wells. Onshore and offshore operators have employed a variety of methods for managing drilling wastes. In the offshore, options are limited to discharge, underground injection, and transport back to shore for disposal. Onshore operators have wider range of options some wastes are managed onsite while others are removed to offsite commercial disposal facilities. Employed onshore waste management options include land-spreading, land-farming and landfill, evaporations and burial onsite, underground injection, incineration and other thermal treatment, bioremediation and composting, and reuse and recycling. Water based mud is a water based mud with the basic elements which consisted of mostly bentonite and water. Bentonite is a clay mineral in montmorillonite group which its chemical composition consist of silica oxide (SiO_2), aluminum oxide (Al_2O_3), and water (H_2O). These compositions are similar to Kaolin and Ball Clay that are used as major raw materials in ceramic industry.

Therefore, the idea to reuse the drilling mud waste as a raw material for building brick and ceramic tiles could reduce transportation cost in disposal process and could also add value to the waste from petroleum well drilling.

1.2 Research objectives

The objectives of this research is to study the possibility to use the drilling mud wastes from petroleum drilling well as a raw material for ceramic tile and building brick production. The properties of ceramic tile and building brick areaccording to the ISO 10545-3: 1995 (Ceramic Tiles - part 3), Thai Industrial Standard (TIS) 2398 Part 3-2553, the American Society for Testing and Materials ASTM C67-11 (Standard test method for sampling and test Brick and Structural Clay Tile) and Thai Industrial Standard (TIS) 77-2545. The physical properties of the samples were determined for the water absorption, apparent porosity, relative density, bulk density and compressive strength.

1.3 Research methodology

1.3.1 Literature review

Relevant topic and previous research results have been reviewed in order to understand the drilling mud waste characteristics and its ability to use as a raw material in ceramic tile and building brick making.A summary of the literature review will be given in the thesis.

1.3.2 Samples preparation

Onshore water-based drilling mud wastes will be collected, prepared,and tested in the laboratories at Suranaree University of Technology. Waste samples were determined the particle size distribution by wet sieve. The waste samples were dried and sieved through mesh no.200 for ceramic samples testing. The chemical compositions of the waste samples were characterized by X-ray diffraction (XRD) and X-ray fluorescence (XRF) techniques.

The waste samples were fabricated into the cylindrical shape and fired at 800-1,200°C for compressive strength testing and their physical properties testingsuch as water absorption, apparent porosity, apparent relative density and bulk density.

The compressive strength and absorption test for building brick were according to Thailand Industrial Standard: Building Brick (TIS 77 -2545) and ASTM C67-11.

The water absorption and apparent relative porosity, relative density, bulk density test were according to Thailand Industrial standard: Ceramic Tiles (TIS 2398 Part 3-2555) and ISO 10545-1995.

1.3.3 Results conclusion, recommendations and thesis writing

The results were described to determine the reliability and accuracy of the measurements. Performance of the waste sample was discussed based on the test results. All research activities, method and results were documented and complied in the thesis.

Research methodology of this study are summarized and shown in Figure 1.1.

1.4 Scope and limitations of the study

The study had been scoped and tested only on the water based drilling mud wastes from drill holes of Thailand onshore Tertiary basin, including Fang, Lampang, Mae Tha, and Phitsanulok basin. X-ray Diffraction (XRD) and X-ray Fluorescence (XRF) methods had been conducted to identify samples mineral and chemical analysis. The water based drilling mud wastes were fabricated into cylindrical shape samples for testing the water absorption, apparent porosity, apparent relative porosity and bulk density according to TIS 2398 Part 3-2555 and ISO 10545-1995. Compressive strength test had been conducted according to the ASTM C67-11(Standard test method for sampling and test Brick and Structural Clay Tile) and Thai Industrial Standard 77-2545 and ISO 10545-3: 1995 (Ceramic Tiles - part 3).

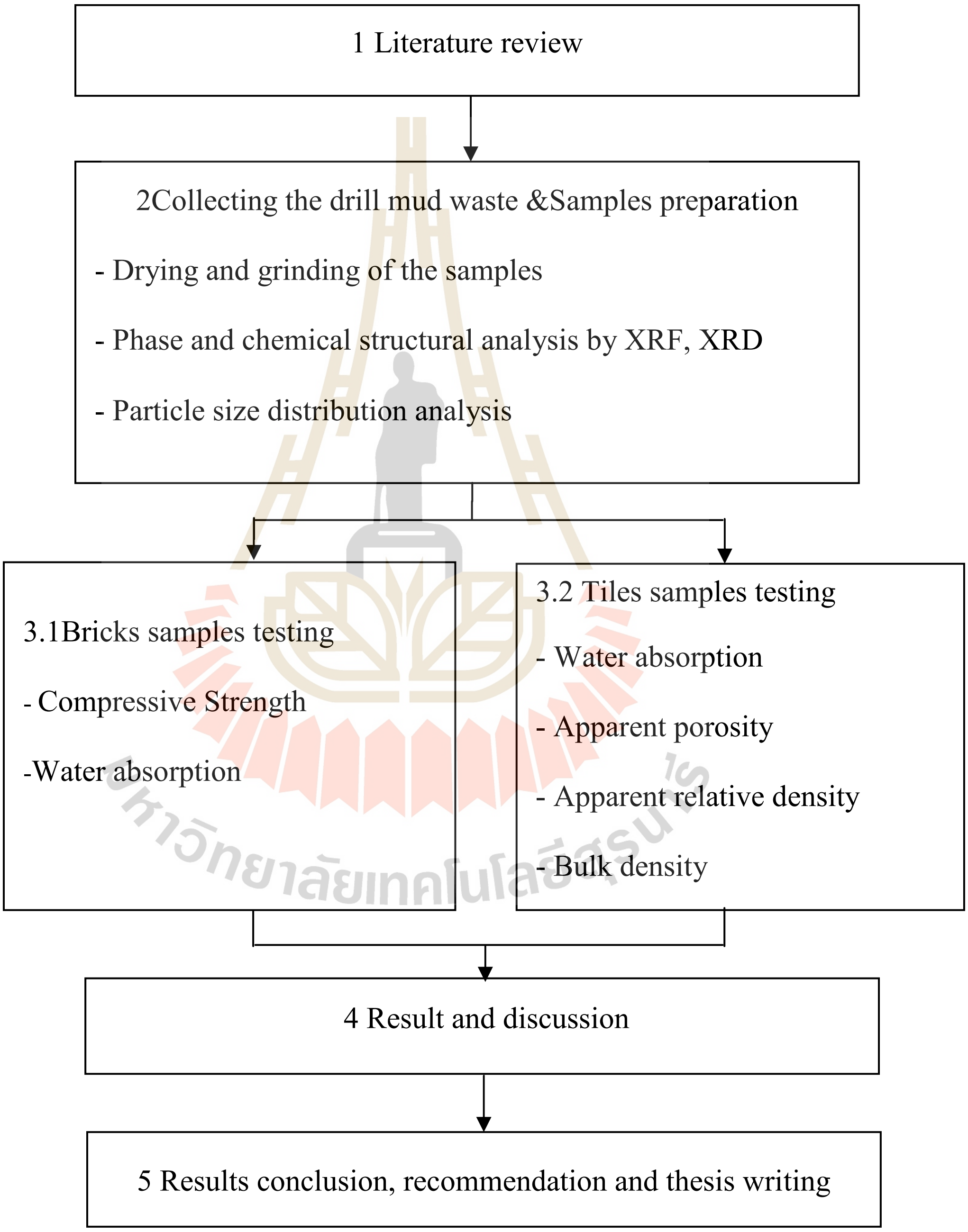

Figure 1.1 Research methodology

1.5 Thesis contents

Chapter I introduces the thesis by briefly describing the background and rationale of study. The research objectives, methodology, scope and limitations are also identified. **Chapter II** summarizes the literature review and theory. **Chapter III** describes the sample preparation and experimental procedure **Chapter IV** describes and discusses the results from the experimental procedure. **Chapter V** concludes the research results and given some recommendations for the future study.

CHAPTER II

LITERATURE REVIEW

2.1 Introduction

This chapter summarizes theory and the related research works for the literature review carried out to improve an understanding of the drilling mud waste characteristics and its ability to use as a raw material in ceramic tile and building brick making. The contents include the recent research results and utilization of the water base drilling mud waste.

2.2 Drilling fluid in petroleum drilling industry

Drilling fluids are a complex system of water based mud (WBM), oil based mud (OBM) or synthetic based fluids with several chemical and mineral additives (Ghazia, 2011).

2.2.1 Water based mud

A water based mud is one that uses water for the liquid phase and commercial clays for viscosity. The continuous phase can be fresh water, brackish water, seawater, or concentrated brines containing any soluble salt. The used commercial clays may be bentonite, attapulgite, sepiolite, or polymer. The use of other components such as thinners, filtration-control additives, lubricants, orinhibiting salts in formulating a particular drilling fluid is determined by the type of system to drill the formations safely and economically. Some of the major systems, including fresh water fluid, brackish or seawater fluid, saturated salt fluid, inhibited fluid, lime fluid, potassium fluid, polymer based fluid, and brine are used in drilling, completion or work-over operations (Ghazia, 2011).

2.2.2 Oil based mud

Unlike to water based mud which water is the continuous phase, oil based mud system consisted of diesel oil formed the continuous phase in the water-in-oil emulsion. In this way oil based mud, have the water content between 3 to 5% or as much as 20% to 40% (in case of invert emulsions) water content. Oil based mud Low-gravity solids content in oil-based mud has to be monitored closely because solids do not hydrate and often causes low-gravity solids contents to exceed acceptable levels. This results the reduction of penetration rate, formation damage and increase in the risk of differential sticking. Since oil based mud contain substantially less colloidal particles, they exhibit a spurt fluid loss. To avoid the high filtration ratio the high pressure and high temperature monitored during the drilling will be important keys to protect the excessive filtration or filter cake buildup. (Ghazia, 2011).

2.3 Oil well drilling waste used as construction material

Souza and Holanda (2005) had studied the densification behavior of petroleum waste bearing clay-based ceramic bodies. Petroleum waste bearing clay-based ceramic bodies for application in structural ceramic products was described. Oily wastes were produced from oil rigs during the liquid/solid impurities separation step. The waste was added in gradual proportions to akaolinite clay from zero up to 20 wt%, in order to study its effect on the densification behavior of the fired samples (linear shrinkage, water absorption and apparent density). Ultimate compressive strength had been also assessed. The samples were unidirectional dry pressed into a cylindrical steel die and fired at temperatures ranging from 750 to 1,100 °C. XRD and SEM were used to identify the present phases and degree of densification. The results revealed that the addition of petroleum waste was responsible for the inclusion of barite and quartz particles to the clay powder and it also affected to the densification behavior of the kaolinite clay. Significant morphological changes and phase transformations occurred during sintering.

Bernado *et al.* (2007) used oil well-derived drilling waste (muddy and rocky) and electric arc furnace slag as alternative raw materials in clinker production. It was founded that the manufacturing process of waste–based clinkers was environmentally compatible and related to cements similar to performance the common hydraulic binders.

Medhat and Tarek (2010) had studied oil based mud waste used in Belayium oil field, Egypt. The field has approximately 100 offshore and 113 onshore wells. They studied the influence of oil well drilling waste, basically oil based mud waste, on the engineering characteristics of the manufactured environmental friendly, sufficient performing red clay building brick. Compositions of the used materials as well as physico-mechanical characteristics of fired briquettes were also investigated. The laboratory results demonstrated that the water absorption, bulk density, efflorescence and compressive strength of the fired briquettes were met the acceptable limits of Egyptian Standard No. 204-2005 for clay masonry units used for load and non-load bearing walls construction. The reuse of this waste material in the building industry will contribute to the protection of the environment through waste minimization and beneficial income to the community through the utilization process in building industry.

Orolinova *et al.* (2012) investigated the changes in structure, surface area and porosity of monomineral fraction of the local bentonite upon heating at 300, 500 and 650 °C. Infrared (IR) spectroscopy, Differential Thermal Analysis (DTA), X-Ray diffraction (XRD) and N_2 adsorption method were employed for the analyses. Experimental results revealed that the basal spacing of the montmorillonite was 1.50 nm, but it decreased to 0.98 nm after thermal treatment. This decrease was attributed to the loss of interlamellar water, finally a phase transformation occured. Changes of the crystal structure related with the decrease of the value of specific surface area and total pore volume.

Souza *et al.*(2013) had studied the sintering behavior of vitrified ceramic tiles incorporated with petroleum waste focus on the sintering behavior of vitrified floor tiles containing petroleum waste. It was founded that the concentration affected sintering behavior, microstructural and physical properties of the vitrified floor tiles.

In Thailand, there is no any research on using water based drilling mud wastes from petroleum well as raw material in ceramic tile and building brick making. Therefore, this research aims to study the possibility to use this waste material as one of raw material in ceramic tile and building brick making industry in the future.

2.4 Classification of ceramic tiles

Ceramic tiles can be classified into 3 groups according to their method of manufacture and their water absorption. The groups do not presuppose the usage of the products. The Classification of ceramic tiles with respect to water absorption and shaping are shown in Table 2.1 and 2.2.

Table 2.1 Classification of ceramic tiles with respect to water absorption (E_b) and shaping (after TIS 2508-2555 Ceramic tile)

Shaping	**Group I** $Eb \leq 3\%$	**Group II$_a$** $3\% < E_b \leq 6\%$	**Group II$_b$** $6\% < E_b \leq 10\%$	**Group III** $E_b > 10\%$
A **Extruded**	Group AI$_a$ $E_b \leq 0.5\%$	Group AII$_{a-1}$[1]	Group AII$_{b-1}$[1]	Group AIII
	Group AI$_b$ $0.5 < Eb \leq 3\%$	Group AII$_{a-2}$[1]	Group AII$_{b-2}$[1]	
B **Dry pressed**	Group BI$_a$ $E \leq 0{,}5\%$	Group BII$_a$ (Appendix A)	Group BII$_b$ (Appendix A)	Group BIII[2] (Appendix A)
	Group BI$_b$ $0{,}5 < Eb \leq 3\%$			

1) Groups AII$_a$ and AII$_b$ are divided into two parts (Parts 1 and 2) with different products specifications.
2) Group BIII covers glazed tiles only. There is a low quantity of dry-pressed unglazed tiles produced with water absorption greater than 10 % that is not covered by this product group.

Table 2.2 Classification and features of ceramic tiles (afterwww.homemartnkc.com /products-dec-tiles.php)

Types of tiles	**Texture**	**Glazed**	**Load (kg/cm^2)**	**Water absorption (%)**	**Usability**
Wall Tiles	Earthenware	Glazed	≥ 230	≥ 17.0	A common wall.
Floor Tiles	Stoneware	Glazed	≥ 350	≥ 6.0	General flooring.
Homogeneous Tiles	Porcelain	Unglazed	≥ 450	≥ 0.1	Heavy use areas (load).
Mosaic Tiles	Porcelain	Glazed Unglazed	≥ 400	≥ 1.0	Pool, exterior wall decoration.
Glazed Porcelain Tiles	Porcelain	Glazed	≥ 450	≥ 0.5	Heavy use areas, decoration.

2.5 Classification of bricks

Building brick can be classified and featured by the maximum water absorption and the minimum compressive strength of specimen testing. The classification and features of bricks are shown in Table 2.3 and 2.4.

Table 2.3 Classification and features of bricks(afterTIS 77-2545)

Grade quality	**Size (mm) length x width x height**
A, B and C	140 x 65 x 40
	190 x 90 x 40
	190 x 90 x 65
	190 x 90 x 90

Table 2.4 Classification of bricks (after TIS 77-2545)

Grade Quality	**The minimum Compressive strength (MPa)**		**The maximum Water absorption (%)**	
	Average (5 lumps)	**Each lump**	**Average (5 lumps)**	**Each lump**
A	21	17	17	20
B	17	15	22	25
C	10	9	not defined	not defined

CHAPTER III

RESEARCH METHODOLOGY

3.1 Introduction

This chapter describes the experimental procedure and the characterization of the water based drilling mud wastes. This chapter includes the sample collection, sample preparation, testing instruments and experimental methods.

3.2 Sample collection and preparation

3.2.1 Sample collection

Water based drilling mud waste samples used in this research had been collected from several drill holes at northern of Thailand onshore Tertiary basin, including Fang (sample C_1, C_2 and C_3), Lampang (sample L), Mae Tha (sample M), and Phitsanulok basin (sample P_1 and P_2). Raw water based drilling mud wastes used in this study were collected from the drilling plant as shown in Figure 3.1 and Table 3.1. They were collected, packed in a gallon, and transported from drilling site to the Geotechnology and Ceramic Engineering Laboratory at Suranaree University of Technology, NakhonRatchasima province.

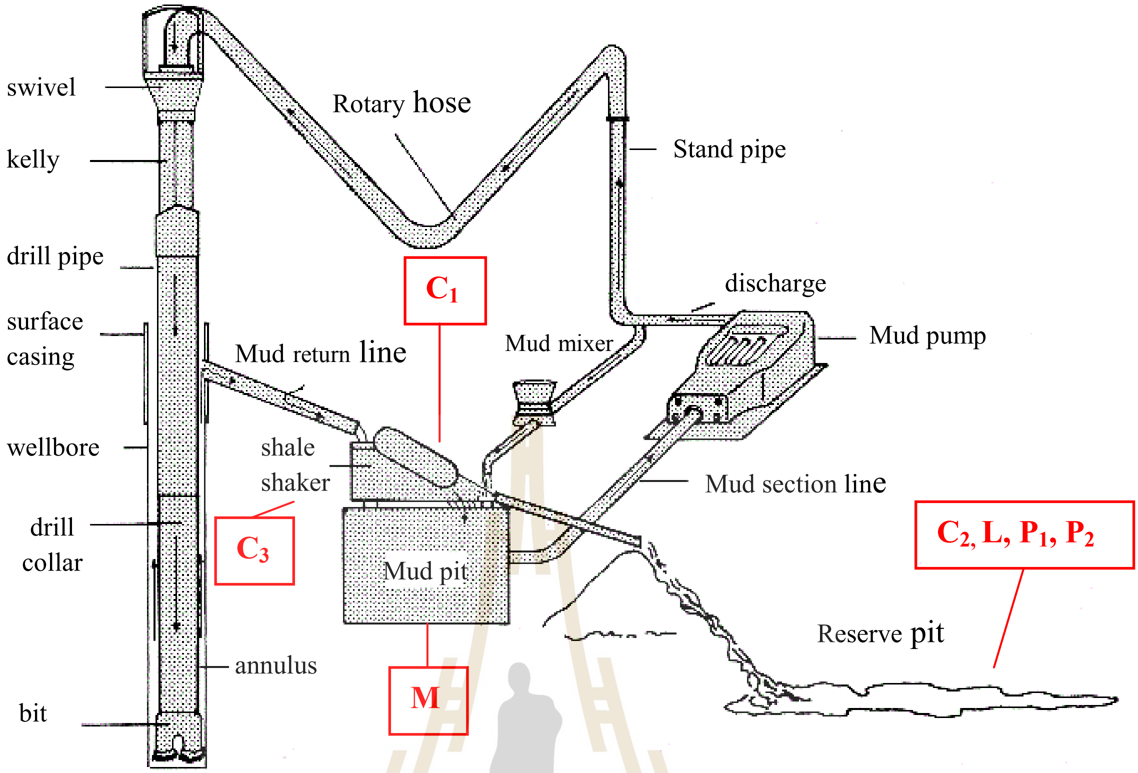

Figure 3.1 Raw water based drilling mud wastes used in this study (after www.kgs.ku.edu)

Table 3.1 Sources of the sample

Sample code	Basin
C_1, C_2, C_3	Fang
L	Lampang
M	Mae Tha
P_1	Phitsanulok (lankrabue)
P_2	Phitsanulok

3.2.2 Sample preparation

Water based drilling mud wastes were percolated out and dried under sunlight. The moisture was removed one more time in a hot-air oven at 100°C for at least 24 hours as shown in Figure 3.2 and 3.3. The dried mud wastes were sieved through a mesh no. 200. The dried mud waste retaining on the mesh of the size was grounded by a milling machine and sieved through the mesh again. Dried drilling mud waste powder from the oven was stored in a plastic box with a tight lid to prevent moisture.

Particle size distribution was determined by sieve analysis method and particle size less than 200 mesh were analyzed by using Horiba-Partica (LA-950) Laser diffraction particle size analysis (Figure 3.4).

Figure 3.2 Mud wastes were filtrated and dried under sunlight

Figure 3.3 Baked mud waste was dried at 100°C for at least 24 hours

Figure 3.4 Horiba-Partica (LA-950)

Dried and grounded mud waste powder were unidirectional pressed in a cylindrical steel mold in diameter of 1 cm and height of 2 cm by applying 320 psi pressure mold and hold 10 seconds, then they were pressed to 640 psi and hold for 1 minute to obtain ceramic tile samples (Figure 3.5). The samples were fired at 800, 900, 1,000, 1,100, 1,150, and 1,200°C, respectively. The drilling mud waste from petroleum drill holes of Phitsanulok basin (P_1) were molded in a steel box in dimension of 6.5x14x4 cm according to TIS 77-2545 to obtain building brick samples (Figure 3.6) and fired at 1,000°C for physical properties testing.

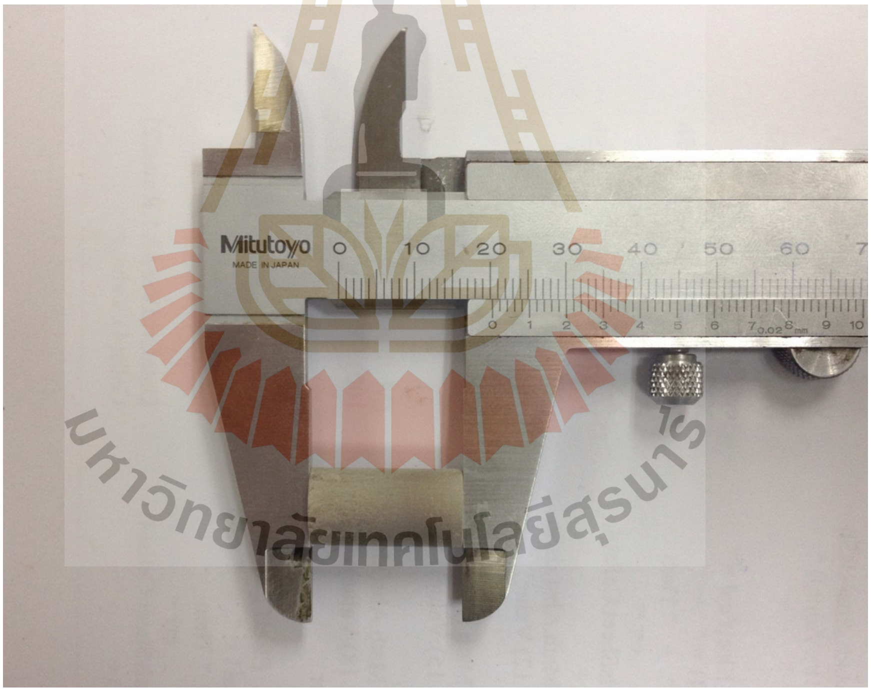

Figure 3.5 Ceramic cylindrical sample

Figure 3.6 Building brick sample

3.3 Physical properties testing

3.3.1 Volume shrinkage

The percent of shrinkage of sample were determined by measured volume of the fired sample and dried sample. The percent of shrinkage can be calculated by equation 3.1 (ชาญ จรรยาวนิชย์, 2536):

$$\% \ V_s = \frac{V_d - V_f}{V_d} \times 100 \tag{3.1}$$

where V_s = Volume shrinkage (%)

V_d = Dry Volume (cm^3)

V_f = Fired Volume (cm^3)

3.3.2 Compressive strength

Compressive strength is the mechanical properties of the material to withstand the forces acting in a specific cross-sectional area in kilograms per square centimeter (kg/cm^2) or Megapascal (MPa). Compressive strength of a compressible material can be calculated by equation 3.2 (TIS 77-2545):

$$C = \frac{W}{A} \tag{3.2}$$

where C = compressive strength of the samples (kg/cm^2)

W = load (kg)

A = cross-sectional area of the sample (cm^2)

Figure 3.7 Instron Universal Testing Systems for compressive strength testing

Ceramic tile samples were tested their compressive strength by using the Instron Universal Testing system (100kN) at the cross speed of 0.1 mm/min at the Ceramic Engineering Laboratory as shown in Figure 3.7 and building brick samples were tested compressive strength by using the compressive strength tester (Figure 3.8) at Civil Engineering Laboratory, Suranaree University of Technology.

Figure 3.8 Compressive strength tester (ELE International)

3.3.3 Water absorption

The percentage of water absorption of ceramic samples tiles were determined by boiling samples in the water and soaking for 3 hours. The water absorption was later calculated by equation 3.3 (ISO 10545 part 3 or TIS 2398-2553):

$$E = \frac{m_2 - m_1}{m_1} \times 100 \tag{3.3}$$

where E = Water absorption (%)

m_1 = the mass of dried tile (grams)

m_2 = the mass of the wet tile after boiling in the water (grams), (the saturated weight in water)

3.3.4 Apparent porosity

The apparent porosity (P), expressed as a percentage, is the ratio of the open pores volume (V_o) and external volume (V). The percentage of apparent porosity of ceramic tiles samples were determined by boiling samples in the water and soaking for 3 hours. The water absorption was calculated by equation 3.4 (ISO 10545 Part 3 or TIS 2398-2555):

$$P = \frac{V_o}{V} \times 100 \tag{3.4}$$

External volume (V), expressed in cubic centimeters, can be calculated by equation 3.5:

$$V = m_2 - m_3 \tag{3.5}$$

where m_3= the sample mass of the suspension in water (suspended samples weight in water), (grams)

Volume of open pores (V_o) expressed in cubic centimeters and can be calculated by equation 3.6:

$$V_o = m_2 - m_1 \quad (3.6)$$

3.3.5 Apparent relative density

Apparent relative density (T) of the impervious portion of the test specimen, the apparent relative density can be calculated by equation 3.7 (ISO 10545 Part3):

$$T = \frac{m_1}{m_1 - m_3} \quad (3.7)$$

3.3.6 Bulk density

The bulk density (B) is the density of the material composed of solid, closed and open pores expressed in grams per cubic centimeters. The bulk density can be calculated by equation 3.8 (ISO 10545 Part3):

$$B = \frac{m_1}{V} \quad (3.8)$$

Figure 3.9 Herzog compress machine

3.3.7 X-ray fluorescence and X-ray diffraction analysis

The samples preparation sieved by the mesh No. 200 (0.075 mm) and was dried at 100°C in the oven for 24 hours**.** Chemical compositions of dried mud waste powder samples phase analysis were determined by X-ray fluorescence (XRF) method by using WD-XRF model Panalytical-Axios MAX (Figure 3.10). The objective of XRF analysis is to determine oxide concentrations in samples. Samples 0.3 to 1.0 grams were compacted by compress machine (Figure 3.9) and hold for 2-3 minutes. The results of this analysis were presented in peak of major elements before matched by software in XRF analyzer for finding quantity of major elements. XRF analyzes determine the chemistry of a sample by measuring the fluorescent (or secondary) X-ray emitted from a sample when it is excited by a primary X-ray source. XRF Spectra with varying intensities are created and will be present in the spectrum, the peaks energy identified the element, and the X-ray peak height/intensity is generally indicative of its concentration.

Figure 3.10 X-ray fluorescence spectrometer (Panalytical-Axis MAX)

X-ray diffraction (XRD) was also conducted to analyze the minerals and chemical phases of dried mud wastes by Bruker-D2 Phaser (Figure 3.11). Amount of 1.0 to 1.5 grams of samples powder were pressed in a sample holder by a thin glass until outer surface smooth. The incident X-ray beam is diffracted by innumerous crystallites in specific 2 Theta directions. Data is recorded diffraction angle range from 10 to 80, step size of 0.2 seconds and increment of each step of 0.02. The quantitative phase analysis was determined by Rietveld refinement Software analysis.

Figure 3.11 Bruker (D2 Phaser) X-ray diffractrometer

CHAPTER IV

RESULTS AND DISCUSSION

4.1 Introduction

This chapter describes the results of the experimental procedure and discusses in the different sources of the drilling mud wastes. Moreover, the physical properties of the drilling mud waste samples were evaluated and classified for the ceramic tile and the building brick standard as referred to after passed through sieve number 200 mesh.

4.2 Particle size analysis

The particle size distribution of dried mud wastes samples were determined by using the laser diffraction particle size analyzer and the results are shown in Figure 4.1. Particle size of sample C_1, C_2 and C_3 are larger than the particle size of P_1, P_2, L and M as shown in Figure 4.1. The mean diameter of C_1, C_2 and C_3sample are 69.73, 66.30, 67.70 μm, respectively. The mean diameter of P_1 and P_2 are 17.16, 6.42 μm, respectively. L and M samples have the mean diameter of 16.32 μm and 32.68 μm, respectively.

The drilling mud waste from P_2 showed the smallest particle size and it was also found that the distribution of each sample was unevenly distributed. The residue weight on the sieve size number 200 mesh and the yield of the waste for each sample were shown in Table 4.1.

Table 4.1 Weight ratio of the different samples after sieving through 200 mesh

Samples	The residual weight on sieve number 200 mesh (%)	The weight passed sieve number 200 mesh (%)
C_1	81.88	18.12
C_2	65.65	34.35
C_3	43.10	56.90
L	80.71	19.29
M	82.19	17.81
P_1	62.70	37.30
P_2	66.78	33.22

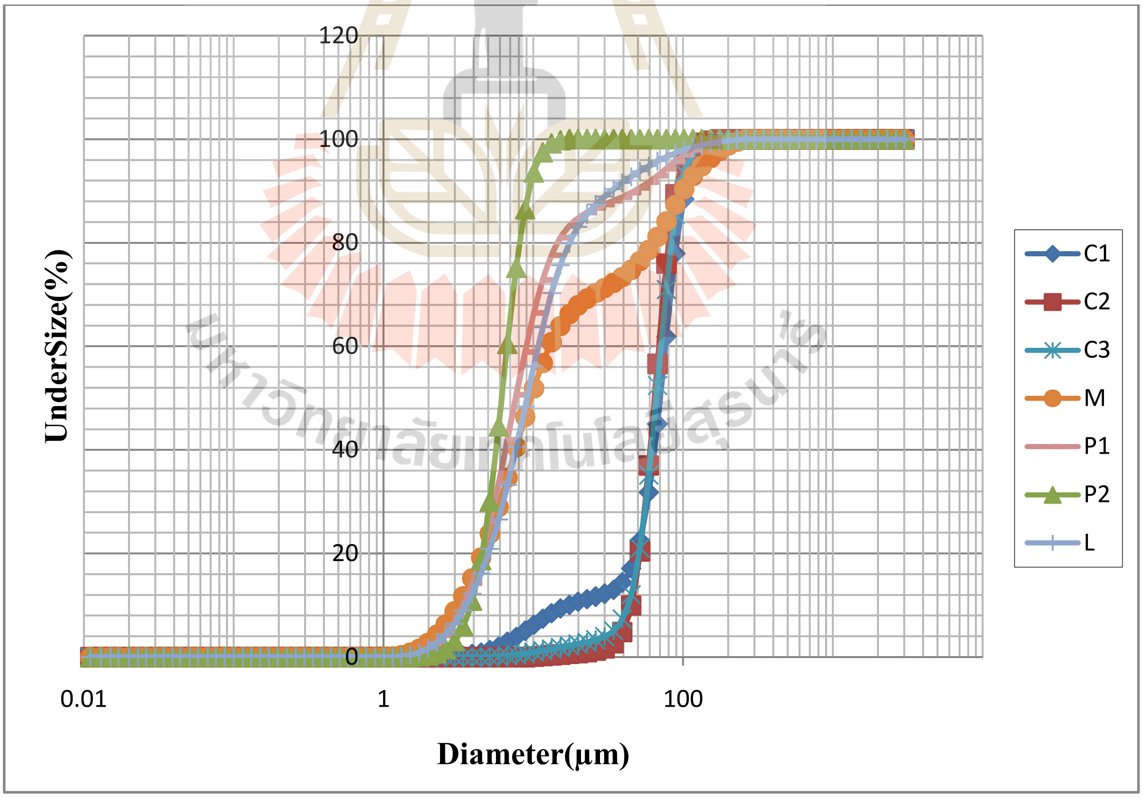

Figure 4.1 Particle size analysis of the different drilling mud wastes

4.3 Chemical analysis

To determine the elements and the mineral compositions of the collected water based drilling mud wastes, XRF and XRD analyses were conducted for this purpose. The elements and mineral compositions of the collected water based drilling mud waste dried powder sample. Results are shown in Table 4.2 and Figure 4.2 to 4.7, respectively.

Results of chemical analyses indicated that the mineral composition of the water based drilling mud wastes used in this study were mainly quartz with a less among of feldspar, kaolinite and barite.

Table 4.2 Quantitative of elements for water based drilling mud wastes analyzed by X-ray fluorescence (XRF)

Element	**Drilling mud waste sample (%)**						
	C_1	**C_2**	**C_3**	**L**	**M**	**P_1**	**P_2**
Na	0.97	0.10	0.60	0.65	0.86	0.6	0.48
Mg	0.75	1.23	1.30	1.66	2.09	1.86	2.26
Al	5.16	12.21	10.92	21.85	21.27	22.34	15.66
Si	57.29	76.87	46.31	44.18	50.27	54.96	59.39
P	0.29	0.22	-	-	0.11	0.06	0.12
S	0.79	0.54	1.38	0.63	0.98	0.1	0.10
Cl	1.03	0.07	0.56	0.26	0.45	0.22	0.25

Table 4.2 Quantitative of elements for water based drilling mud wastes analyzed by X-ray fluorescence (XRF) (continued)

Element	Drilling mud waste sample (%)						
	C_1	C_2	C_3	L	M	P_1	P_2
K	4.45	6.37	6.02	4.74	5.56	4.76	4.57
Ca	7.23	-	12.21	14.37	1.43	2.38	-
Ti	0.54	1.71	0.81	0.97	1.04	1.1	1.22
Cr	-	0.07	-	0.02	0.03	0.04	0.06
Mn	0.27	0.33	0.27	0.09	0.17	0.2	0.21
Fe	11.92	-	19.40	8.28	12.34	11.4	15.36
Co	-	0.07	0.07	-	-	0.02	0.04
Ni	0.06	0.03	0.09	-	-	0.02	0.04
Cu	-	0.02	0.06	0.03	0.02	0.02	0.02
Ga	-	-	-	-	0.03	-0	-
Rb	-	0.08	-	0.09	0.08	0.08	-
Zr	-	-	-	-	-	-	0.04
Mo	9.26	-	-	-	-	-	-
Ba	-	-	-	2.20	3.31	0.22	0.20
Ce	-	0.10		-	-	1.1	-

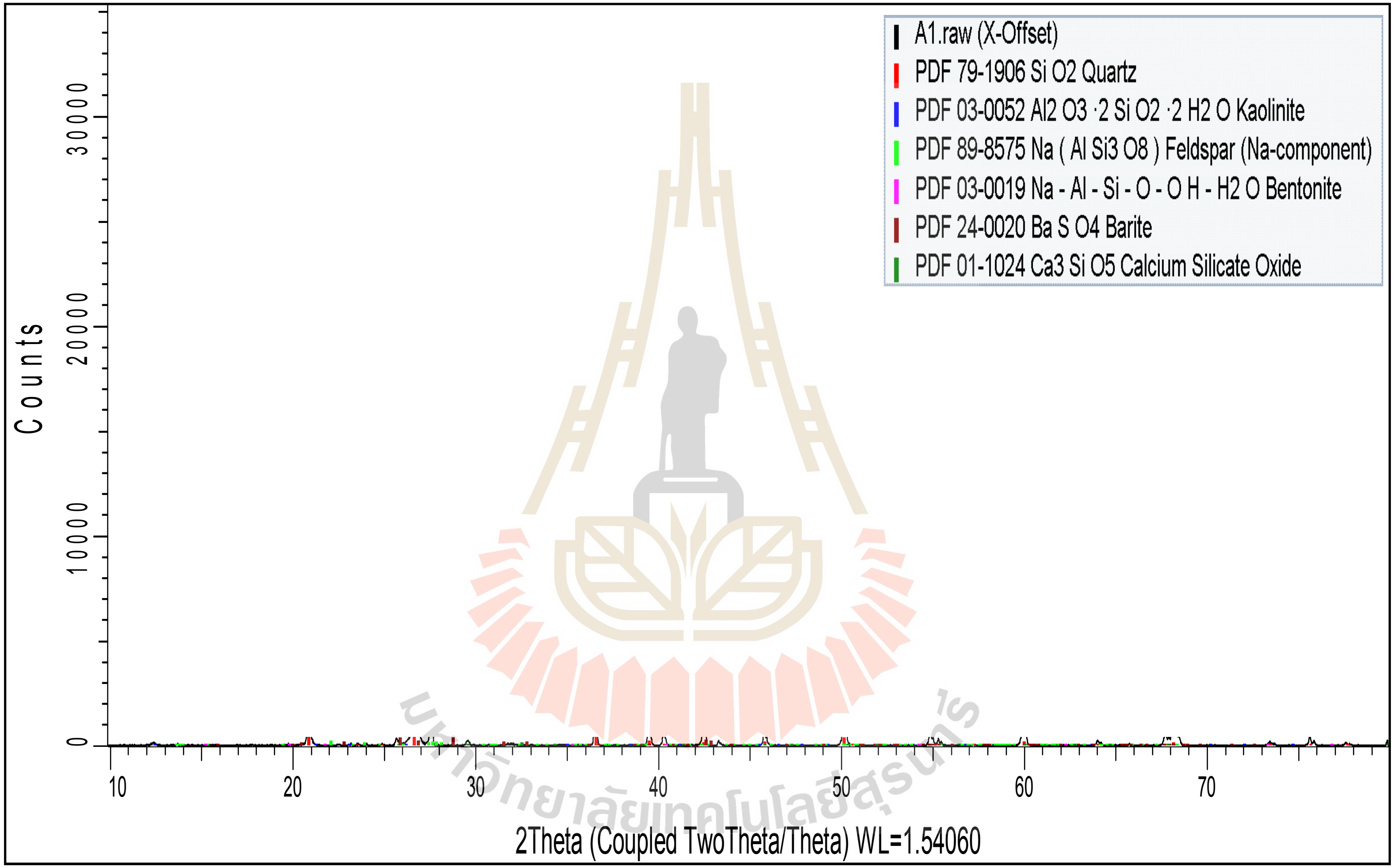

Figure 4.2 XRD pattern from sample C_1

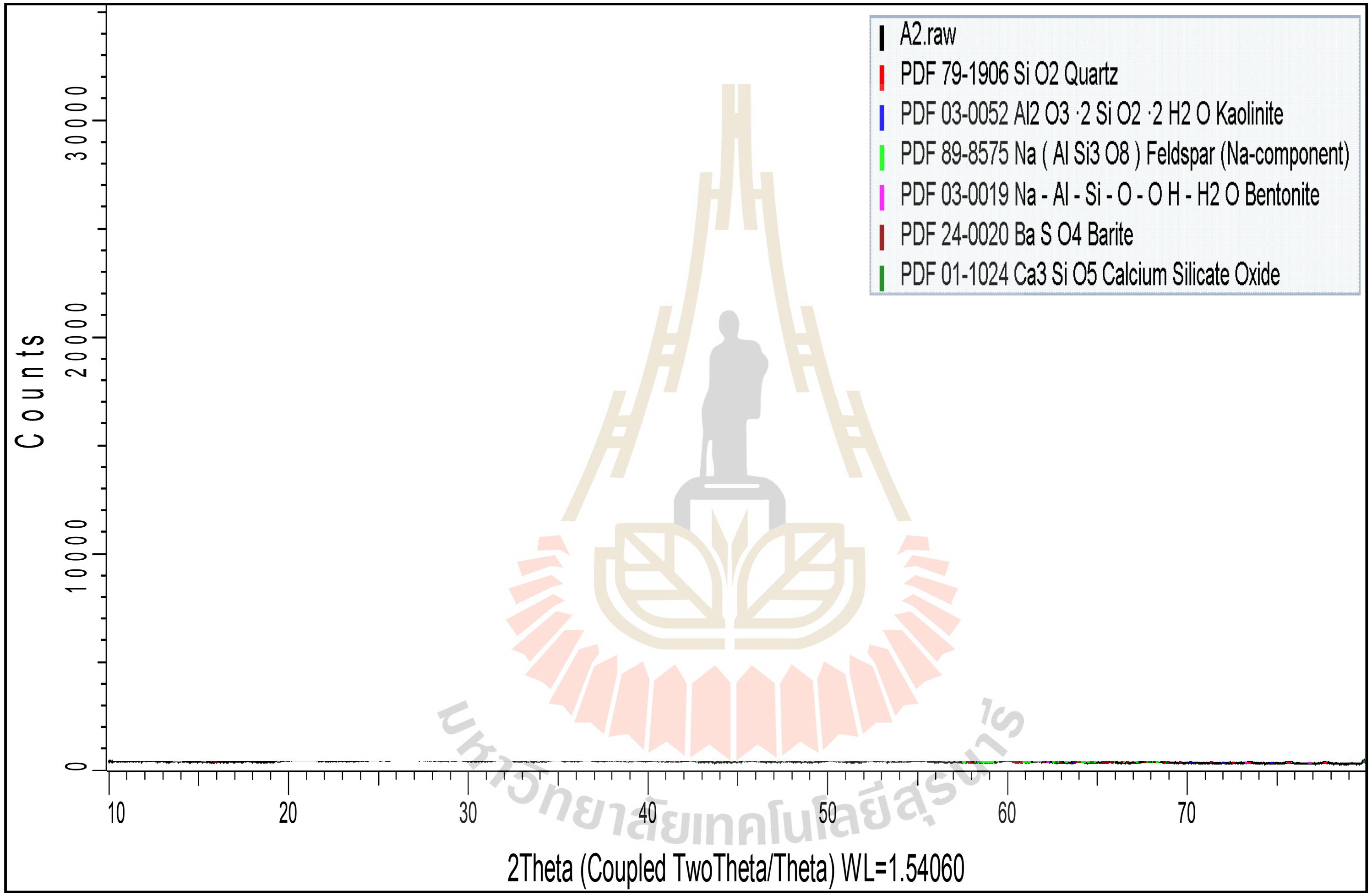

Figure 4.3 XRD pattern from sample C_2

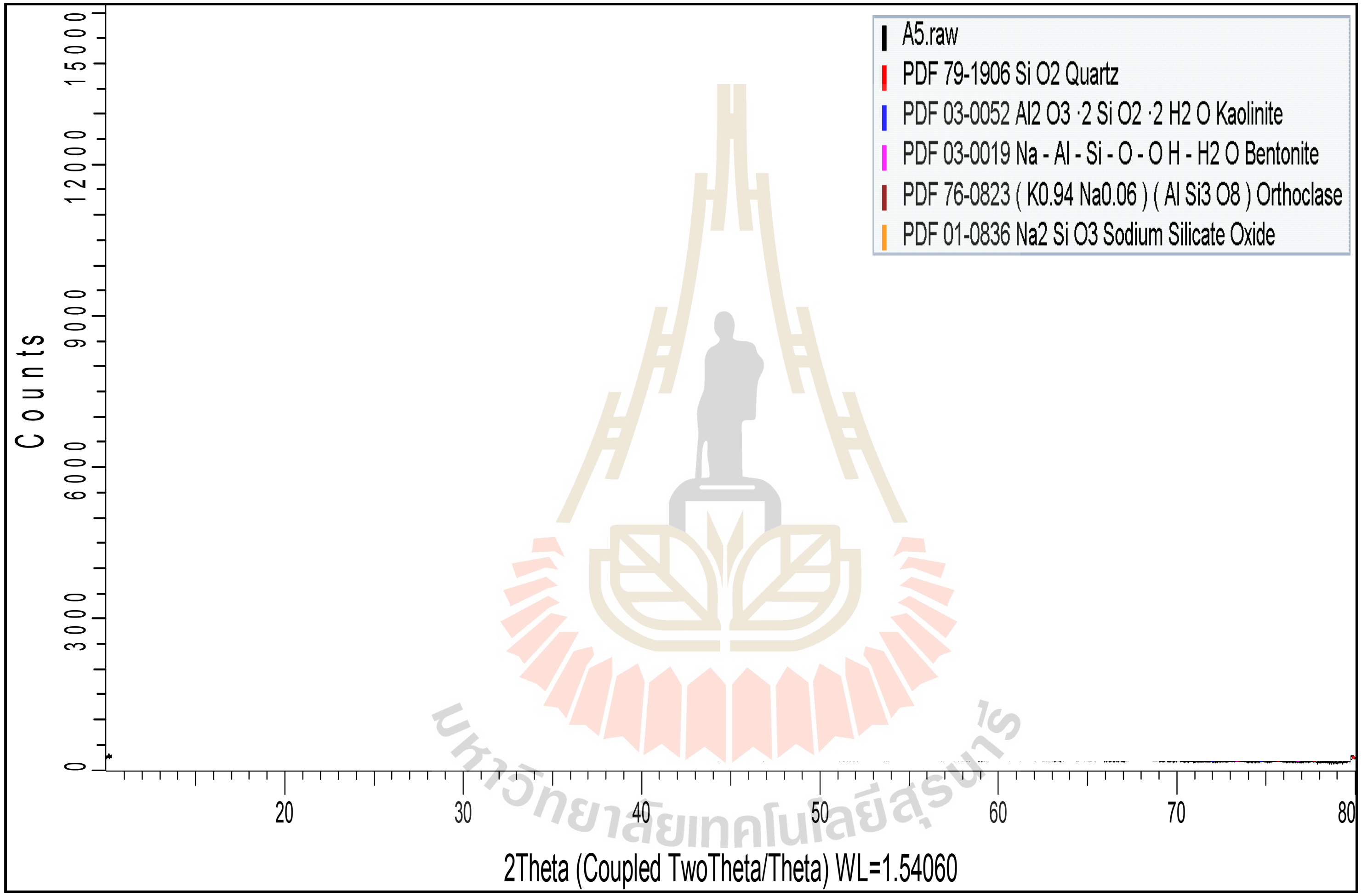

Figure 4.4 XRD pattern from sample C_3

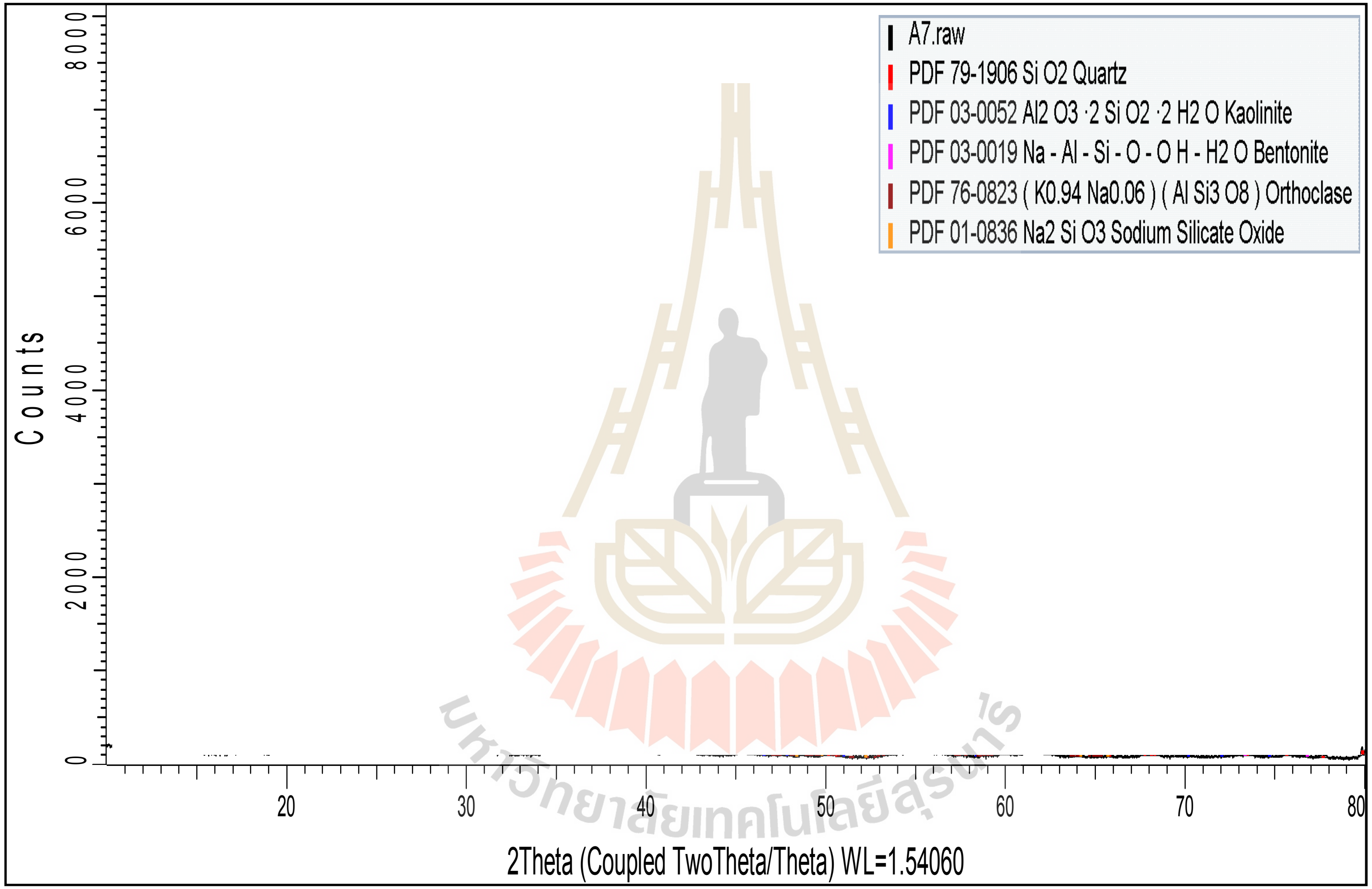

Figure 4.5 XRD pattern from sample P_1

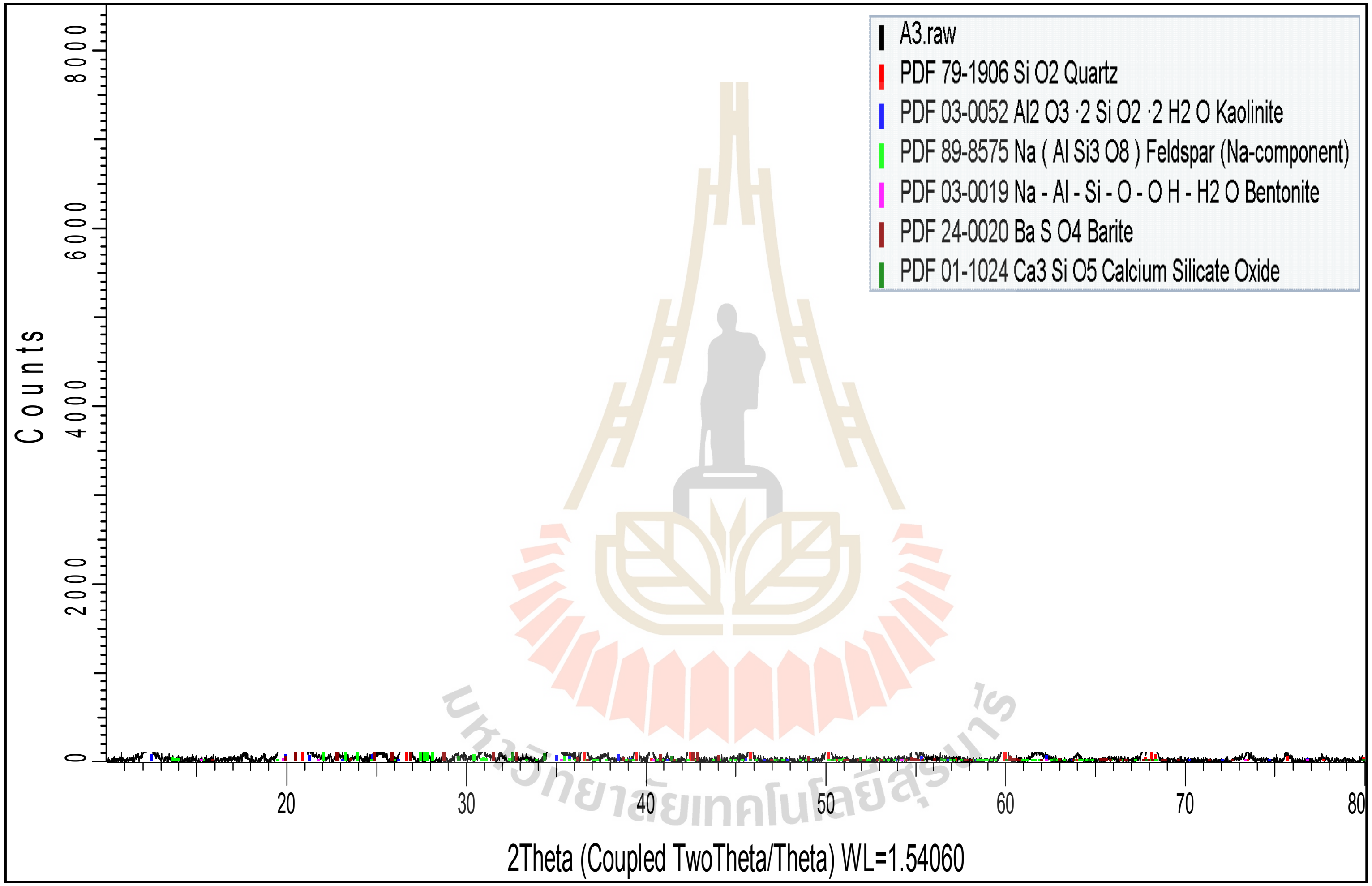

Figure 4.6 XRD pattern from sample P_2

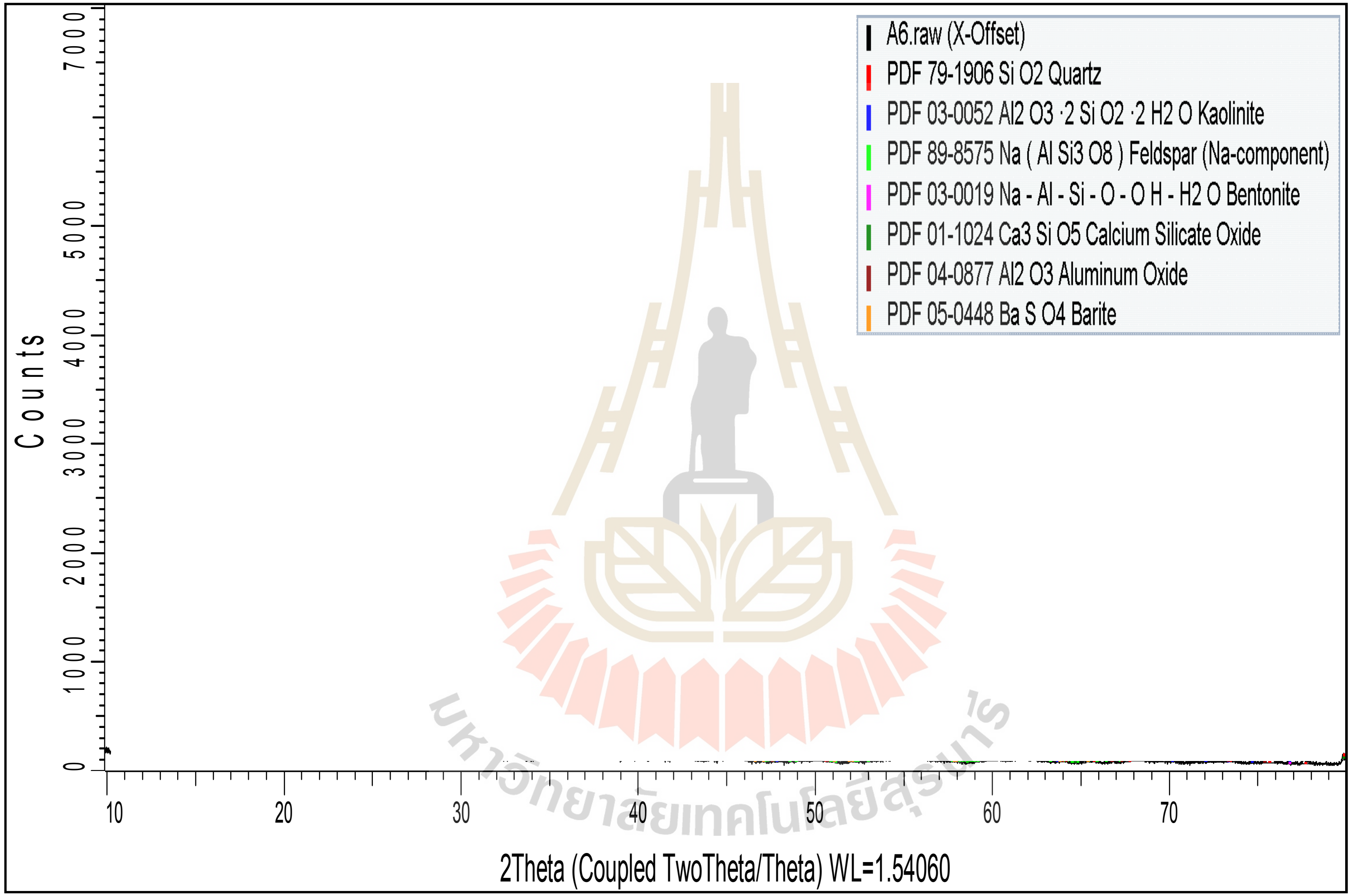

Figure 4.7 XRD pattern from sample M

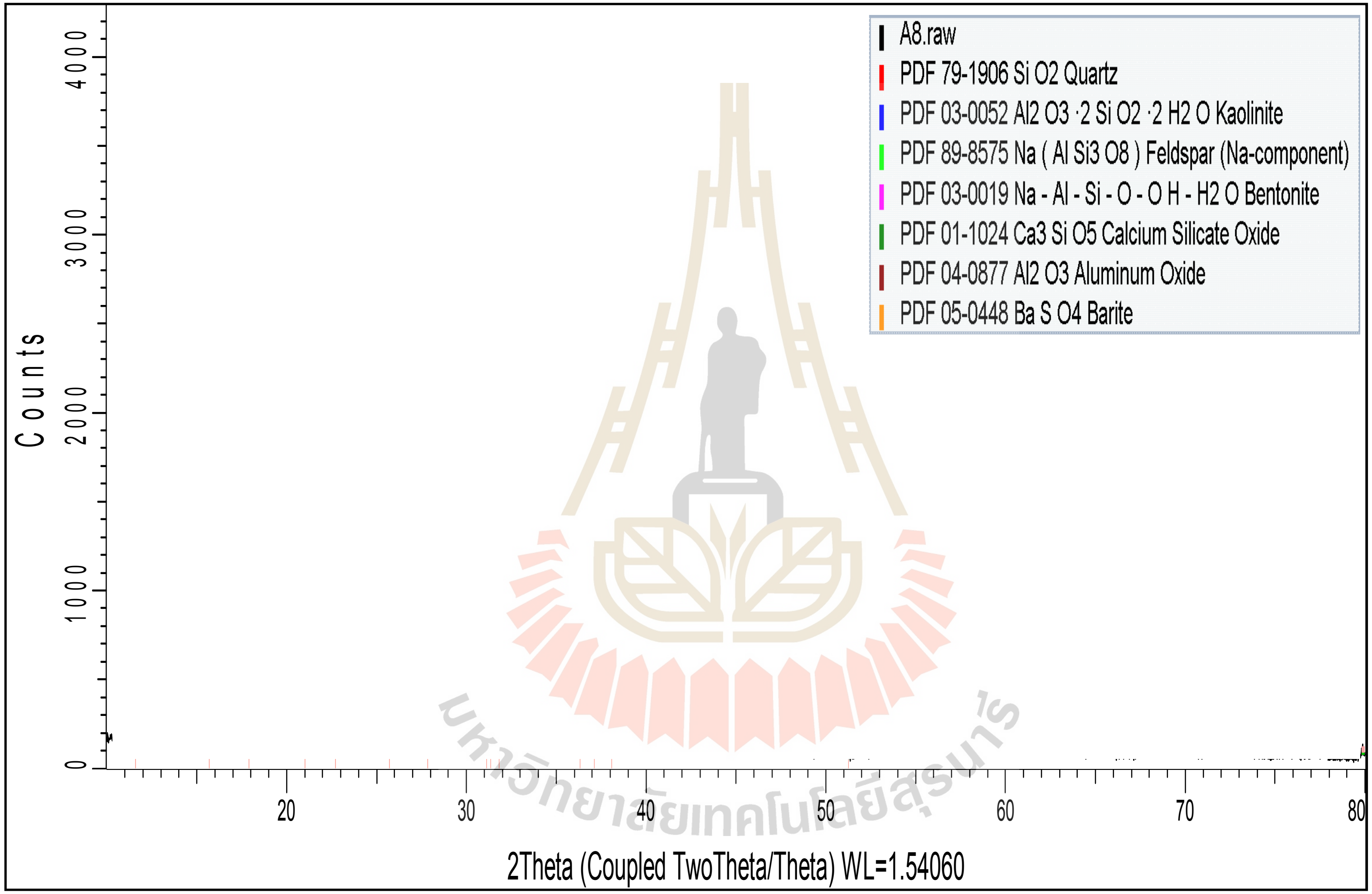

Figure 4.8 XRD pattern from sample L

4.4 Physical property testing

4.4.1 Shrinkage

The percentage of shrinkage after fired samples at various temperatures shown in Figure 4.9. The volumes shrinkage of sample C_1, C_2 and C_3 were 4.13 to 27.60, 2.44 to 33.94 and 4.13 to 27.60 percent, respectively. The volume shrinkage of sample P_1, P_2, L and M were 2.05 to 28.08, 6.28 to 24.92, 1.29 to 27.23 and 2.34 to 22.66 percent, respectively. It was observed that the volume of samples decreased with the firing temperature increased.

The volume shrinkage percent of sample C_3 was the highest, whereas the volume shrinkage percent of sample M was the lowest when fired at 1,150°C.

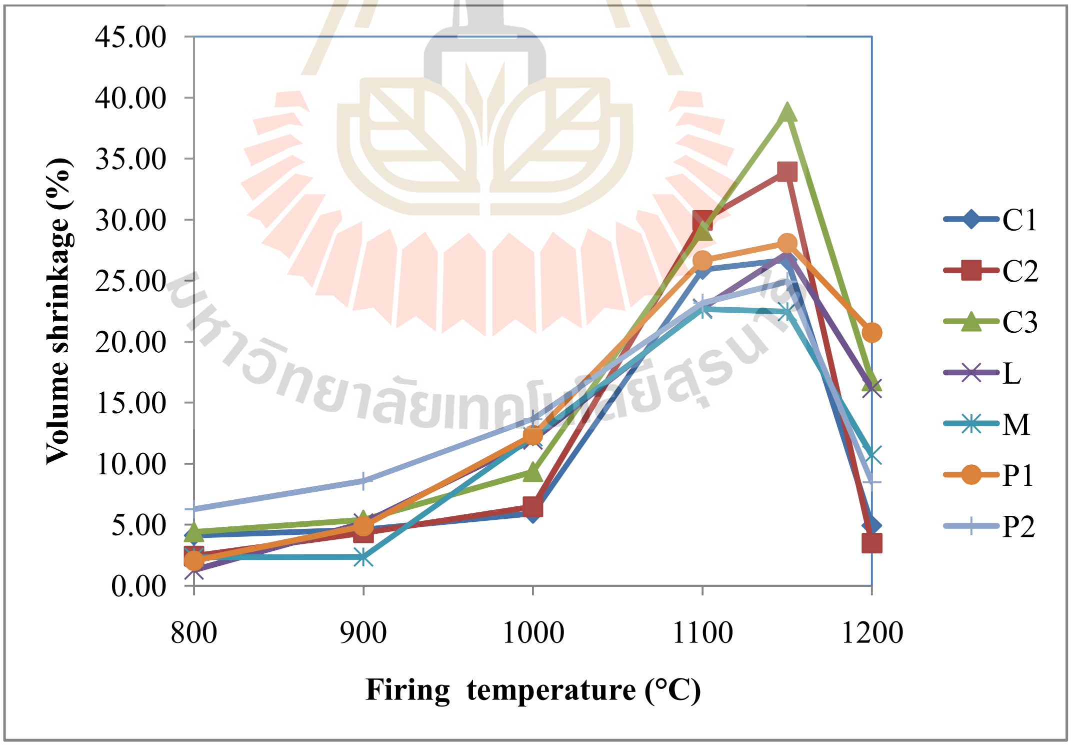

Figure 4.9 The relationship between shrinkage percent and the firing temperature of samples

Table 4.3 Volume shrinkage percent at the tested firing temperature

Sample	Volume shrinkage (%) at the tested firing temperature (°C)					
	800°C	900°C	1,000°C	1,100°C	1,150°C	1,200°C
C_1	4.13	4.58	5.92	25.90	26.70	4.93
C_2	2.44	4.34	6.47	29.94	33.94	3.49
C_3	4.40	5.41	9.33	29.10	38.87	16.76
L	1.29	5.13	11.94	22.76	27.23	16.17
M	2.34	2.37	12.20	22.66	22.47	10.71
P_1	2.05	4.89	12.34	26.66	28.08	20.75
P_2	6.28	8.57	13.68	23.17	24.92	8.47

4.4.2 Water Absorption

The water absorption measurement of ceramic tile and building brick samples were conducted according to TIS 2398 part 3-2553 and TIS 77-2545 standard respectively. The relationship between water absorption of ceramic tile samples from various sources and firing temperature are presented in Figure 4.10, while the percent water absorption of ceramic tile samples from each source are plotted with the firing temperature separately as shown in Figure 4.11 to 4.17, respectively.

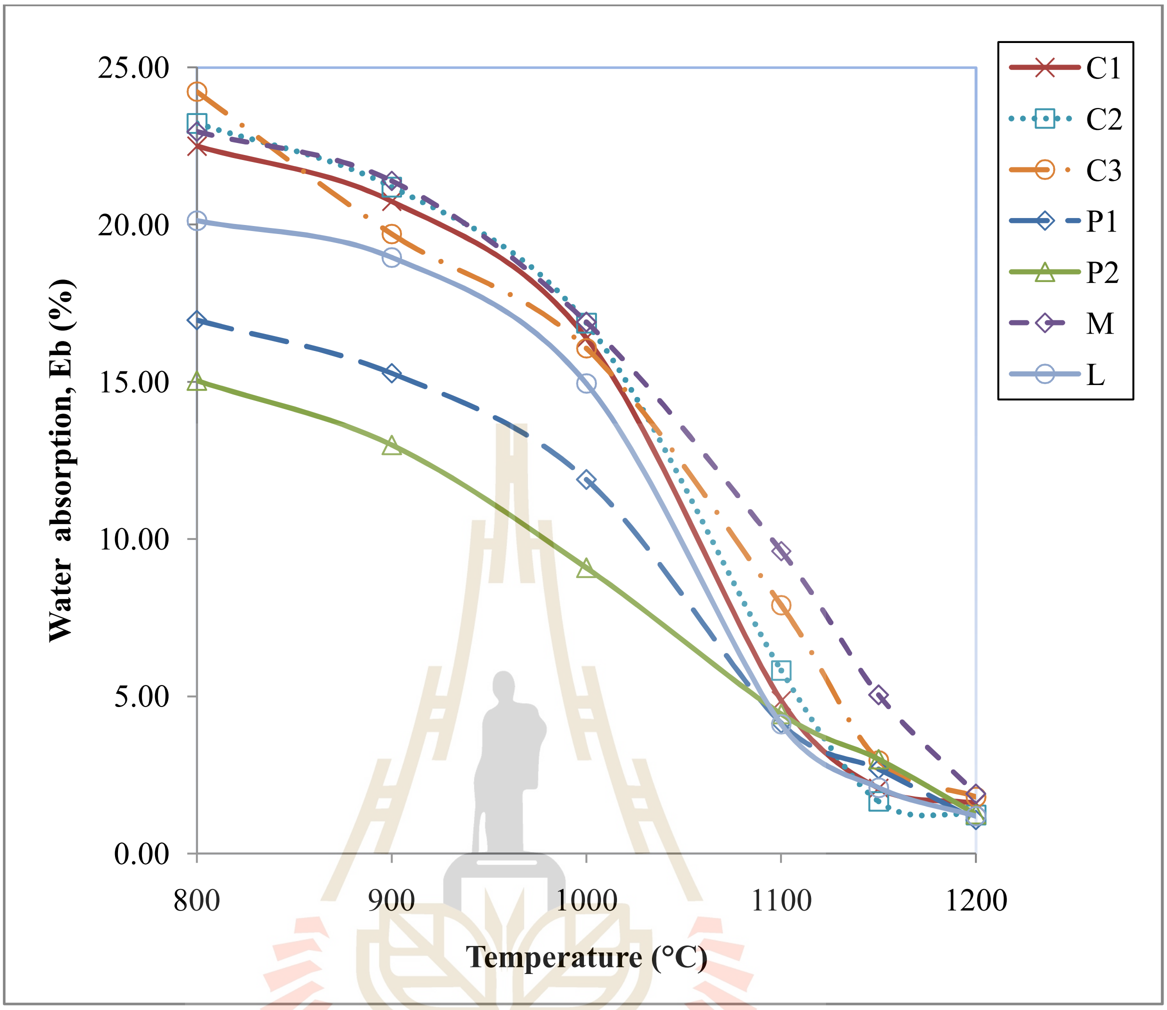

Figure 4.10 The water absorption percent of ceramic tile samples from various sources versus the firing temperature

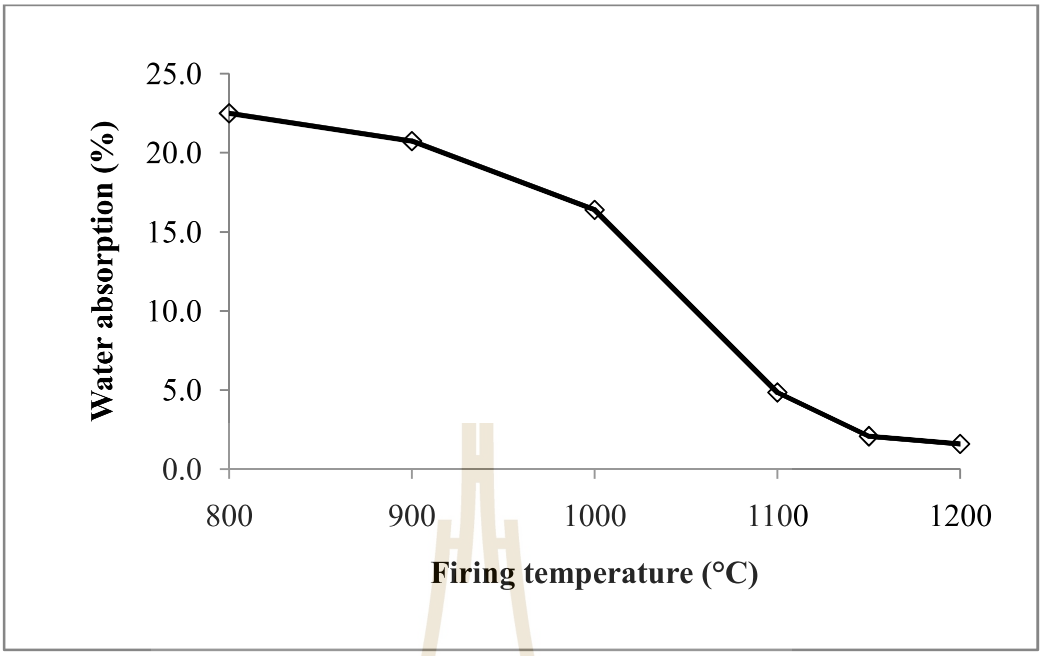

Figure 4.11 The water absorption of sample C_1 versus the firing temperature

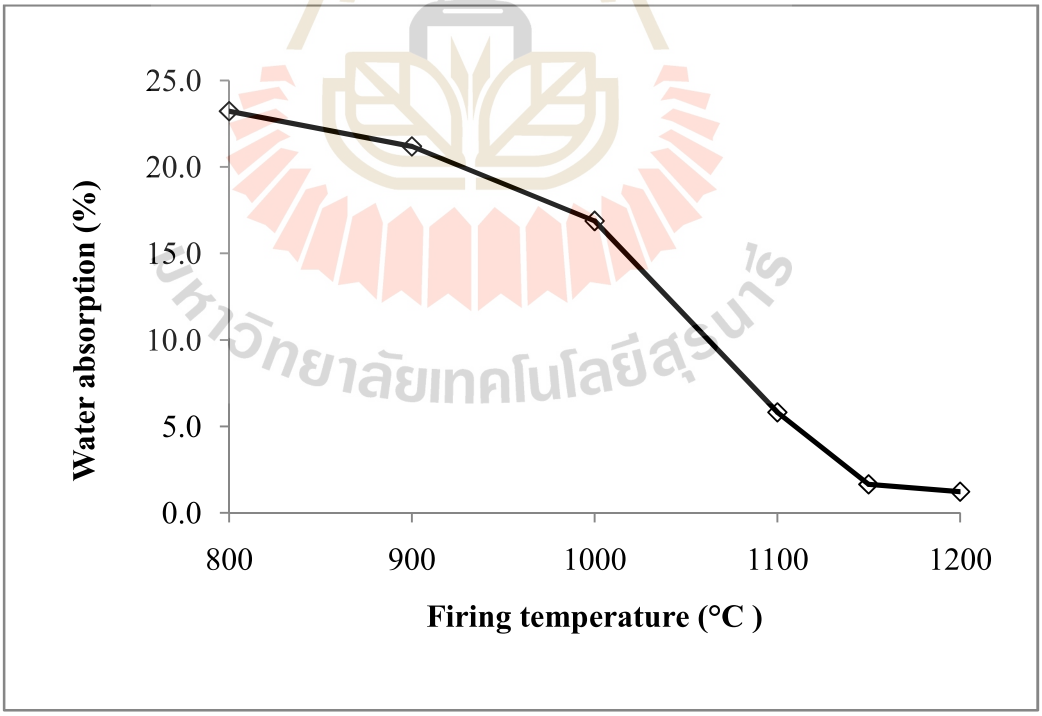

Figure 4.12 The water absorption of sample C_2 versus the firing temperature

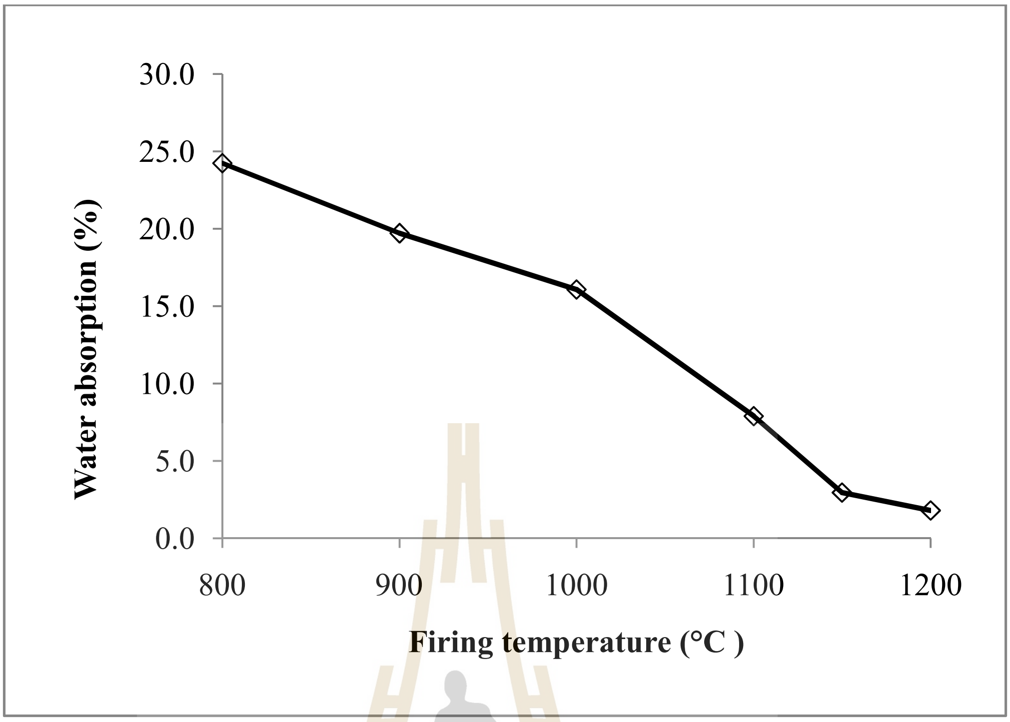

Figure 4.13 The water absorption of sample C_3 versus the firing temperature

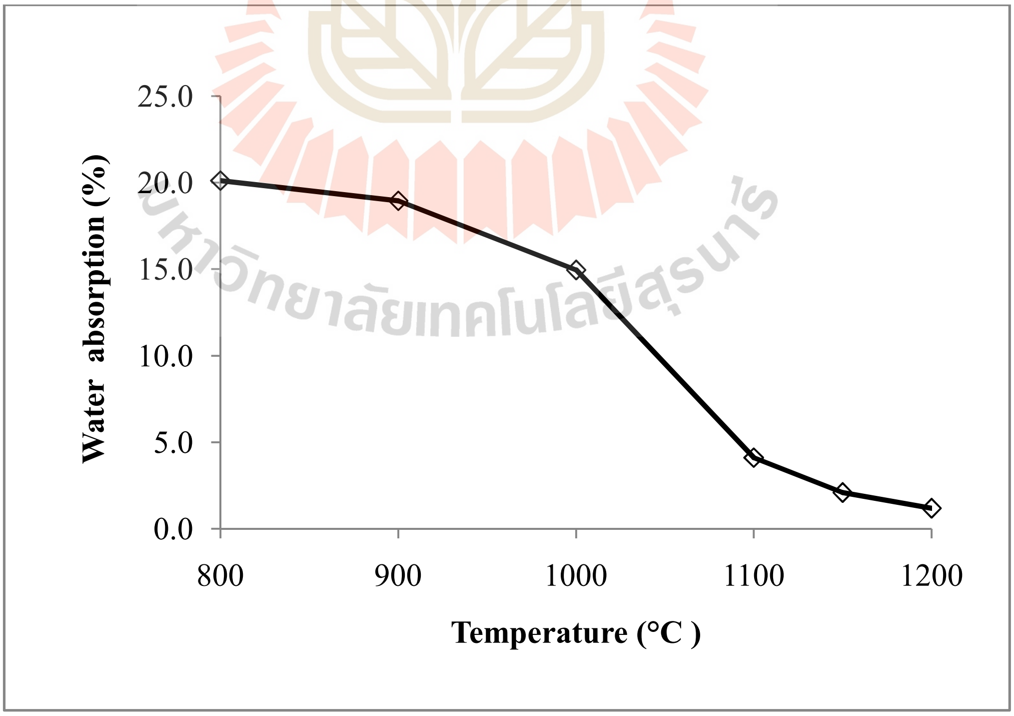

Figure 4.14 The water absorption of sample L versus the firing temperature

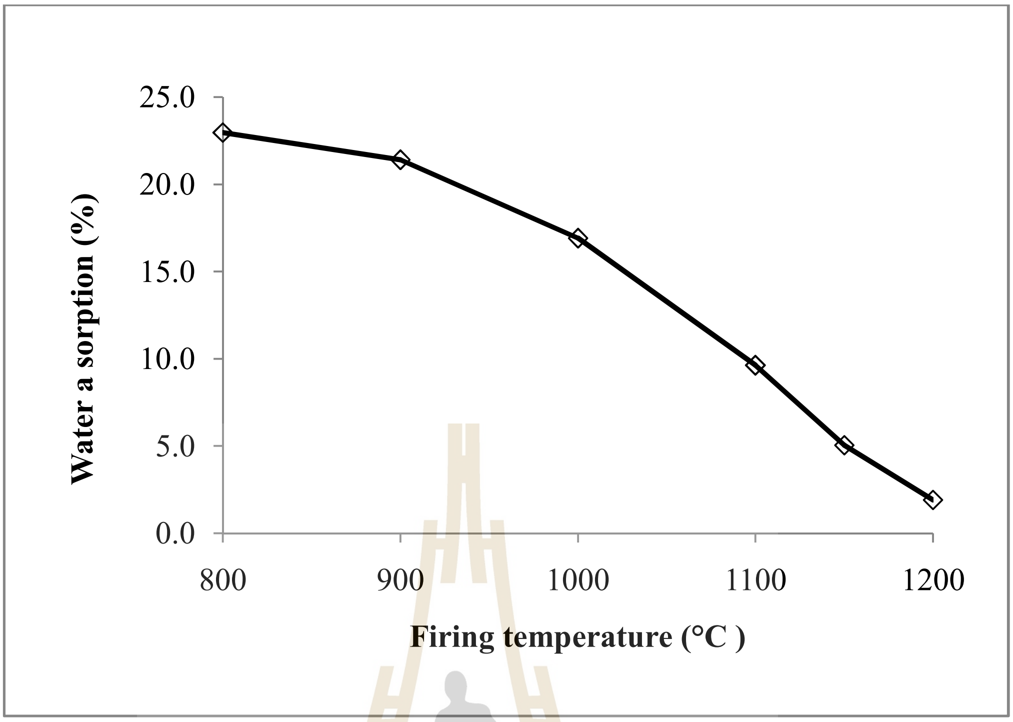

Figure 4.15 The water absorption of sample M versus the firing temperature

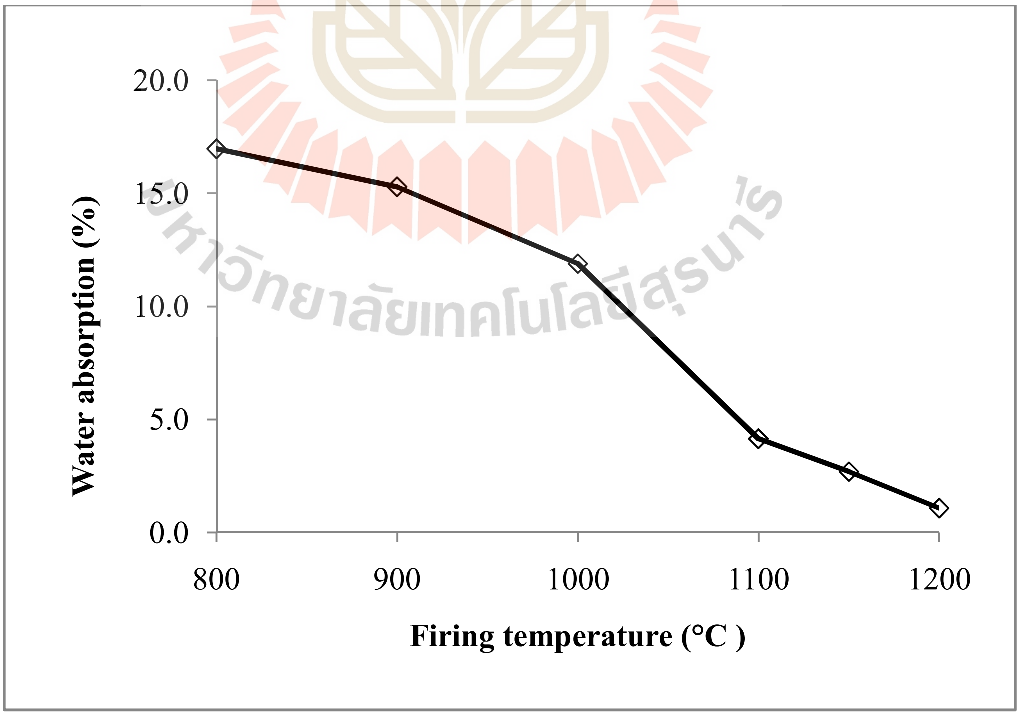

Figure 4.16 The water absorption of sample P_1 versus the firing temperature

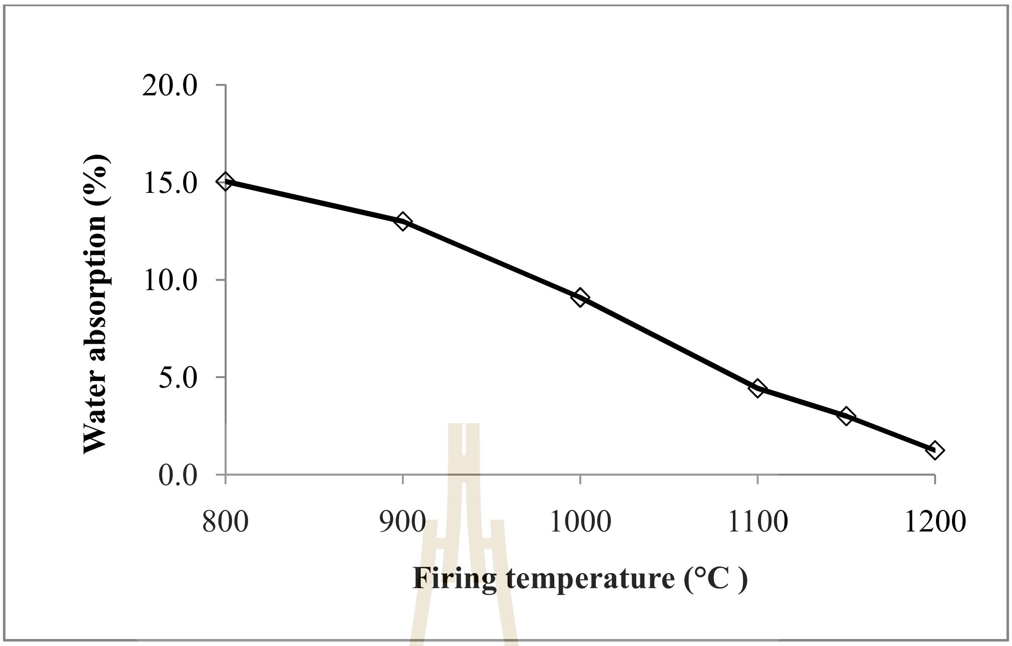

Figure 4.17 The water absorption of sample P_2 versus the firing temperature

Results of the water absorption measurement in Figure 4.10 show that the water absorption of samples decreased when the firing temperature increased. Samples fired range from 800 to 1,000°C have the water absorption more than 10 percent and can be classified into the Group BIII according to the referenced ceramic tile standard. Samples fired at higher than 1,100°C have water absorption range from 6 to 10 percent and can be classified into the Group BII_a. However, M and P_2 samples show very low water absorption in range of 3 to 6 percent, therefore, they can be classified into the Group BII_b.

Building brick samples made from drilling mud waste only from a drill hole of Phitsanulok basin (P_1) and fired at 1,000°C were also conducted the water absorption measurement. Results of the measurement are presented in Table A10.

Results of the water absorption measurement indicated that the average water absorption of 15 building brick samples for P_1 was 12.98 percent.

This low water absorption of the ceramic tile and brick samples may cause from its low permeability character which is resulted from high kaolinite and a clay mineral content.

4.4.3 Apparent porosity

The apparent porosity was determined only on the ceramic tile samples according to the TIS 2398 Part 3-2553 standard. The apparent porosity of ceramic tile samples made from drilling mud wastes of drill holes at Fang, Lampang, Mae Tha and Phitsanulok basin are presented in Table A16 to A22. The apparent porosity of ceramic tile samples from various sources versus the firing temperature are plotted in Figure 4.18, while the apparent porosity of ceramic tile samples from each source are plotted versus the firing temperature separately in Figure 4.19 to Figure 4.25, respectively.

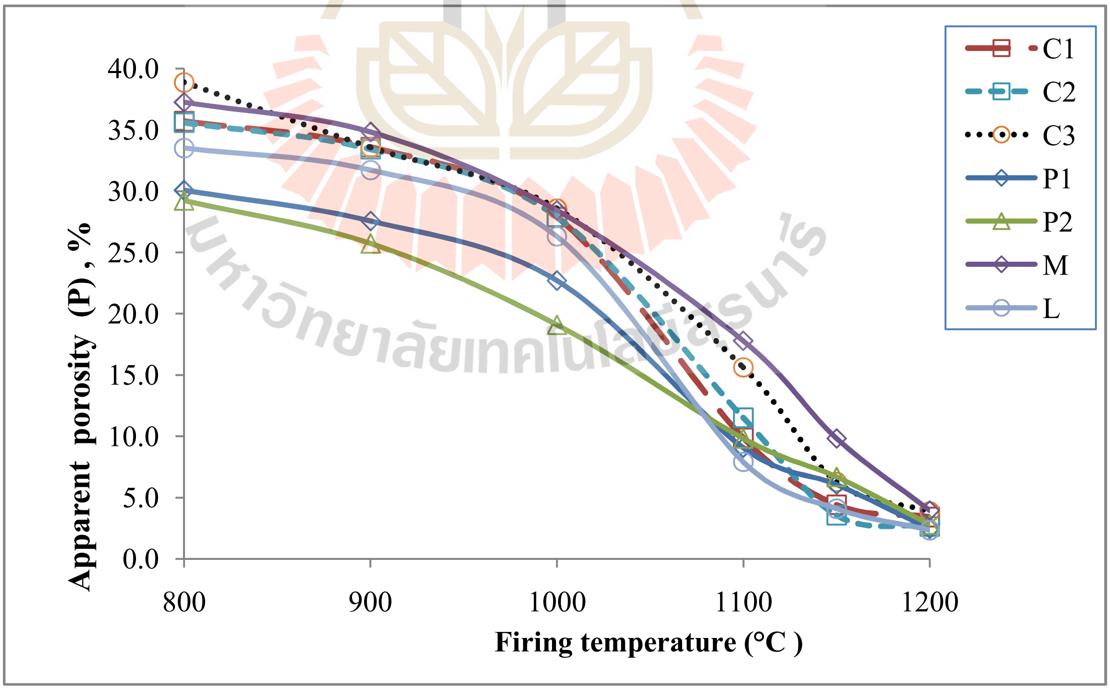

Figure 4.18 The apparent porosity percent of ceramic tile samples from various sources versus the firing temperature

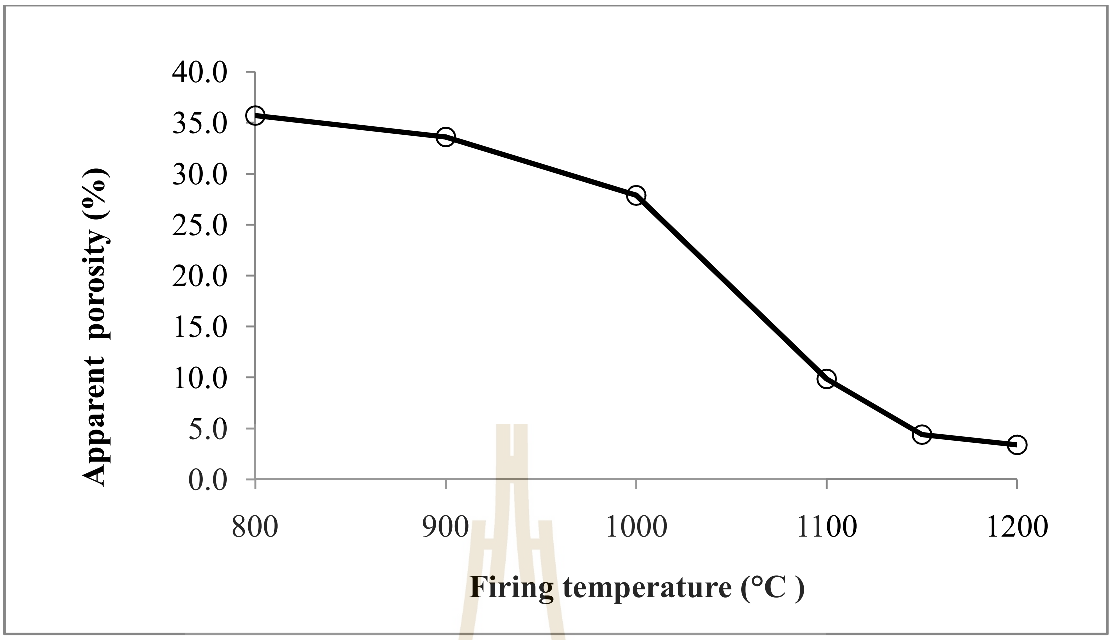

Figure 4.19 The apparent porosity percent of sample C_1 versus the firing temperature

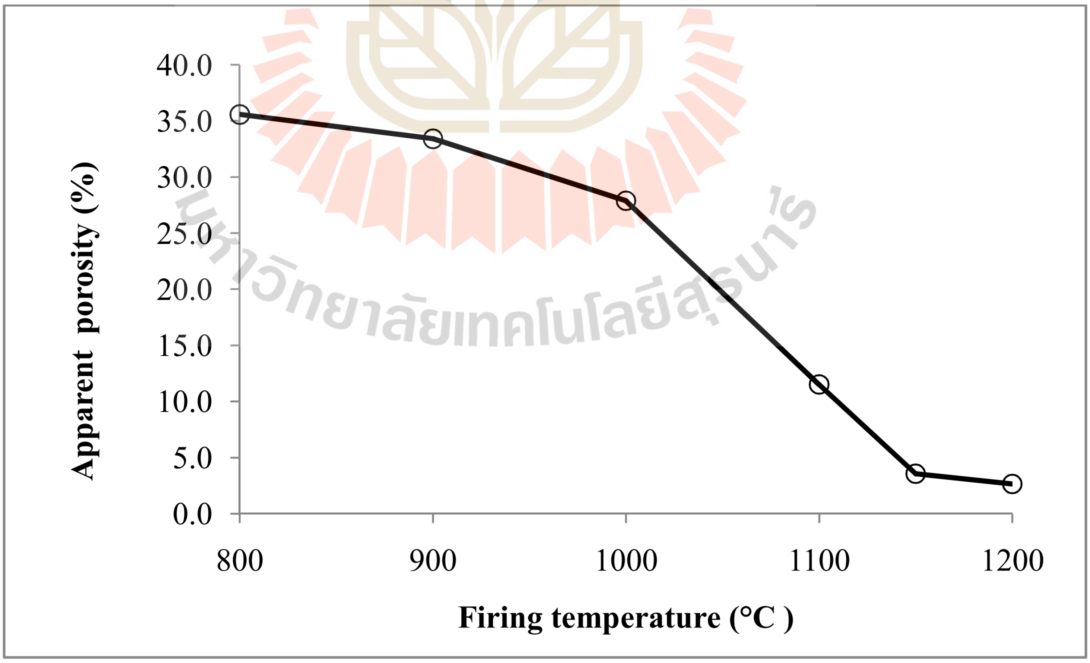

Figure 4.20 The apparent porosity percent of sample C_2 versus the firing temperature

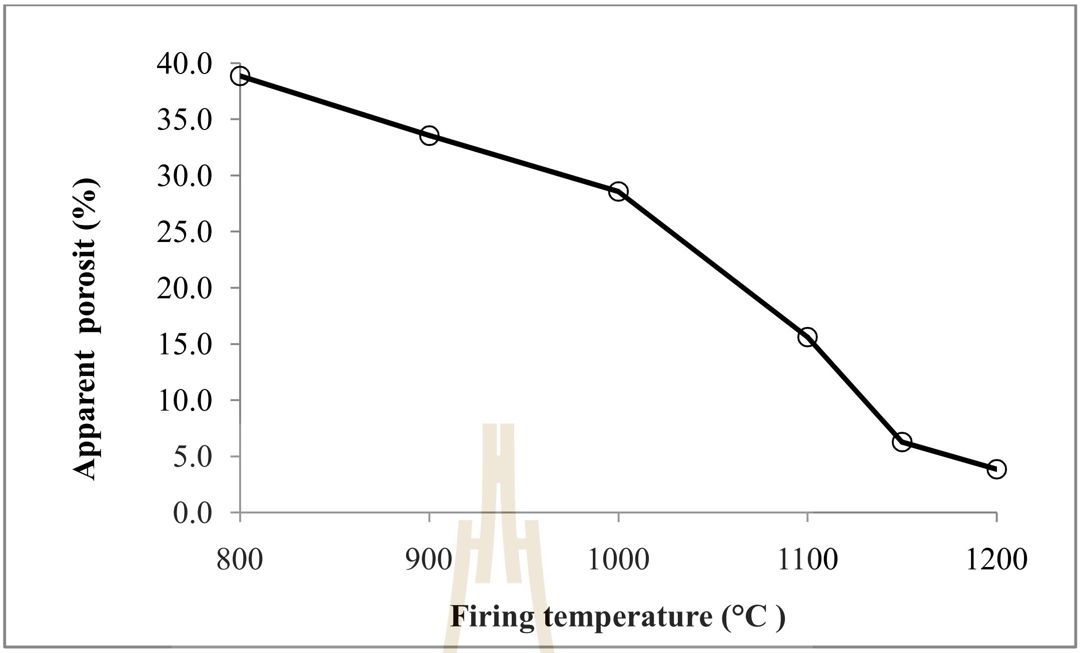

Figure 4.21 The apparent porosity percent of sample C_3 versus the firing temperature

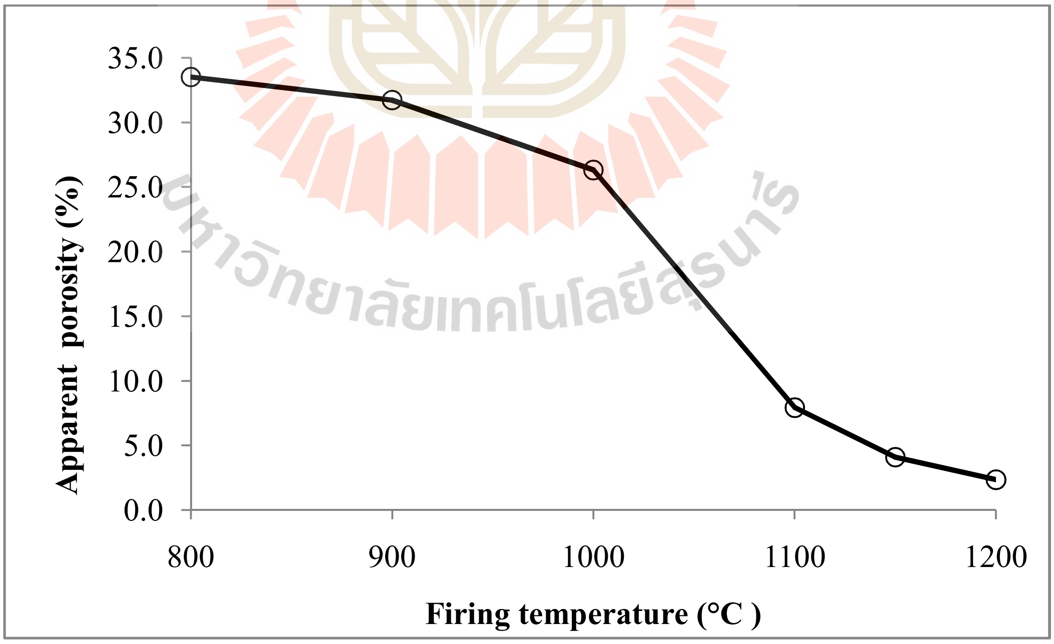

Figure 4.22 The apparent porosity percent of sample L versus the firing temperature

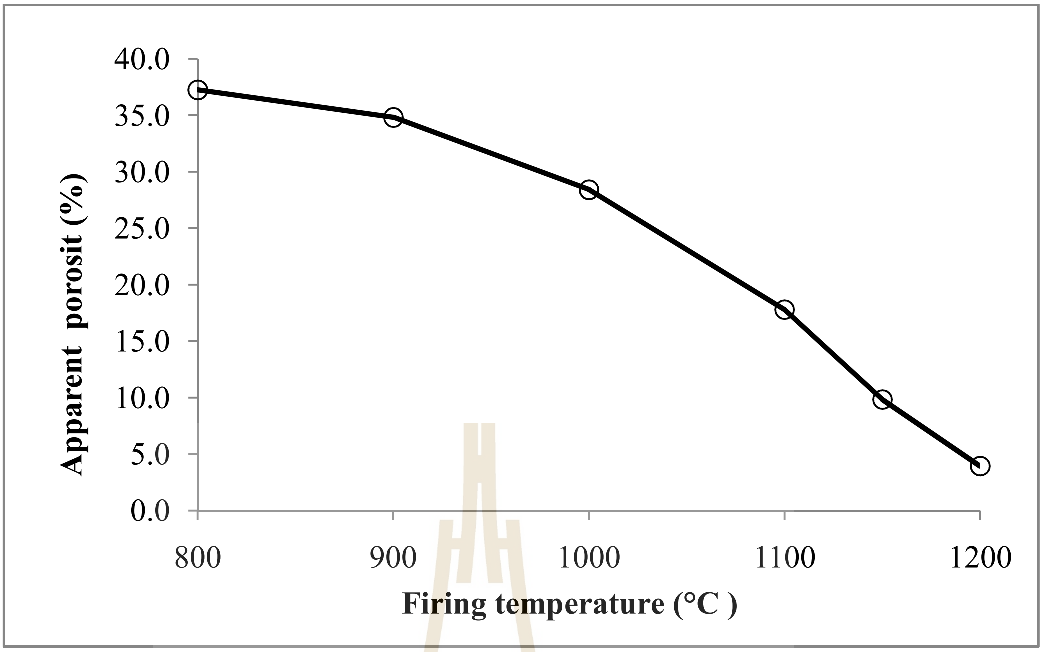

Figure 4.23 The apparent porosity percent of sample M versus the firing temperature

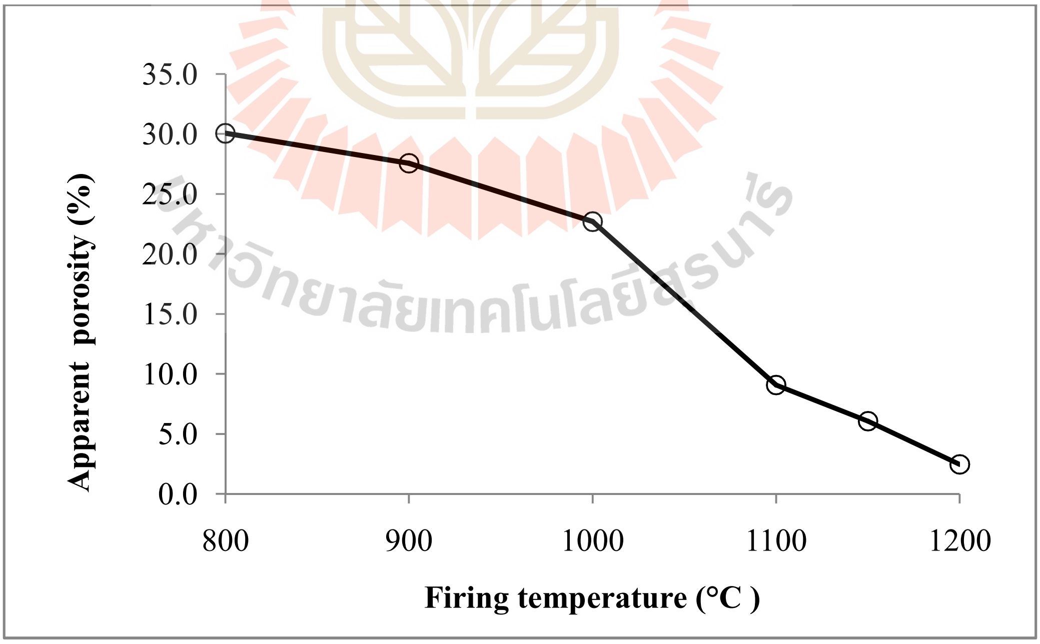

Figure 4.24 The apparent porosity percent of sample P_1 versus the firing temperature

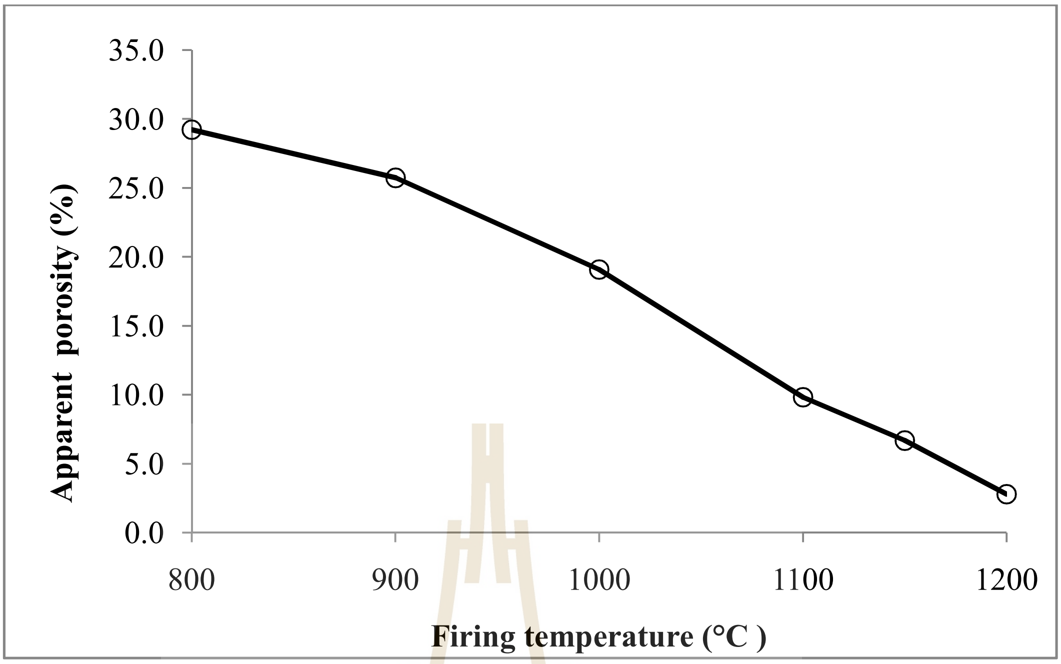

Figure 4.25 The apparent porosity percent of sample P_2 versus the firing temperature

Results from apparent porosity measurement of ceramic tile samples indicated that the apparent porosity of ceramic tile samples decreased when the firing temperature increased. When the clay and minerals in the drilling mud waste were fired at high temperature, the porosity of samples became lower and resulting in the low water absorption.

4.4.4 Apparent relative density

The apparent relative density was determined only on the ceramic tile samples according to the TIS 2398 Part 3-2553 standard. The results of apparent relative density measurement of ceramic tile samples are shown in Table A23 to A29. The apparent relative density of ceramic tile samples from various source versus firing temperature are plotted all together in Figure 4.26. The apparent relative density of ceramic tile samples from each source was plotted versus firing temperature separately in Figure 4.27 to 4.33, respectively. From the plots it was observed that the apparent relative density of ceramic tiles decreases with the firing temperature increased.

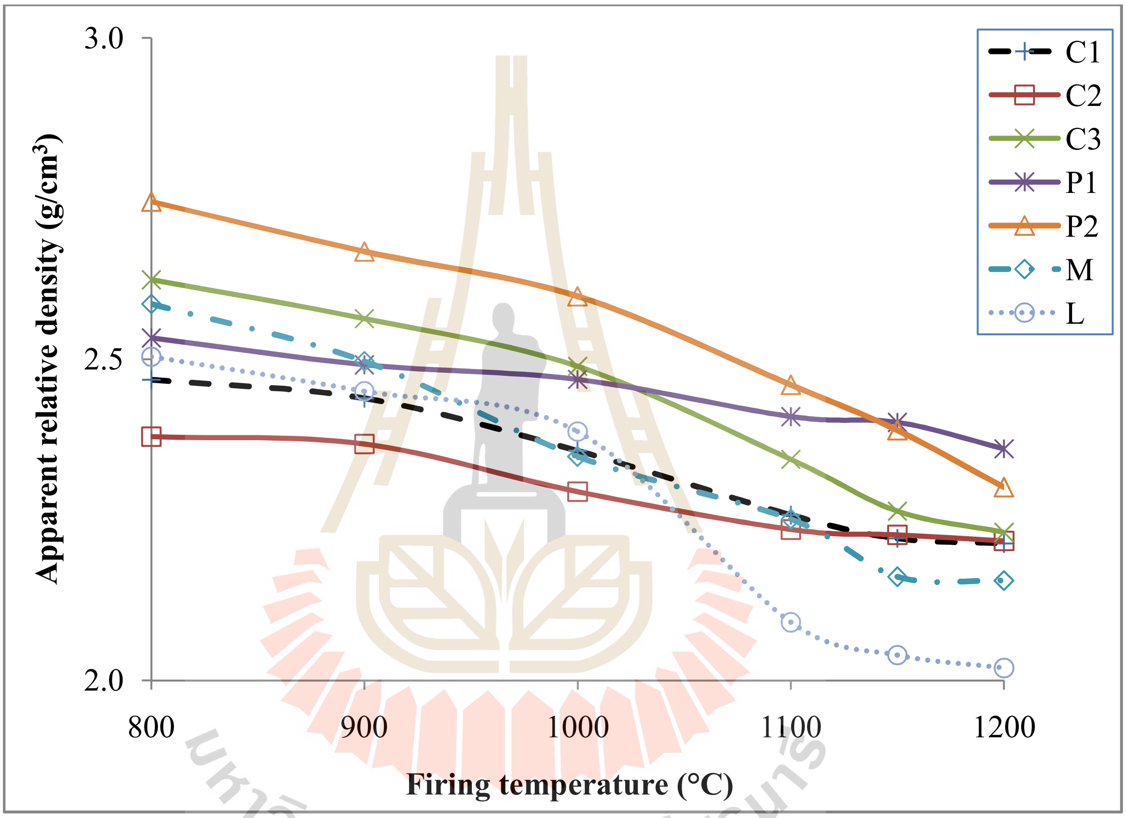

Figure 4.26 The apparent relative density of ceramic tile samples from various sources versus the firing temperature

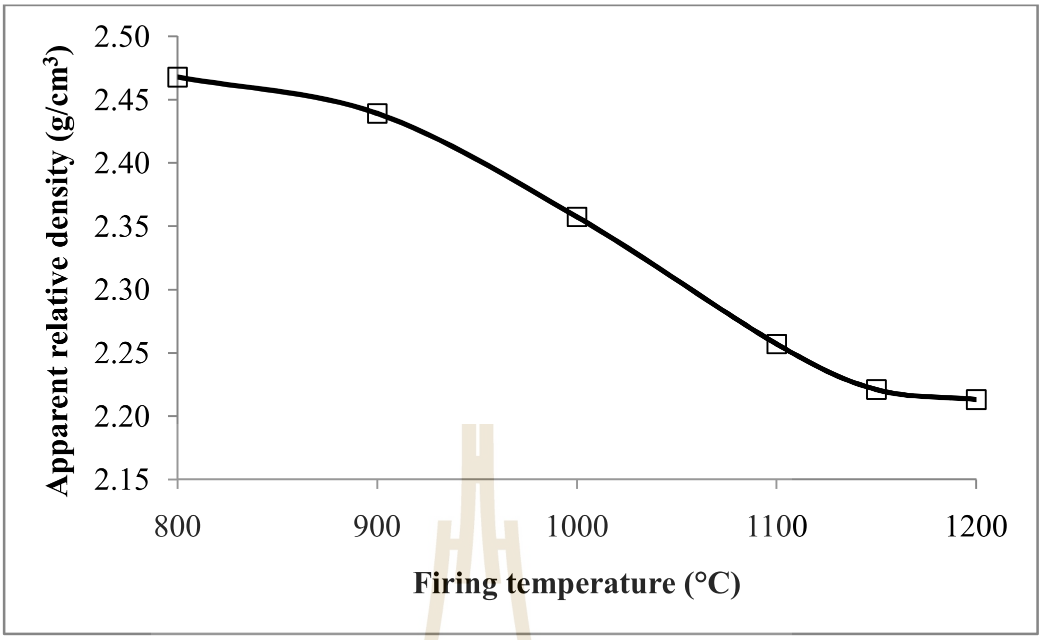

Figure 4.27 The apparent relative density of sample C_1 versus the firing temperature

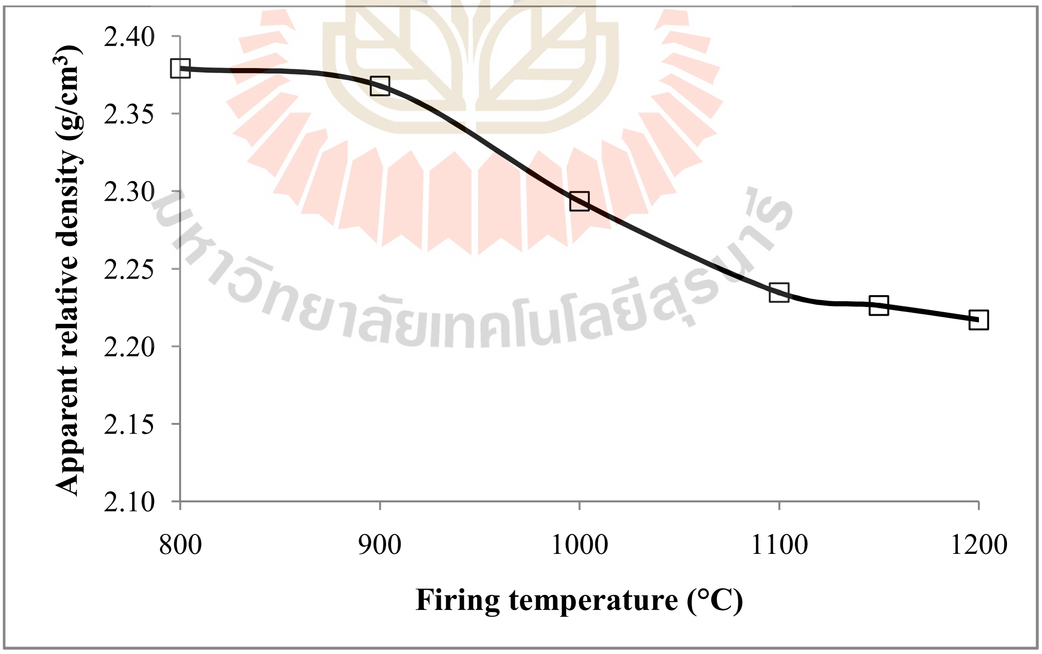

Figure 4.28 The apparent relative density of sample C_2 versus the firing temperature

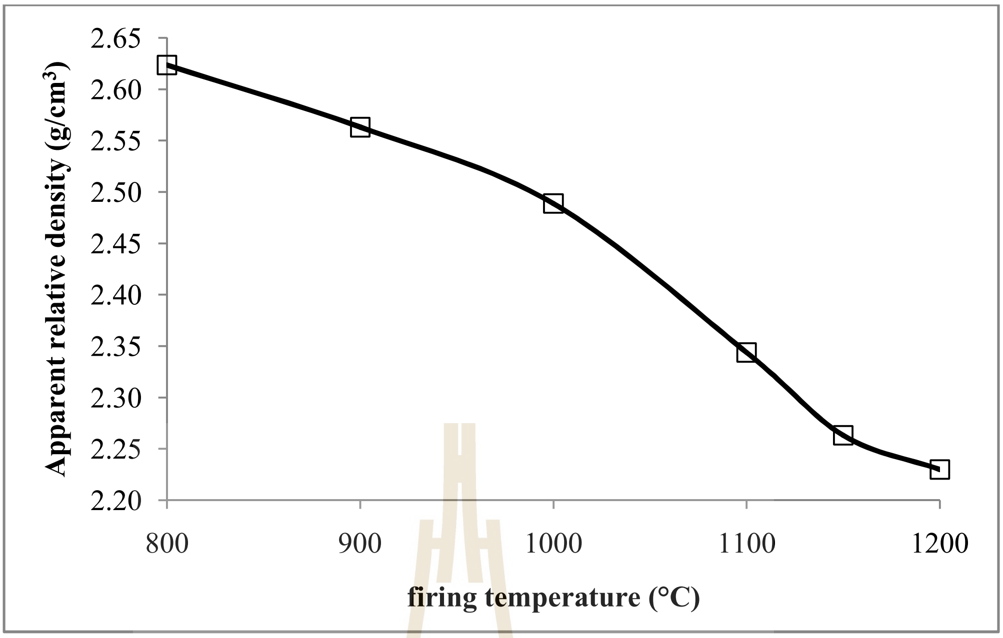

Figure 4.29 The apparent relative density of sample C3 versus the firing temperature

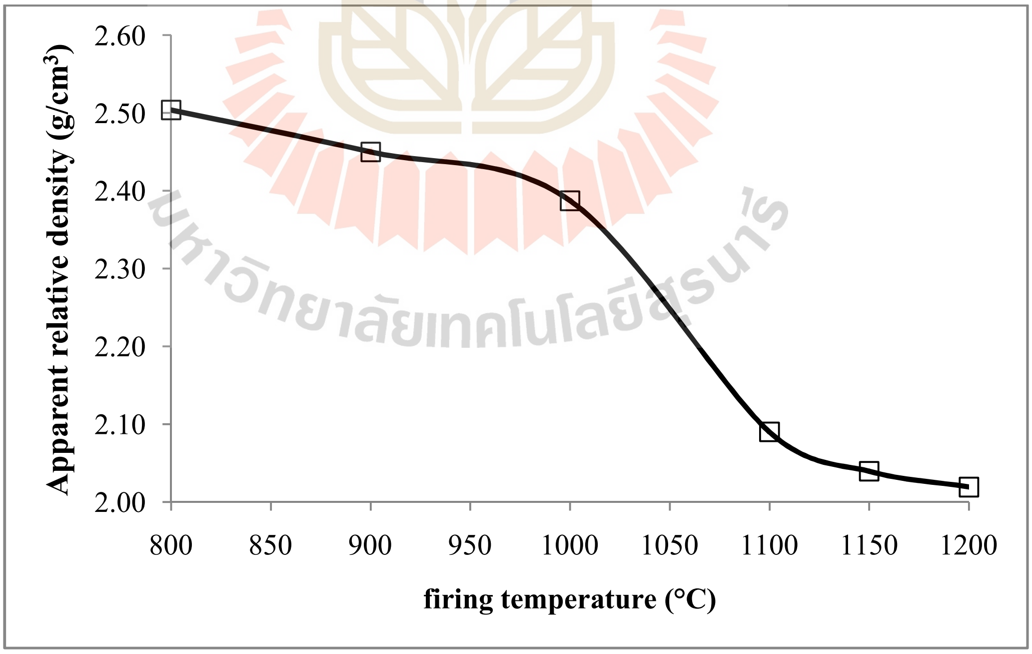

Figure 4.30 The apparent relative density of sample L versus the firing temperature

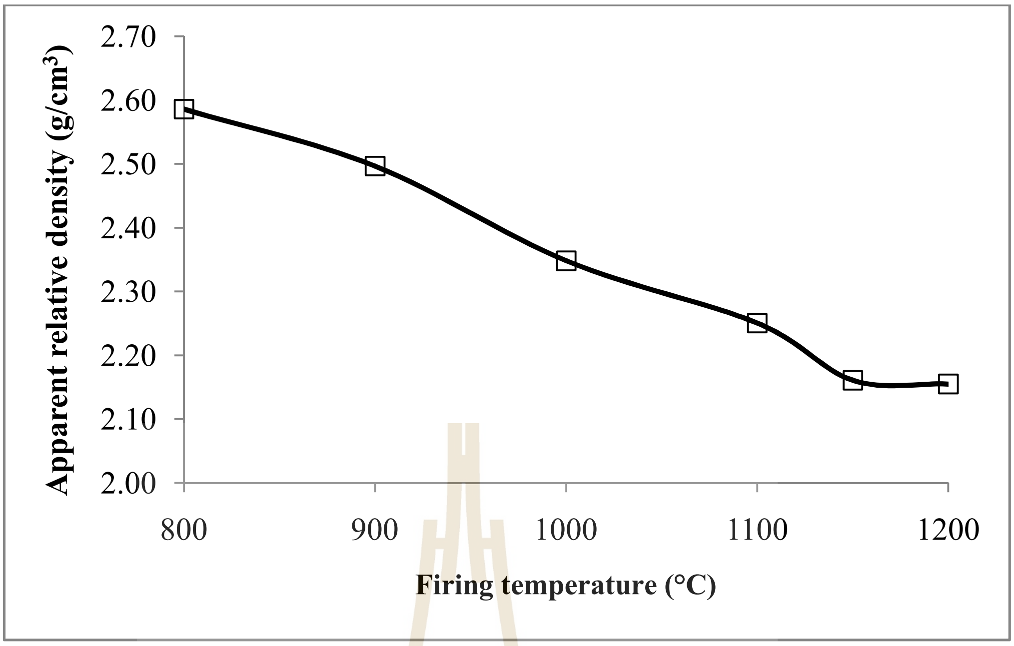

Figure 4.31 The apparent relative density of sample M versus the firing temperature

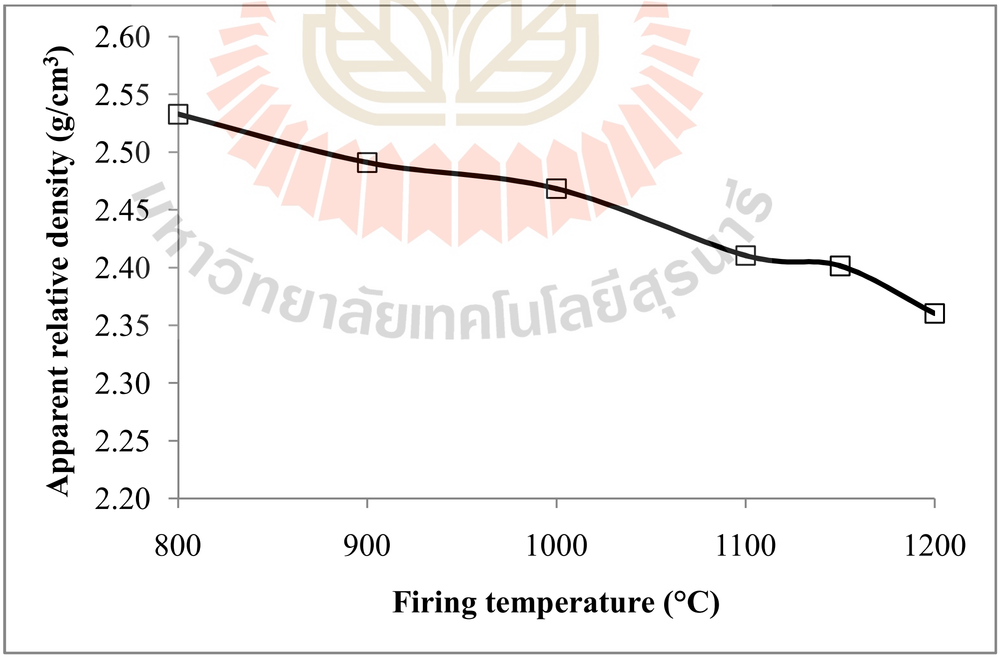

Figure 4.32 The apparent relative density of sample P_1 versus the firing temperature

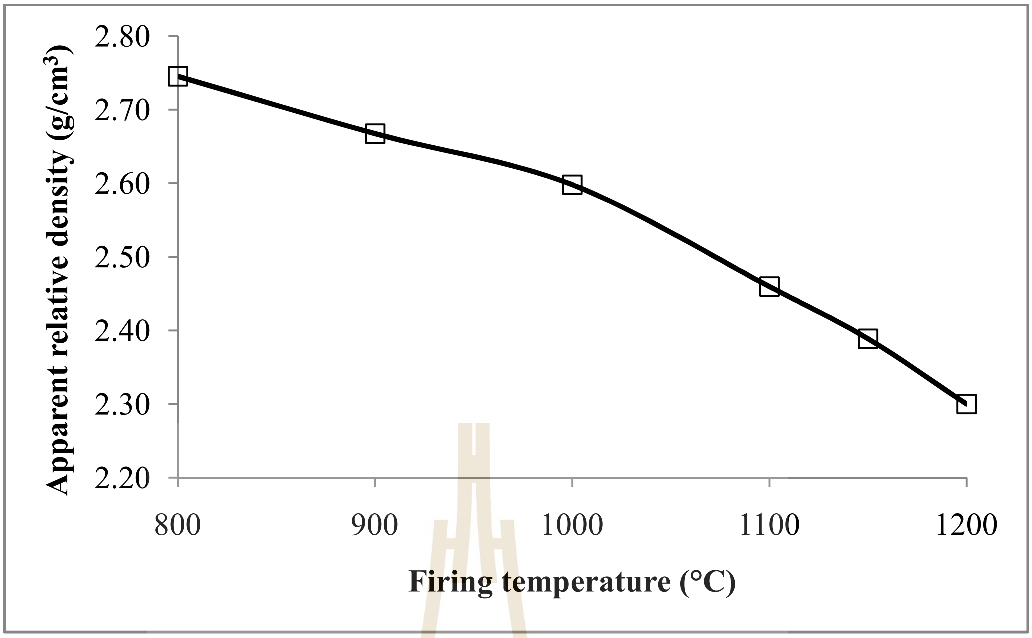

Figure 4.33 The apparent relative density of sample P_2 versus the firing temperature

4.4.5 Bulk density

The bulk density was determined only on the ceramic tile samples according to the TIS 2398-2553 part 3. The results of bulk density measurement of ceramic tile samples are shown in Table A30 to A36. The bulk density only of ceramic tile samples from various sources versus the firing temperature are plotted all together in Figure 4.34 and the bulk density of ceramic tile samples from each source are plotted versus firing temperature separately as shown in Figure 4.35 to 4.41, respectively.

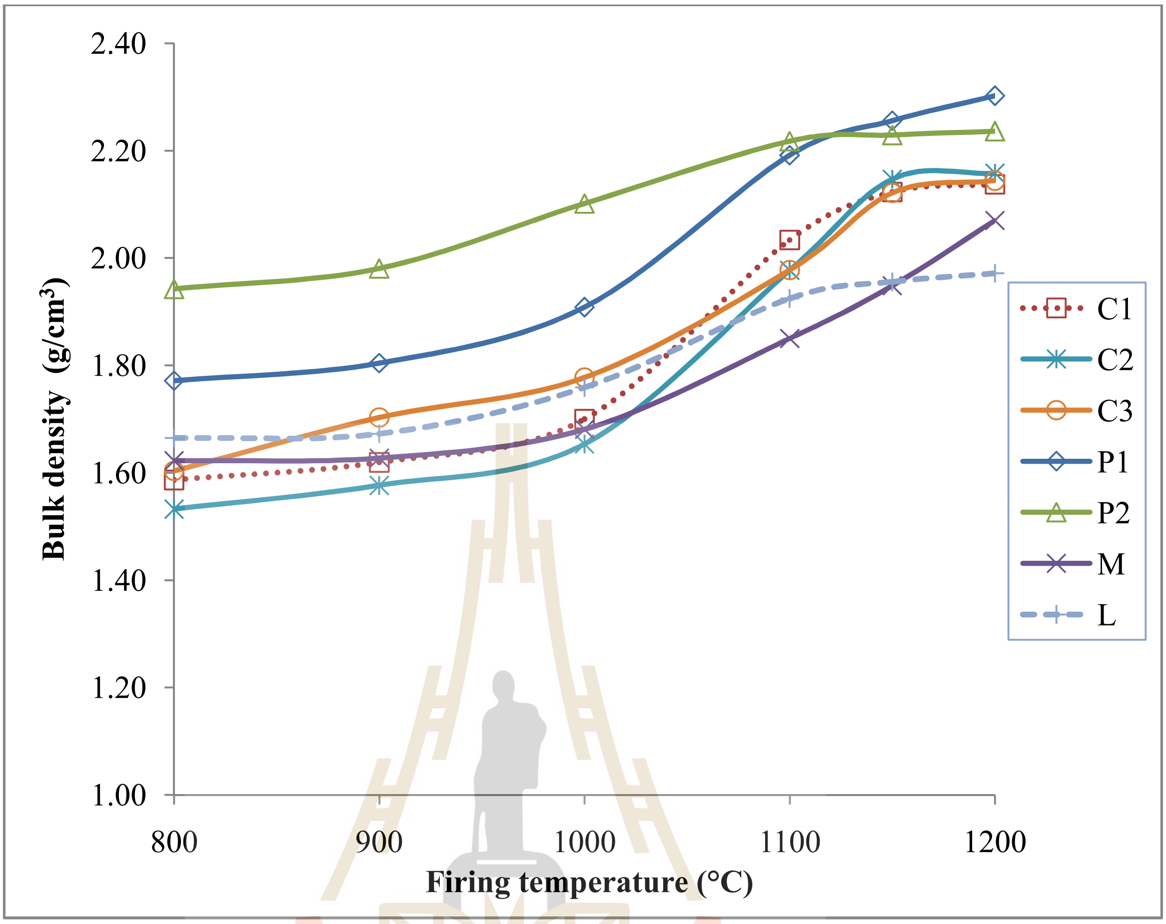

Figure 4.34 The bulk density of ceramic tile samples from various sources versus the firing temperature

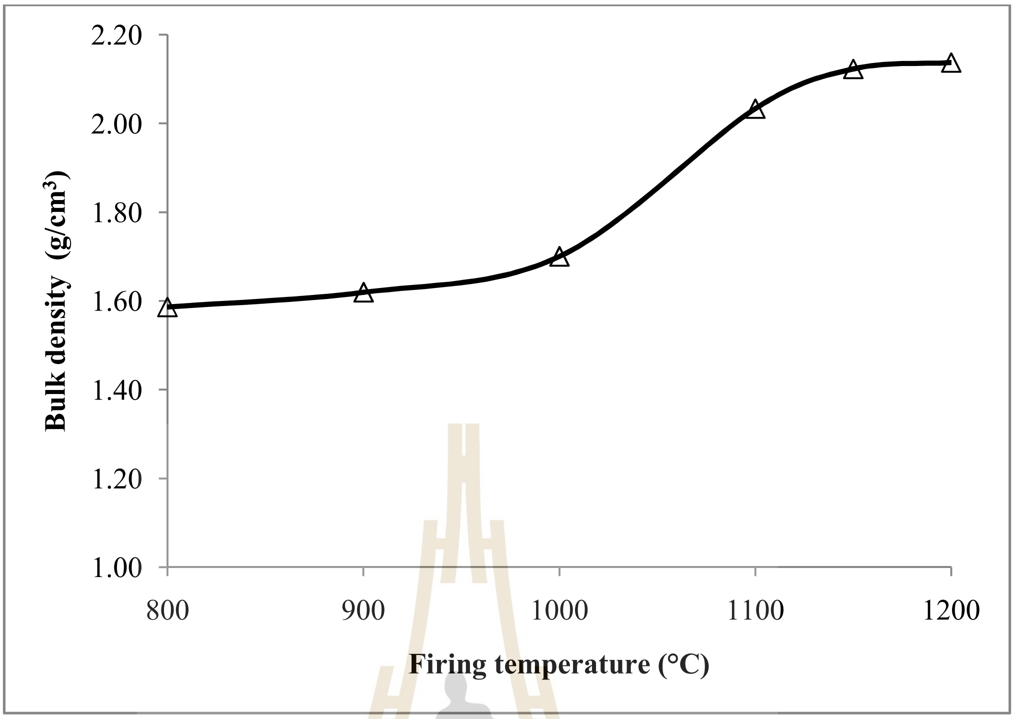

Figure 4.35 The bulk density of sample C_1 versus the firing temperature

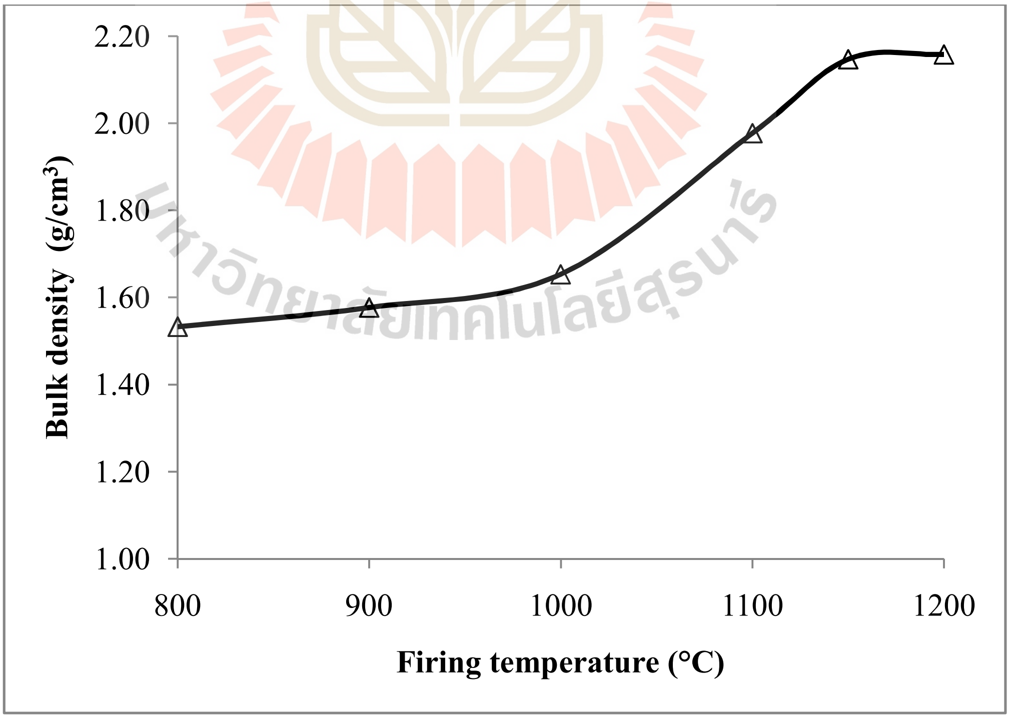

Figure 4.36 The bulk density of sample C_2 versus the firing temperature

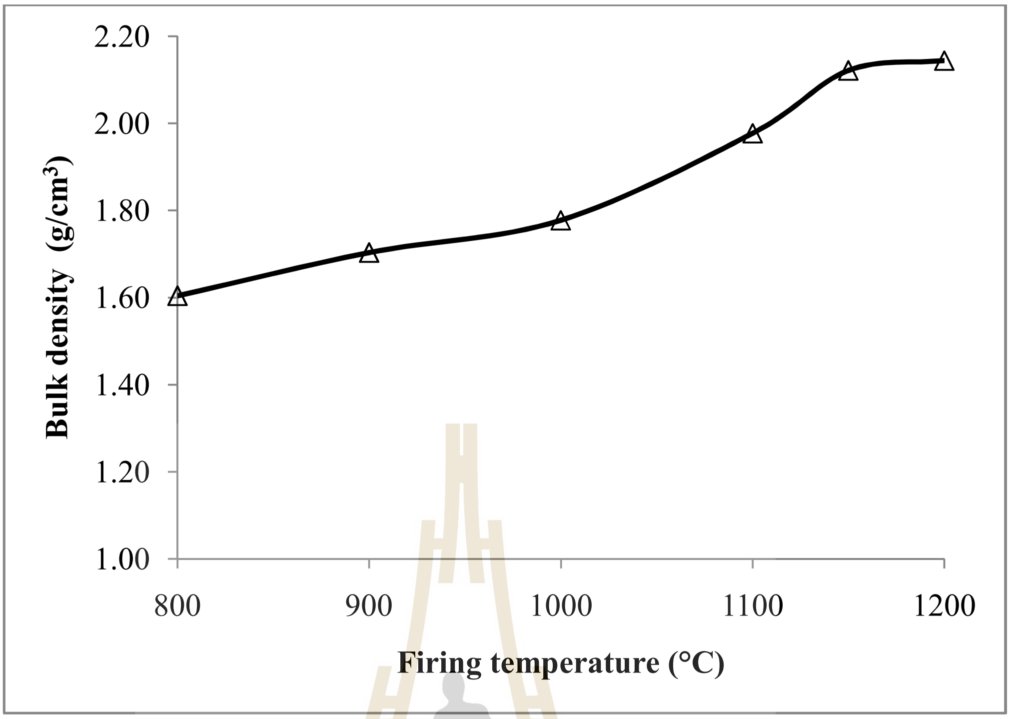

Figure 4.37 The bulk density of sample C_3 versus the firing temperature

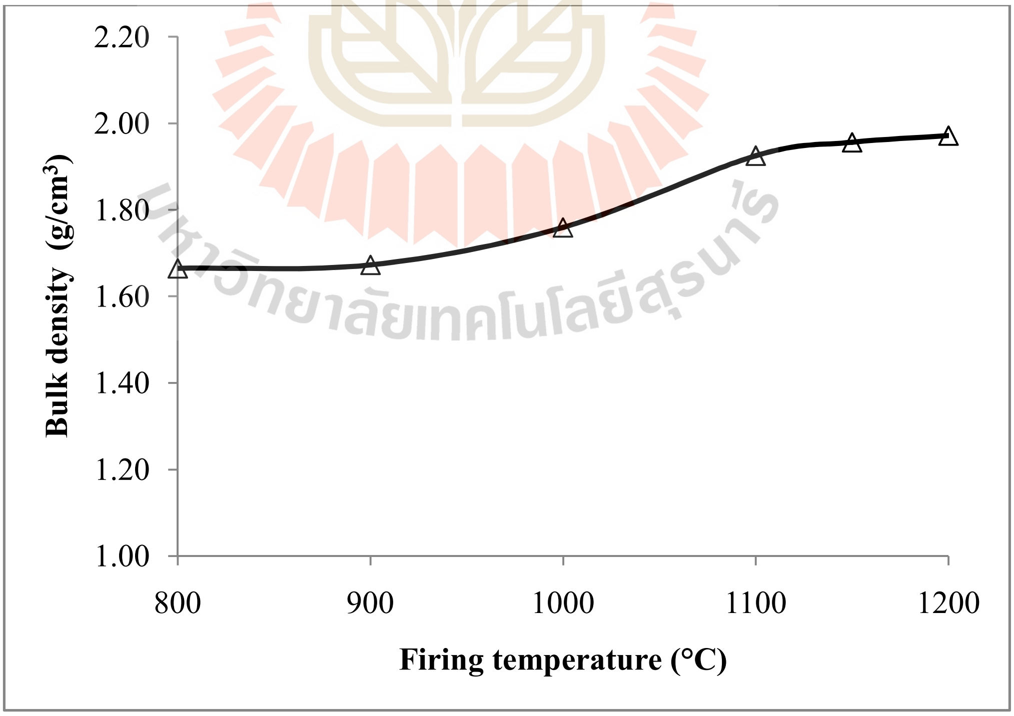

Figure 4.38 The bulk density of sample L versus the firing temperature

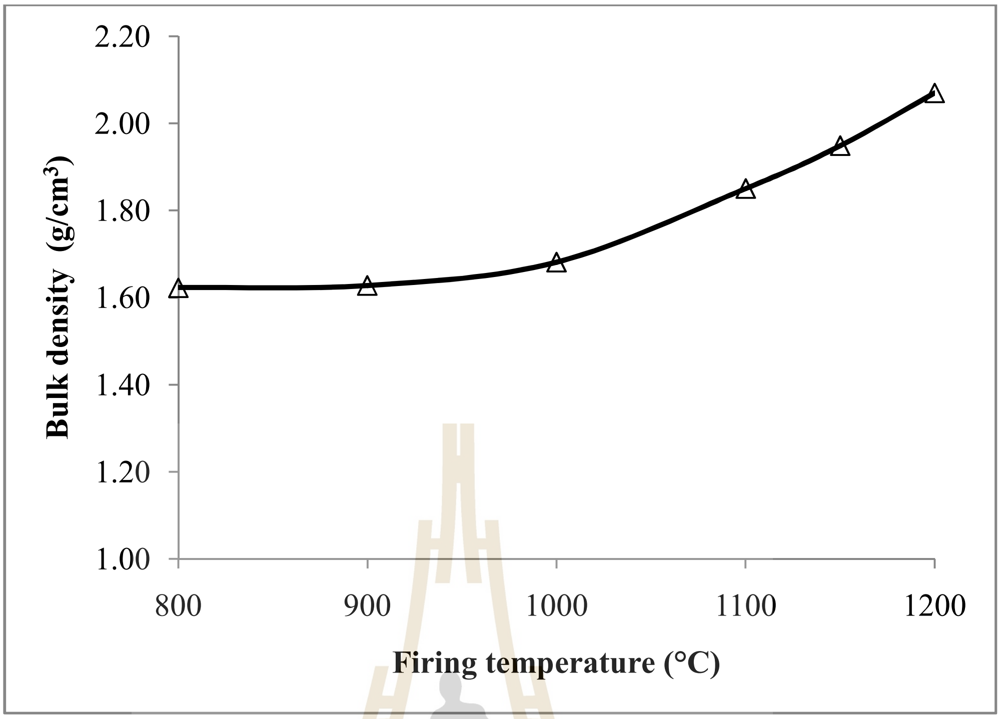

Figure 4.39 The bulk density of sample M versus the firing temperature

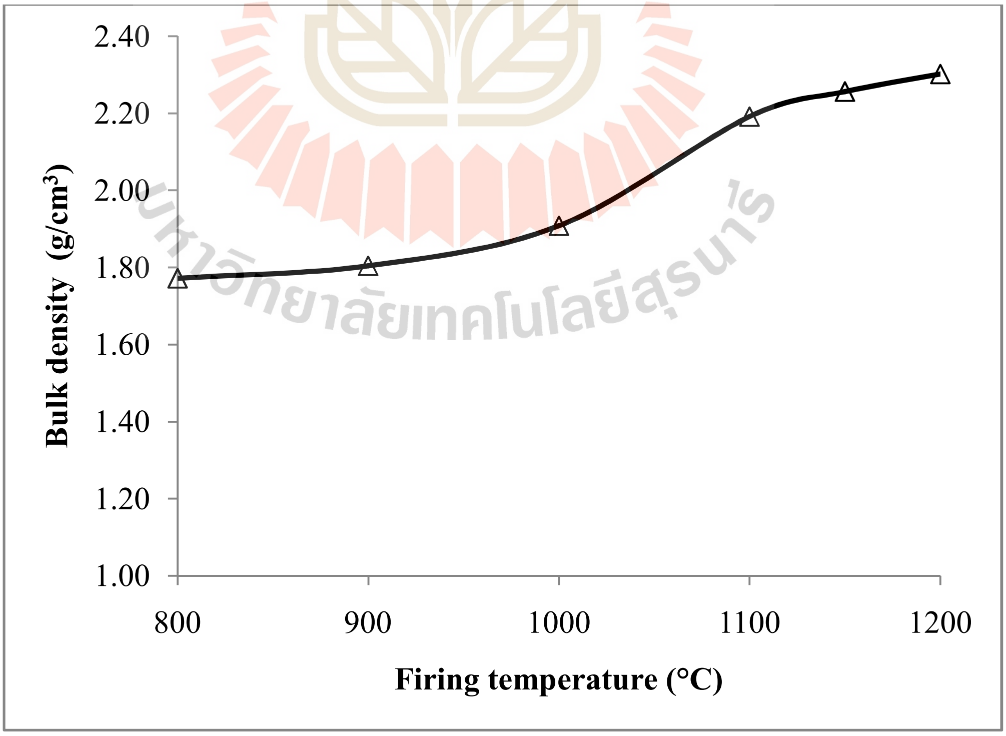

Figure 4.40 The bulk density of sample P_1 versus the firing temperature

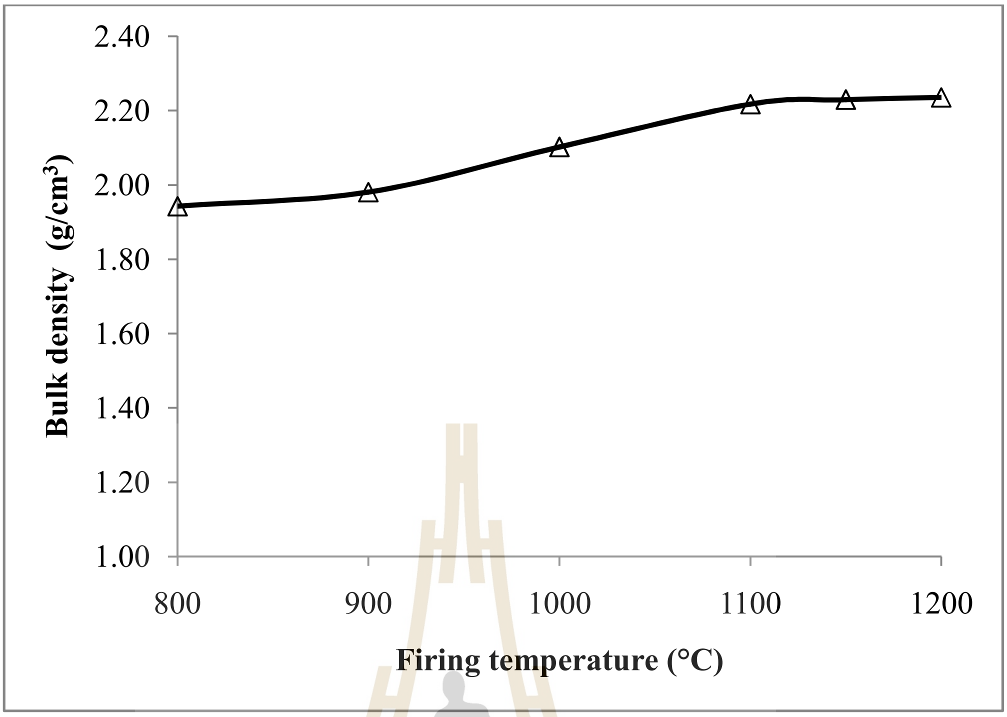

Figure 4.41 The bulk density of sample P_2 versus the firing temperature

. It was observed from the plots that the bulk density of ceramic tile samples increased when the firing temperatures increased.

4.4.6 Compressive strength

The compressive strength of ceramic tile and building brick samples were conducted according to TIS 2398-2553 Part 3and TIS 77-2545 standard, respectively. The compressive strength of ceramic tile samples made from drilling mud wastes of drill holes at Fang, Lampang, Mae Tha and Phitsanulok basin are presented in Table A37 to A42. The average compressive strength of ceramic tile samples from each source is plotted versus the firing temperature separately in Figure 4.42 to Figure 4.48, respectively.

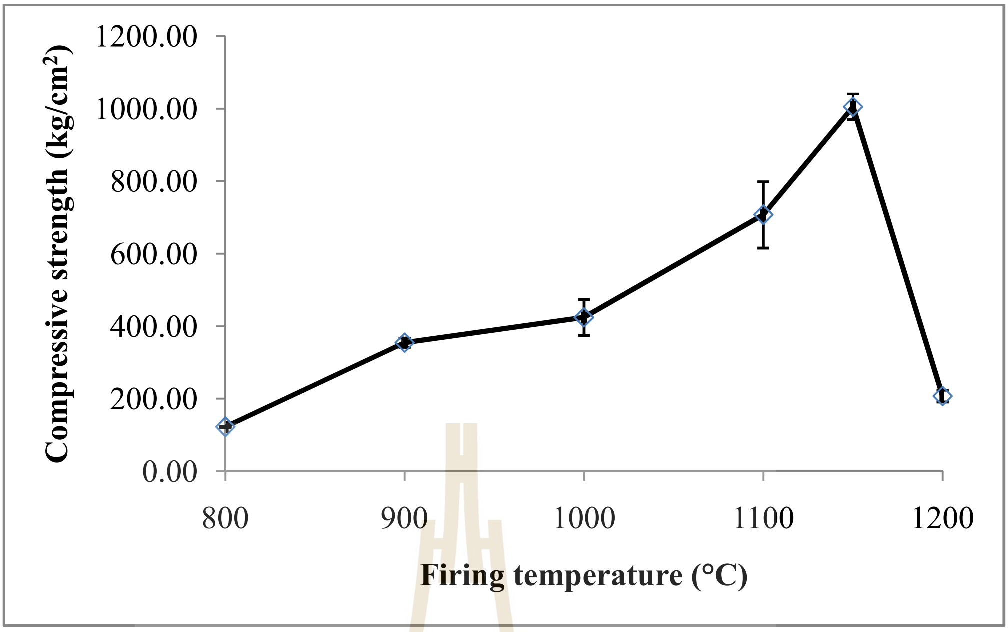

Figure 4.42 The average compressive strength of sample C_1 versus firing temperature

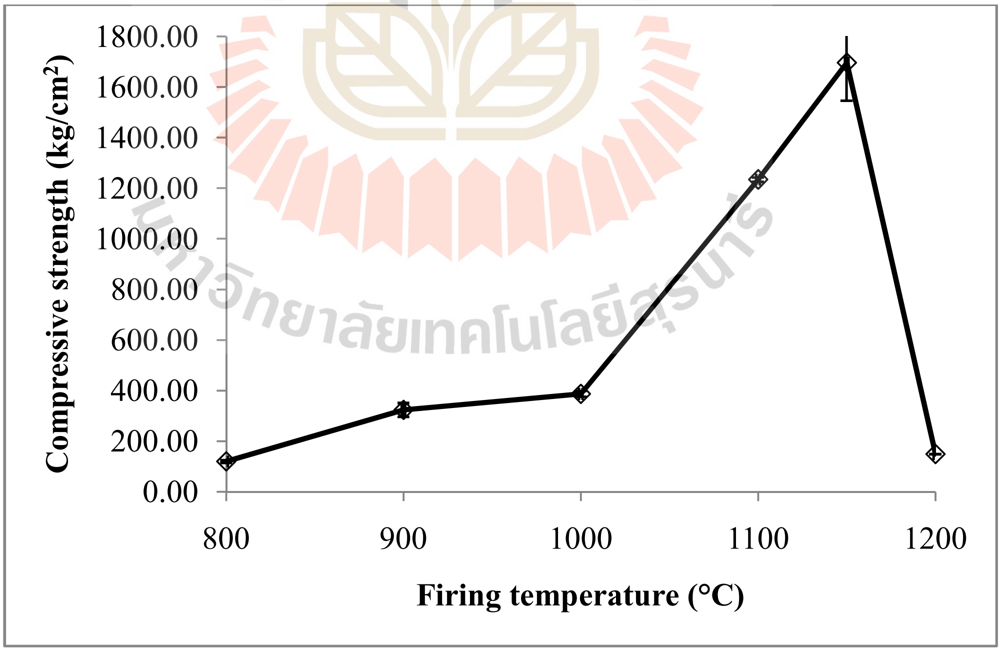

Figure 4.43 The average compressive strength of sample C_2 versus firing temperature

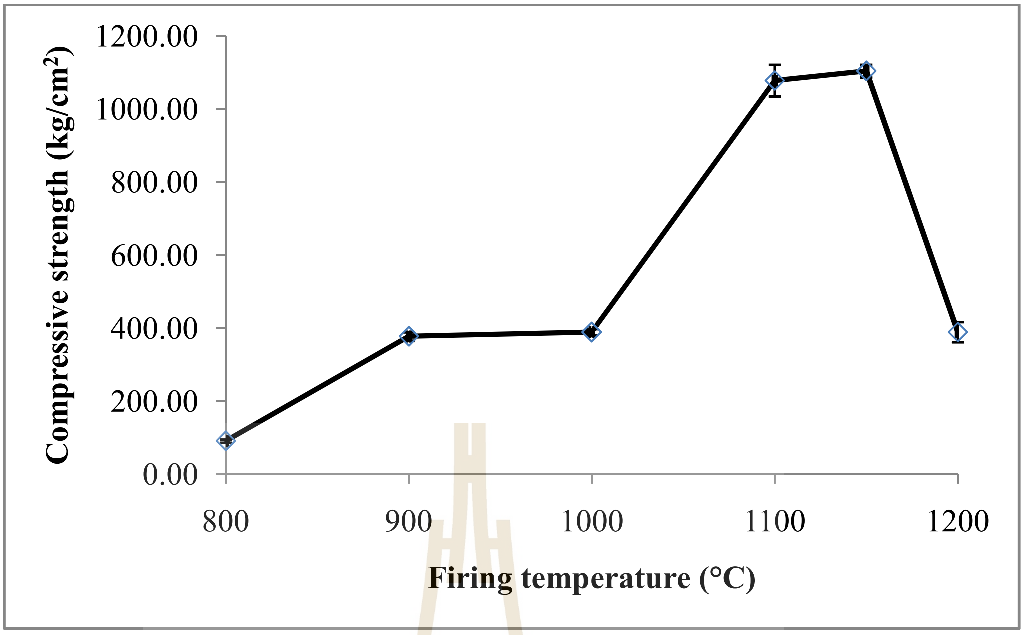

Figure 4.44 The average compressive strength of sample C_3 versus firing temperature

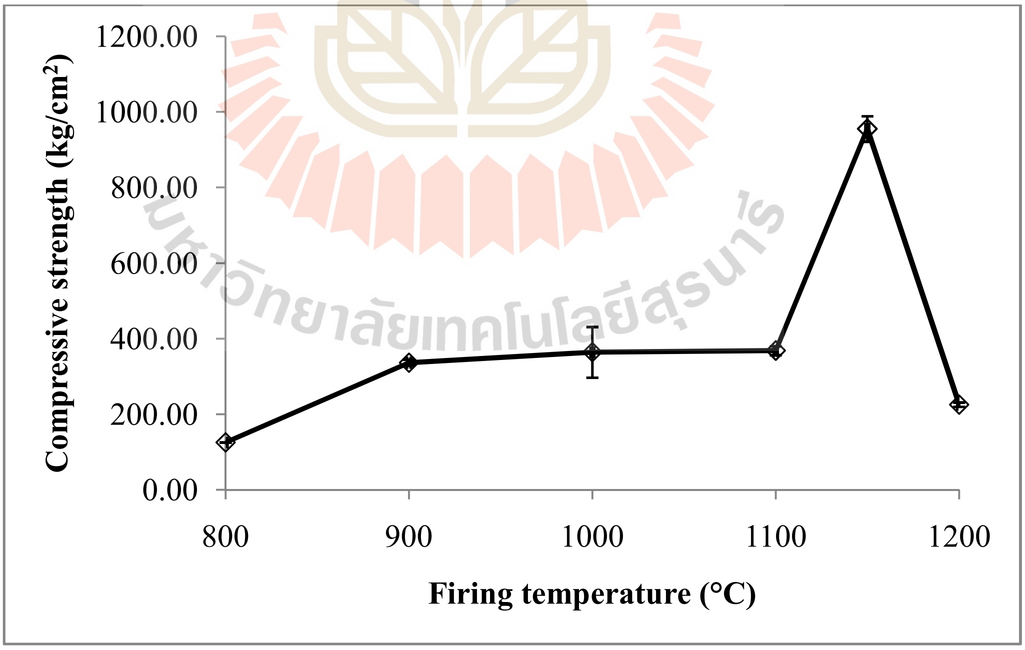

Figure 4.45 The average compressive strength of sample L versus firing temperature

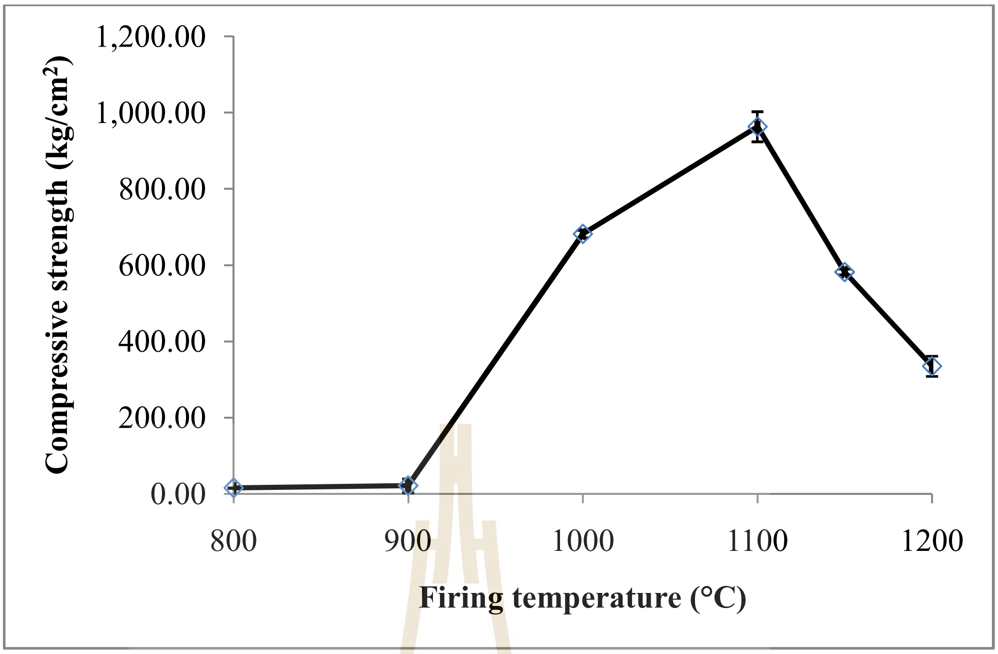

Figure 4.46 The average compressive strength of sample M versus firing temperature

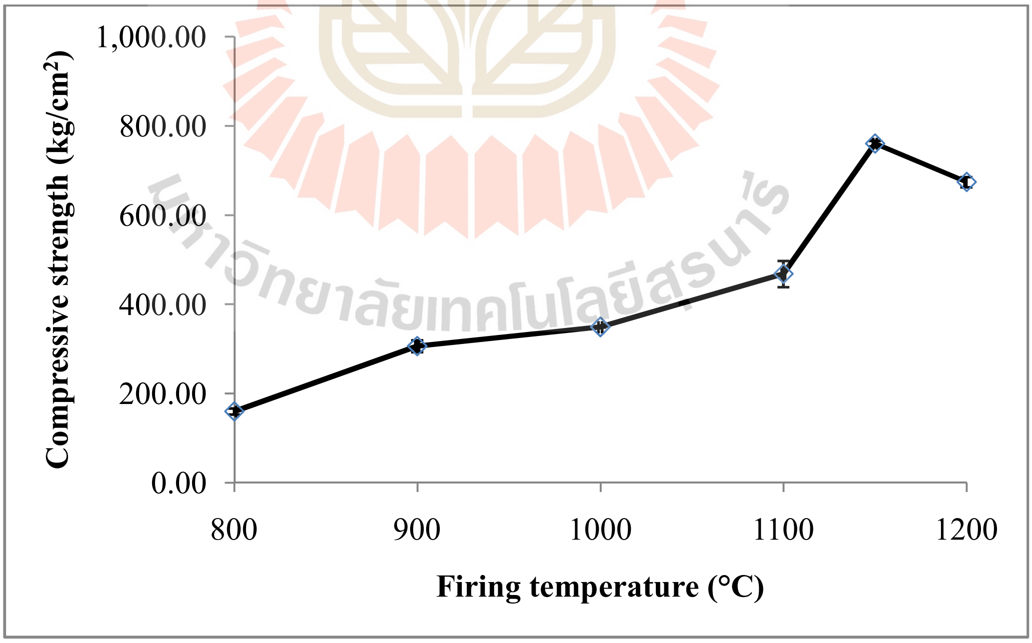

Figure 4.47 The average compressive strength of sample P_1 versus firing temperature

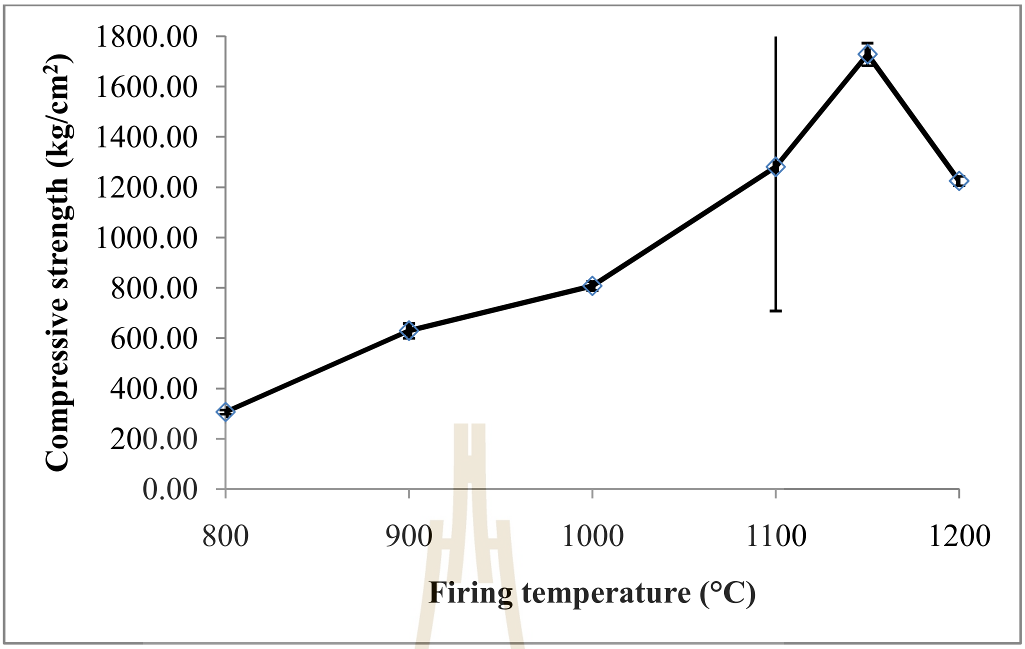

Figure 4.48 The average compressive strength of sample P_2 versus firing temperature

The compressive strength of almost drilling mud waste became higher with increasing the firing temperature. The highest compressive strength of samples was obtained when firing at 1,150°C. However, the compressive strength for all samples decreased after firing at 1,200°C. It indicated that all drilling mud waste were able to melt at 1,200°C due to the high content of fluxing mineral in waste.

In addition, the compressive strength measurement of building brick samples made of drilling mud waste only from a drill hole of Phitsanulok basin (P_1) was indicated that the average compressive strength of 5 building brick samples was 21.12 MPa or 215.33 kg/cm^2.

The high compressive strength of the ceramic tile and building brick samples may result from their high silica content which enhanced the strength property of ceramic tile after firing.

.

4.5 Ceramic tile and building brick classification

Ceramic tile classification

According to the TIS 2508-2555 standard and the water absorption measurement results, the ceramic tile samples made from water based drilling mud wastes fired from 800 to 1,000°C can be classified into Group BIII. Ceramic tile samples fired at 1,100°C can be classified into the Group BII_a except M and P_2 which are belong to the Group BII_b. However, all sample fired at 1,150 and 1,200 were classified into Group BI_b and can be used as a raw material for making the floor tile because they have the average minimum compressive strength more than 230 kg/cm^2.

Table 4.4 Classification of ceramic tile samples following with the water absorption percent

Sample	Firing temperature (°C)	Water absorption (%)	Group
C_1	800	22.495	BIII
	900	20.744	BIII
	1,000	16.396	BIII
	1,100	4.858	BII_a
	1,150	2.077	BI_b
	1,200	1.595	BI_b

Table 4.4 Classification of ceramic tile samples following with the water absorption percent (continued)

Sample	Firing temperature (°C)	Water absorption (%)	Group
C_2	800	23.218	BIII
	900	21.194	BIII
	1,000	16.869	BIII
	1,100	5.82	BII_a
	1,150	1.655	BI_b
	1,200	1.223	BI_b
C_3	800	24.231	BIII
	900	19.703	BIII
	1,000	16.072	BIII
	1,100	7.895	BII_b
	1,150	2.959	BI_b
	1,200	1.795	BI_b
P_1	800	16.963	BIII
	900	15.277	BIII
	1,000	11.89	BIII
	1,100	4.138	BII_a
	1,150	2.684	BI_b
	1,200	1.069	BI_b
P_2	800	15.044	BIII
	900	12.993	BIII
	1,000	9.084	BIII
	1,100	4.432	BII_a
	1,150	2.998	BI_b
	1,200	1.251	BI_b

Table 4.4 Classification of ceramic tile samples following with the water absorption percent (continued)

Sample	Firing temperature (°C)	Water absorption (%)	Group
L	800	20.125	BIII
	900	18.956	BIII
	1,000	14.953	BIII
	1,100	4.113	BII_a
	1,150	2.09	BI_b
	1,200	1.187	BI_b
M	800	22.957	BIII
	900	21.391	BIII
	1,000	16.899	BIII
	1,100	9.615	BII_b
	1,150	5.043	BII_a
	1,200	1.903	BI_b

Building brick classification

According to ASTM C67-11 and TIS.77-2545 standard, the brick samples made from water based drilling mud wastes in this study (P_1) fired at 1,000°C can be classified into Grade A brick. This is because after firing at 1,000°C, P_1 samples have the average water absorption of 12.98 percent and the average minimum compressive strength of 21 MPa or 215.33 kg/cm^2.

CHAPTER V

CONCLUSION AND RECOMMENDATIONS

5.1 Conclusions

The results of particle size distribution by particle size analysis, XRF and XRD analyses and some physical properties of ceramic tile and building bricksamples made from water based drilling mud wastes collected from petroleum drill holes of Fang, Lampang, Mae Tha and Phitsanulok basin which were tested according to the ISO 10545-3: 1995 (Ceramic Tiles - part 3), the TIS 2398 Part 3-2553, the ASTM C67-11 and the TIS 77-2545 standard can be summarized as follows.

5.1.1 Particle size analysis

The results from particle size analysis after sieving passed 200 mesh number revealed that samples from Fang Basin(C_1, C_2 and C_3) had the particle size larger than those of Lampang (L), Mae Tha (M) and Phitsanulok basin (P_1 and P_2). Themean particle size of sample C_1, C_2 and C_3 were 69.73, 66.30, and 67.70 µm, respectively. Whereas the mean size diameter of sample P_1,P_2, Land M were17.16, 6.42,16.32 and 32.68 µm, respectively.

5.1.2 Chemical analysis

The results from XRF and XRD analysis revealed that these drilling mud wastes were mainly composed of high quartz, kaolinite and some minor mineral including albite, calciteand barite.

5.1.3 Physical property testing

5.1.3.1 Shrinkage

The volume shrinkage percent after samplesfiring at various temperatures were decreased with the firing temperature increased. Thevolume shrinkage percent of sample C_3 was the highest, whereasthevolume shrinkage percent of sample M was thelowest when fired at the same temperature.

5.1.3.2 Ceramic Tile

The results of physical property measurement of the ceramic tile according to the ISO 10545-3: 1995 (Ceramic Tiles - Part 3) and the TIS 2398 Part 3-2553can be summarized in Table 5.1.

Table 5.1 Physical properties of ceramic tile samples made from water based drilling mud wastes collected from petroleum drill holes of Fang (sample C), Lampang (sample L), Mae Tha (sample M) and Phitsanulok basin (sample P)

Sample	Temp. (°C)	Water absorption (%)	Apparent porosity (%)	Apparent relative density (g/cm^3)	Bulk density (g/cm^3)	Compressive strength (kg/cm^2) avg. (±S.D.)
C_1	800	22.495	35.697	2.468	1.587	122.40 ± 1.94
	900	20.744	33.597	2.439	1.620	355.14 ± 12.56
	1,000	16.396	27.876	2.357	1.700	424.50 ± 49.32
	1,100	4.858	9.881	2.257	2.034	707.45 ± 91.57
	1,150	2.077	4.409	2.221	2.123	1005.47 ± 35.35
	1,200	1.595	3.409	2.213	2.138	207.69 ± 16.15

Table 5.1 Physical properties of ceramic tile samples made from water based drilling mud wastes collected from petroleum drill holes of Fang (sample C), Lampang (sample L), Mae Tha (sample M) and Phitsanulok basin (sample P) (Continued)

Sample	Temp. (°C)	Water absorption (%)	Apparent porosity (%)	Apparent relative density (g/cm^3)	Bulk density (g/cm^3)	Compressive strength (kg/cm^2) avg.(±S.D.)
C_2	800	23.218	35.584	2.379	1.533	119.67 ± 4.96
	900	21.194	33.415	2.368	1.577	323.545 ± 27.81
	1,000	16.869	27.896	2.294	1.654	387.19 ± 11.10
	1,100	5.82	11.509	2.235	1.977	1234.03 ± 8.36
	1,150	1.655	3.553	2.226	2.147	1696.96 ± 150.87
	1,200	1.223	2.641	2.217	2.158	149.07 ± 0.67
C_3	800	24.231	38.865	2.624	1.604	91.14 ± 4.51
	900	19.703	33.555	2.563	1.703	377.66 ± 11.89
	1,000	16.072	28.571	2.489	1.778	389.27 ± 8.77
	1,100	7.895	15.615	2.344	1.978	1078.40 ± 43.09
	1,150	2.959	6.276	2.263	2.121	1104.30 ± 17.16
	1,200	1.795	3.849	2.23	2.144	389.59 ± 27.50
P_1	800	16.963	30.053	2.533	1.772	160.05 ± 6.94
	900	15.277	27.565	2.491	1.804	306.52 ± 12.94
	1,000	11.89	22.691	2.468	1.908	349.03 ± 0.47
	1,100	4.138	9.07	2.41	2.192	468.50 ± 29.45
	1,150	2.684	6.055	2.401	2.256	760.77 ± 6.53
	1,200	1.069	2.46	2.36	2.302	674.40 ± 11.45
P_2	800	15.044	37.253	2.745	1.943	306.33 ± 8.30
	900	12.993	34.814	2.668	1.981	629.10 ± 29.51
	1,000	9.084	28.408	2.598	2.102	807.49 ± 17.88
	1,100	4.432	17.789	2.46	2.218	1280.75 ± 572.52
	1,150	2.998	9.826	2.389	2.229	1728.452 ± 44.88
	1,200	1.251	3.939	2.3	2.236	1224.96 ± 18.68

Table 5.1 Physical properties of ceramic tile samples made from water based drilling mud wastes collected from petroleum drill holes of Fang (sample C), Lampang (sample L), Mae Tha (sample M) and Phitsanulok basin (sample P) (Continued)

Sample	**Temp. (°C)**	**Water absorption (%)**	**Apparent porosity (%)**	**Apparent relative density (g/cm^3)**	**Bulk density (g/cm^3)**	**Compressive strength (kg/cm^2) avg.(±S.D.)**
L	800	20.125	33.506	2.504	1.665	125.22 ± 0.09
	900	18.956	31.714	2.45	1.673	336.60 ± 8.17
	1,000	14.953	26.305	2.387	1.759	364.17 ± 67.00
	1,100	4.113	7.917	2.09	1.925	368.21 ± 11.51
	1,150	2.09	4.088	2.039	1.956	955.11 ± 33.56
	1,200	1.187	2.341	2.019	1.972	225.52 ± 5.76
M	800	22.957	29.228	2.586	1.623	15.25 ± 0.71
	900	21.391	25.74	2.497	1.628	21.19 ± 18.23
	1,000	16.899	19.094	2.348	1.681	681.83 ± 9.68
	1,100	9.615	9.829	2.251	1.85	963.27 ± 39.43
	1,150	5.043	6.684	2.161	1.949	582.21 ± 7.82
	1,200	1.903	2.797	2.155	2.07	334.78 ± 26.38

It can be observed from Table 5.1 that the compressive strength of all samples fired at temperature range from 800 to 1,150°C increases with the firing temperature increases. However, the compressive strength of samples fired at 1,200°C had been decreased due to the phase changingand became melting after firing at the temperature higher than 1,200°C.

Therefore, it can be concluded that ceramic tile samples made from water based drilling mud waste collected from all tested sites can be used as a raw material for ceramic tile making. However, water based drilling mud waste collected from Phitsanulok and Fang basin are considered to be the best raw material. This is because their ceramic tile samples show the lowest water absorption percent and the highest compressive strength property comparing to samples from other siteswhen fired at the same temperature.

5.1.3.3 Building brick

Building brick samples made from water based drilling mud waste collected only from petroleum drill holes of Phitsanulok basin (P_1) were conducted the water absorption and compressive strength measurement according to the ASTM C67-11 and the TIS 77-2545.The results of the tests are shown in Table 5.2.

Table 5.2 Average water absorption percent and average compressive strength of building brick samples made from water based drilling mud wastes collected from petroleum drill holes of Phitsanulok basin (P_1)fired at 1,000°C

Water absorption (Percent)	Compressive strength	
	(kg_f/cm^2)	MPa
12.98	215.33	21.12

The high compressive strength of the building brick samples (P_1) may be resulted from its high silica content (54.96 wt.%). It also showed slightly low water absorption percent. This low water absorption percent can indicate the low permeability character of the brick sample, which is resulted from its high kaolinite and clay mineral content as well.

5.1.4 Ceramic tile and building brick classification

5.1.4.1 Ceramic tile classification

According to the TIS 2508-2555, the ceramic tile samples made from water based drilling mud wastes fired from 800 to 1,000°C can be classified into Group BIII due to their water absorption are more than 10 percent. These samples could be used as a raw material for making the wall tile and floor tile because they have the average minimum compressive strength more than 230 and 350 kg/cm^2, respectively. Sample C_1, C_2, L, P_1 and P_2 fired at 1,100°C can be classified into Group BII_a because their water absorption are less than 6 percent, except M and P_2 which are belong to Group BII_b. However, samples fired at 1,150 and 1200 °C can be classified into group BI_b and can be used as a raw material for making the floor tile because they have the average compressive strength more than 350 kg/cm^2.

5.1.4.2 Building brick classification

According to ASTM C67-11 and TIS.77-2545 the brick samples made from water based drilling mud wastes from Phitsanulok basin (P_1) can be classified into Grade A brick.This is because they havethe average minimum compressive strength more than 21 MPa or 215.33 kg/cm^{2}and the average water absorption of 12.98 percent.

5.2 Recommendations

Although this study reported that the water based drilling mud waste could be used as a raw material for ceramic tile and building brick making, some control factors needed to define and control in the future, such as; 1) sites and place to collect drilling mud waste should be the same for all samples at any the drilling rig site, 2) some additive, e.g. rice husk ash, should be mixed with the drilling mud waste and tested the compressive strength and water absorption of the tile and brick samples before and after mixing the additive.

REFERENCES

ชาญ จรรยาวนิชย์. (2536). **การอบแห้งผลิตภัณฑ์เซรามิกส์**.เอกสารการสัมมนาวิชาการเซรามิกส์เพื่อภาคอุตสาหกรรม. บริษัทเคลย์แอนด์ มิเนอร์รัลส์ (ประเทศไทย) จำกัด รังสิต ประทุมธานี.

ธนวัชโพคะรัตน์ศิริ.(2554). **เอกสารประกอบการสอน CE 311 Structural Materials and Testing.** ภาควิชาวิศวกรรมโยธา คณะวิศวกรรมศาสตร์มหาวิทยาลัยเชียงใหม่.

ปรีดาพิมพ์ขาวขำ.(2539).**เซรามิกซ์.** (พิมพ์ครั้งที่4). กรุงเทพฯ:โรงพิมพ์แห่งจุฬาลงกรณ์มหาวิทยาลัย.

สุธรรม ศรีหล่มสัก(2543).**เอกสารประกอบการสอนวิชา 506303 Drying and Firing(Drying of Ceramics).**สาขาวิชาวิศวกรรมเซรามิก สำนักวิชาวิศวกรรมศาสตร์มหาวิทยาลัยเทคโนโลยีสุรนารี. (สงวนลิขสิทธิ์).

อายุวัฒน์ สว่างผล.(2543).**วัตถุดิบที่ใช้แพร่หลายในงานเซรมิกส์ (Raw Materials of Ceramaics).** กรุงเทพฯ : โอเดียนสโตร์.

Darley H.C.H. and Gray G.R. (1988). **Composition and Properties of Drilling and Completion Fluids, Fifth Edition**. Gulf Publishing Company, HoustonTX.

Delmar H. Larsen.(1996). **USE OF CLAY IN DRILLING FLUIDS.** [On-line].Available: http://web.pdx.edu/~pmoeck/phy381/Topic5a-XRD.pdf

Medhat S. E. and Tarek A.O.(2010). **Influence of Oil WellDrilling Waste on the Engineering Characteristics of Clay Bricks: Journal of American Science.**[On- line].Available**:** http://www.jofamericanscience.org/journal/am-sci/am0

607/06_2749_am0607_48_54.pdf.

Mian M.A.(1992)**. Petroleum Engineering Handbook For The Practicing Engineer, VolII**.PennWell Publishing, TulasOklahom.

OrolinovaZ.,Mockovciakova A., Dolinska S. andBriancinJ. (2012).**Effect of thermal treatment on the bentonite properties**. [On-line].Available:http://www.arhivzatehnickenauke.com/files/arhiv7/uticaj_termicke_obrade_na_betonitska_svojstva.pdf(Access date : 14 June 2013)

Pollution Control Department, Ministry of natural resources and environment Thailand.(2004).**Soil quality standard.** [On-line].Available://www.pcd.go.th/info_serv/reg_std_airsnd03.html

Scott A S.(2012).**Introduction to X-Ray Powder Diffraction DataAnalysis.**Center for Materials Science and Engineering at MIT. [On-line].Available: http://prism.mit.edu/xray (Access date : 12June 2013)

SouzaA.J., PinheiroB.C.A. and HolandaJ.NF.(2013).**Sintering Behavior ofVitrified Ceramic Tiles Incorporated with Petroleum Waste.** [On-Line]. Available:http://dx.doi.org/10.5772/53256http://cdn.intechopen.com/pdfs/42534/InTechSintering_behavior_of_vitrified_ceramic_tiles_incorporated_with_petroleum_waste.pdf.(Access date : 15 June 2013)

APPENDIX A

EXPERIMENTAL DATA

Parameters for all tested classification of ceramic tiles sample

Table G.1 — Requirements for dry-pressed ceramic tiles with low water absorption Group BI_a, $E \leq 0,5$ %

Dimensions and surface quality	Surface S of the product (cm²)				Test
	$S \leq 90$	$90 < S \leq 190$	$190 < S \leq 410$	$S > 410$	
Length and width The manufacturer shall choose the work size as follows: a) for modular tiles in order to allow a nominal joint width of between 2 mm and 5 mm[1)]; b) for non-modular tiles so that the difference between the work size and the nominal size is not more than ± 2 % (max. ± 5 mm). The deviation, in percent, of the average size for each tile (2 or 4 sides) from the work size (W).	± 1,2 %	± 1,0 %	± 0,75 %	± 0,6 %	ISO 10545-2
The deviation, in percent, of the average size for each tile (2 or 4 sides) from the average size of the 10 test specimens (20 or 40 sides).	± 0,75 %	± 0,5 %	± 0,5 %	± 0,5 %	ISO 10545-2
Thickness					
a) The thickness shall be specified by the manufacturer.					
b) The deviation, in percent, of the average thickness of each tile from the work size thickness.	± 10 %	± 10 %	± 5 %	± 5 %	ISO 10545-2
Straightness of sides [2)] (facial sides)					
The maximum deviation from straightness, in percent, related to the corresponding work sizes.	± 0,75 %	± 0,5 %	± 0,5 %	± 0,5 %	ISO 10545-2

Figure A1 Classification of ceramic tiles with respect to water absorption and shape

Table G.1 *(continued)*

Dimensions and surface quality	Surface S of the product (cm^2)				Test
	$S \leq 90$	$90 < S \leq 190$	$190 < S \leq 410$	$S > 410$	
Rectangularity [2]					
The maximum deviation from rectangularity, in percent, related to the corresponding work sizes.	± 1,0 %	± 0,6 %	± 0,6 %	± 0,6 %	ISO 10545-2
Surface flatness					
The maximum deviation from flatness, in percent: a) centre curvature, related to diagonal calculated from the work sizes,	± 1,0 %	± 0,5 %	± 0,5 %	± 0,5 %	ISO 10545-2
b) edge curvature, related to the corresponding work sizes;	± 1,0 %	± 0,5 %	± 0,5 %	± 0,5 %	ISO 10545-2
c) warpage, related to diagonal calculated from the work sizes.	± 1,0 %	± 0,5 %	± 0,5 %	± 0,5 %	ISO 10545-2
Surface quality [3]	A minimum of 95 % of the tiles shall be free from visible defects that would impair the appearance of a major area of tiles				ISO 10545-2
Physical properties	**Requirements**				**Test**
Water absorption Percent by mass [8]	≤ 0,5 % Individual maximum 0,6 %				ISO 10545-3
Breaking strength, in N					
a) Thickness ≥ 7,5 mm	Not less than 1 300				ISO 10545-4
b) Thickness < 7,5 mm	Not less than 700				ISO 10545-4
Modulus of rupture, in N/mm^2 Not applicable to tiles with breaking strength ≥ 3 000 N.	Minimum 35 Individual minimum 32				ISO 10545-4
Abrasion resistance					
a) Resistance to deep abrasion of unglazed tiles: removed volume, in cubic millimetres.	Maximum 175				ISO 10545-6
b) Resistance to surface abrasion of glazed tiles intended for use on floors [4].	Report abrasion class and cycles passed				ISO 10545-7
Coefficient of linear thermal expansion [5]					
From ambient temperature to 100 °C.	Test method available				ISO 10545-8
Thermal shock resistance [5]	Test method available				ISO 10545-9
Crazing resistance: glazed tiles [6]	Required				ISO 10545-11
Frost resistance	Required				ISO 10545-12
Coefficient of friction					
Tiles intended for use on floors.	Manufacturer to state value and test method used				ISO 10545-17

Figure A2 Classification of ceramic tiles with respect to water absorption and shape

Table H.1 — Requirements for dry-pressed ceramic tiles with low water absorption Group BI_b, 0,5 % < E ≤ 3 %

Dimensions and surface quality	Surface S of the product (cm²)				Test
	$S \leq 90$	$90 < S \leq 190$	$190 < S \leq 410$	$S > 410$	
Length and width					
The manufacturer shall choose the work size as follows: a) for modular tiles in order to allow a nominal joint width of between 2 mm and 5 mm[1]; b) for non-modular tiles so that the difference between the work size and the nominal size is not more than ± 2 % (max. ± 5 mm). The deviation, in percent, of the average size for each tile (2 or 4 sides) from the work size (W).	± 1,2 %	± 1,0 %	± 0,75 %	± 0,6 %	ISO 10545-2
The deviation, in percent, of the average size for each tile (2 or 4 sides) from the average size of the 10 test specimens (20 or 40 sides).	± 0,75 %	± 0,5 %	± 0,5 %	± 0,5 %	ISO 10545-2
Thickness					
a) The thickness shall be specified by the manufacturer.					
b) The deviation, in percent, of the average thickness of each tile from the work size thickness.	± 10 %	± 10 %	± 5 %	± 5 %	ISO 10545-2
Straightness of sides [2] (facial sides)					
The maximum deviation from straightness, in percent, related to the corresponding work sizes.	± 0,75 %	± 0,5 %	± 0,5 %	± 0,5 %	ISO 10545-2

Figure A3 Classification of ceramic tiles with respect to water absorption and shape

Table H.1 *(continued)*

Dimensions and surface quality	Surface S of the product (cm^2)				Test
	$S \leqslant 90$	$90 < S \leqslant 190$	$190 < S \leqslant 410$	$S > 410$	
Rectangularity 2)					
The maximum deviation from rectangularity, in percent, related to the corresponding work sizes.	± 1,0 %	± 0,6 %	± 0,6 %	± 0,6 %	ISO 10545-2
Surface flatness					
The maximum deviation from flatness, in percent:					
a) centre curvature, related to diagonal calculated from the work sizes;	± 1,0 %	± 0,5 %	± 0,5 %	± 0,5 %	ISO 10545-2
b) edge curvature, related to the corresponding work sizes;	± 1,0 %	± 0,5 %	± 0,5 %	± 0,5 %	ISO 10545-2
c) warpage, related to diagonal calculated from the work sizes.	± 1,0 %	± 0,5 %	± 0,5 %	± 0,5 %	ISO 10545-2
Surface quality 3)	A minimum of 95 % of the tiles shall be free from visible defects that would impair the appearance of a major area of tiles				ISO 10545-2

Physical properties	Requirements	Test
Water absorption Percent by mass 8)	$0,5\ \% < E \leqslant 3\ \%$ Individual maximum 3,3 %	ISO 10545-3
Breaking strength, in N		
a) Thickness $\geqslant$ 7,5 mm	Not less than 1 100	ISO 10545-4
b) Thickness < 7,5 mm	Not less than 700	ISO 10545-4
Modulus of rupture, in N/mm^2 Not applicable to tiles with breaking strength $\geqslant$ 3 000 N.	Minimum 30 Individual minimum 27	ISO 10545-4
Abrasion resistance		
a) Resistance to deep abrasion of unglazed tiles: removed volume, in cubic millimetres.	Maximum 175	ISO 10545-6
b) Resistance to surface abrasion of glazed tiles intended for use on floors 4).	Report abrasion class and cycles passed	ISO 10545-7
Coefficient of linear thermal expansion 5)		
From ambient temperature to 100 °C.	Test method available	ISO 10545-8
Thermal shock resistance 5)	Test method available	ISO 10545-9
Crazing resistance: glazed tiles 6)	Required	ISO 10545-11
Frost resistance	Required	ISO 10545-12
Coefficient of friction		
Tiles intended for use on floors.	Manufacturer to state value and test method used	ISO 10545-17

Figure A4 Classification of ceramic tiles with respect to water absorption and shape

Table J.1 — Requirements for dry-pressed ceramic tiles, Group BII_a, 3 % < E ≤ 6 %

Dimensions and surface quality	Surface S of the product (cm²)				Test
	S ≤ 90	90 < S ≤ 190	190 < S ≤ 410	S > 410	
Length and width The manufacturer shall choose the work size as follows: a) for modular tiles in order to allow a nominal joint width of between 2 mm and 5 mm [1)]; b) for non-modular tiles so that the difference between the work size and the nominal size is not more than ± 2 % (max. ± 5 mm). The deviation, in percent, of the average size for each tile (2 or 4 sides) from the work size (W).	± 1,2 %	± 1,0 %	± 0,75 %	± 0,6 %	ISO 10545-2
The deviation, in percent, of the average size for each tile (2 or 4 sides) from the average size of the 10 test specimens (20 or 40 sides).	± 0,75 %	± 0,5 %	± 0,5 %	± 0,5 %	ISO 10545-2
Thickness					
a) The thickness shall be specified by the manufacturer.					
b) The deviation, in percent, of the average thickness of each tile from the work size thickness.	± 10 %	± 10 %	± 5 %	± 5 %	ISO 10545-2
Straightness of sides [2)] (facial sides)					
The maximum deviation from straightness, in percent, related to the corresponding work sizes.	± 0,75 %	± 0,5 %	± 0,5 %	± 0,5 %	ISO 10545-2

Figure A5 Classification of ceramic tiles with respect to water absorption and shape

Table J.1 *(continued)*

Dimensions and surface quality	Surface S of the product (cm^2)				Test
	$S \leqslant 90$	$90 < S \leqslant 190$	$190 < S \leqslant 410$	$S > 410$	
Rectangularity 2)					
The maximum deviation from rectangularity, in percent, related to the corresponding work sizes.	± 1,0 %	± 0,6 %	± 0,6 %	± 0,6 %	ISO 10545-2
Surface flatness					
The maximum deviation from flatness, in percent:					
a) centre curvature, related to diagonal calculated from the work sizes;	± 1,0 %	± 0,5 %	± 0,5 %	± 0,5 %	ISO 10545-2
b) edge curvature, related to the corresponding work sizes;	± 1,0 %	± 0,5 %	± 0,5 %	± 0,5 %	ISO 10545-2
c) warpage, related to diagonal calculated from the work sizes.	± 1,0 %	± 0,5 %	± 0,5 %	± 0,5 %	ISO 10545-2
Surface quality 3)	A minimum of 95 % of the tiles shall be free from visible defects that would impair the appearance of a major area of tiles				ISO 10545-2
Physical properties	**Requirements**				**Test**
Water absorption Percent by mass	$3\ \% < E \leqslant 6\ \%$ Individual maximum 6,5 %				ISO 10545-3
Breaking strength, in N					
a) Thickness $\geqslant$ 7,5 mm	Not less than 1 000				ISO 10545-4
b) Thickness $<$ 7,5 mm	Not less than 600				ISO 10545-4
Modulus of rupture, in N/mm^2 Not applicable to tiles with breaking strength $\geqslant$ 3 000 N.	Minimum 22 Individual minimum 20				ISO 10545-4
Abrasion resistance					
a) Resistance to deep abrasion of unglazed tiles: removed volume, in cubic millimetres.	Maximum 345				ISO 10545-6
b) Resistance to surface abrasion of glazed tiles intended for use on floors 4).	Report abrasion class and cycles passed				ISO 10545-7
Coefficient of linear thermal expansion 5)					
From ambient temperature to 100 °C.	Test method available				ISO 10545-8
Thermal shock resistance 5)	Test method available				ISO 10545-9
Crazing resistance: glazed tiles 6)	Required				ISO 10545-11
Frost resistance 5)	Test method available				ISO 10545-12
Coefficient of friction					
Tiles intended for use on floors.	Manufacturer to state value and test method used				ISO 10545-17

Figure A6 Classification of ceramic tiles with respect to water absorption and shape

Table J.1 *(concluded)*

Physical properties	Requirements	Test
Moisture expansion, in mm/m 5)	Test method available	ISO 10545-10
Small colour differences 5)	Test method available	ISO 10545-16
Impact resistance 5)	Test method available	ISO 10545-5
Chemical properties		**Test**
Resistance to staining		
a) Glazed tiles	Minimum Class 3	ISO 10545-14
b) Unglazed tiles 5)	Test method available	ISO 10545-14
Resistance to chemicals		
Resistance to low concentrations of acids and alkalis a) glazed tiles; b) unglazed tiles 7).	 Manufacturer to state classification Manufacturer to state classification	 ISO 10545-13 ISO 10545-13
Resistance to high concentrations of acids and alkalis 5).	Test method available	ISO 10545-13
Resistance to household chemicals and swimming pool salts a) glazed tiles; b) unglazed tiles 7).	 Minimum GB Minimum UB	ISO 10545-13
Lead and cadmium release 5)	Test method available	ISO 10545-15

1) Similar joint widths may be used to apply to traditional systems based on non-metric sizes.
2) Not applicable for tiles having curved shapes.
3) Because of firing, slight variations from the standard colour are unavoidable. This does not apply to intentional irregularities of colour variation of the face of tiles (which can be unglazed, glazed or partly glazed) or to the colour variation over a tile area which is characteristic for this type of tile and desirable. Spots or coloured dots which are introduced for decorative purposes are not considered a defect.
4) Reference may be made to annex N of this International Standard for the abrasion resistance classification for all glazed tiles intended for use on floors.
5) Reference may be made to annex P of this International Standard for information regarding requirements which are non-compulsory but which are listed "test method available".
6) Certain decorative effects may have a tendency to craze. They shall be identified by the manufacturer, in which case the crazing test given in ISO 10545-11 is not applicable.
7) If the hue becomes slightly different, this is not considered to be chemical attack.

Figure A7 Classification of ceramic tiles with respect to water absorption and shape

Annex K
(normative)

Dry-pressed ceramic tiles
6 % $< E \leqslant$ 10 %
Group BII_b

K.1 Requirements

Dimensional and surface quality requirements and physical and chemical properties shall be in accordance with table K.1.

Table K.1 — Requirements for dry-pressed ceramic tiles, Group BII_b, 6 % $< E \leqslant$ 10 %

Dimensions and surface quality	Surface S of the product (cm^2)				Test
	$S \leqslant 90$	$90 < S \leqslant 190$	$190 < S \leqslant 410$	$S > 410$	
Length and width					
The manufacturer shall choose the work size as follows: a) for modular tiles in order to allow a nominal joint width of between 2 mm and 5 mm 1); b) for non-modular tiles so that the difference between the work size and the nominal size is not more than ± 2 % (max. ± 5 mm). The deviation, in percent, of the average size for each tile (2 or 4 sides) from the work size (W).	± 1,2 %	± 1,0 %	± 0,75 %	± 0,6 %	ISO 10545-2
The deviation, in percent, of the average size for each tile (2 or 4 sides) from the average size of the 10 test specimens (20 or 40 sides).	± 0,75 %	± 0,5 %	± 0,5 %	± 0,5 %	ISO 10545-2
Thickness					
a) The thickness shall be specified by the manufacturer.					
b) The deviation, in percent, of the average thickness of each tile from the work size thickness.	± 10 %	± 10 %	± 5 %	± 5 %	ISO 10545-2
Straightness of sides 2) (facial sides)					
The maximum deviation from straightness, in percent, related to the corresponding work sizes.	± 0,75 %	± 0,5 %	± 0,5 %	± 0,5 %	ISO 10545-2

Figure A8 Classification of ceramic tiles with respect to water absorption and shape

Table K.1 *(continued)*

Dimensions and surface quality	Surface S of the product (cm^2)				Test
	$S \leq 90$	$90 < S \leq 190$	$190 < S \leq 410$	$S > 410$	
Rectangularity 2)					
The maximum deviation from rectangularity, in percent, related to the corresponding work sizes.	± 1,0 %	± 0,6 %	± 0,6 %	± 0,6 %	ISO 10545-2
Surface flatness					
The maximum deviation from flatness, in percent:					
a) centre curvature, related to diagonal calculated from the work sizes;	± 1,0 %	± 0,5 %	± 0,5 %	± 0,5 %	ISO 10545-2
b) edge curvature, related to the corresponding work sizes;	± 1,0 %	± 0,5 %	± 0,5 %	± 0,5 %	ISO 10545-2
c) warpage, related to diagonal calculated from the work sizes.	± 1,0 %	± 0,5 %	± 0,5 %	± 0,5 %	ISO 10545-2
Surface quality 3)	A minimum of 95 % of the tiles shall be free from visible defects that would impair the appearance of a major area of tiles				ISO 10545-2
Physical properties	**Requirements**				**Test**
Water absorption Percent by mass	$6\ \% < E \leq 10\ \%$ Individual maximum 11 %				ISO 10545-3
Breaking strength, in N					
a) Thickness ≥ 7,5 mm	Not less than 800				ISO 10545-4
b) Thickness < 7,5 mm	Not less than 500				ISO 10545-4
Modulus of rupture, in N/mm^2 Not applicable to tiles with breaking strength ≥ 3 000 N.	Minimum 18 Individual minimum 16				ISO 10545-4
Abrasion resistance					
a) Resistance to deep abrasion of unglazed tiles: removed volume, in cubic millimetres.	Maximum 540				ISO 10545-6
b) Resistance to surface abrasion of glazed tiles intended for use on floors 4).	Report abrasion class and cycles passed				ISO 10545-7
Coefficient of linear thermal expansion 5)					
From ambient temperature to 100 °C.	Test method available				ISO 10545-8
Thermal shock resistance 5)	Test method available				ISO 10545-9
Crazing resistance: glazed tiles 6)	Required				ISO 10545-11
Frost resistance 5)	Test method available				ISO 10545-12
Coefficient of friction					
Tiles intended for use on floors.	Manufacturer to state value and test method used				ISO 10545-17

Figure A9 Classification of ceramic tiles with respect to water absorption and shape

Table K.1 *(concluded)*

Physical properties		Test
Moisture expansion, in mm/m 5)	Test method available	ISO 10545-10
Small colour differences 5)	Test method available	ISO 10545-16
Impact resistance 5)	Test method available	ISO 10545-5
Chemical properties		**Test**
Resistance to staining		
a) Glazed tiles	Minimum Class 3	ISO 10545-14
b) Unglazed tiles 5)	Test method available	ISO 10545-14
Resistance to chemicals		
Resistance to low concentrations of acids and alkalis		
a) glazed tiles;	Manufacturer to state classification	ISO 10545-13
b) unglazed tiles 7).	Manufacturer to state classification	ISO 10545-13
Resistance to high concentrations of acids and alkalis 5).	Test method available	ISO 10545-13
Resistance to household chemicals and swimming pool salts		
a) glazed tiles;	Minimum GB	ISO 10545-13
b) unglazed tiles 7).	Minimum UB	
Lead and cadmium release 5)	Test method available	ISO 10545-15

1) Similar joint widths may be used to apply to traditional systems based on non-metric sizes.
2) Not applicable for tiles having curved shapes.
3) Because of firing, slight variations from the standard colour are unavoidable. This does not apply to intentional irregularities of colour variation of the face of tiles (which can be unglazed, glazed or partly glazed) or to the colour variation over a tile area which is characteristic for this type of tile and desirable. Spots or coloured dots which are introduced for decorative purposes are not considered a defect.
4) Reference may be made to annex N of this International Standard for the abrasion resistance classification for all glazed tiles intended for use on floors.
5) Reference may be made to annex P of this International Standard for information regarding requirements which are non-compulsory but which are listed "test method available".
6) Certain decorative effects may have a tendency to craze. They shall be identified by the manufacturer, in which case the crazing test given in ISO 10545-11 is not applicable.
7) If the hue becomes slightly different, this is not considered to be chemical attack.

Figure A10 Classification of ceramic tiles with respect to water absorption and shape

Annex L
(normative)

Dry-pressed ceramic tiles
$E > 10$ %
Group BIII

L.1 Requirements

Dimensional and surface quality requirements and physical and chemical properties shall be in accordance with table L.1.

Table L.1 — Requirements for dry-pressed ceramic tiles, Group BIII, $E > 10$ %

Dimensions and surface quality	Non-spacer	Spacer	Test
Length (l) and width (w)			
The manufacturer shall choose the work size as follows: a) for modular tiles in order to allow a nominal joint width of between 1,5 mm and 5 mm[1]; b) for non-modular tiles so that the difference between the work size and the nominal size is not more than ± 2 mm. The deviation, in percent, of the average size for each tile (2 or 4 sides) from the work size (W)[7].	$l \leq$ 12 cm: ± 0,75 % $l >$ 12 cm: ± 0,50 %	+ 0,6 % − 0,3 %	ISO 10545-2
The deviation, in percent, of the average size for each tile (2 or 4 sides) from the average size of the 10 test specimens (20 or 40 sides)[7].	$l \leq$ 12 cm: ± 0,5 % $l >$ 12 cm: ± 0,3 %	± 0,25 %	ISO 10545-2
Thickness			
a) The thickness shall be specified by the manufacturer.			
b) The deviation, in percent, of the average thickness of each tile from the work size thickness.	± 10 %	± 10 %	ISO 10545-2
Straightness of sides[2] (facial sides)			
The maximum deviation from straightness, in percent, related to the corresponding work sizes	± 0,3 %	± 0,3 %	ISO 10545-2

Figure A11 Classification of ceramic tiles with respect to water absorption and shape

Table L.1 *(continued)*

Dimensions and surface quality	Non-spacer	Spacer	Test
Rectangularity [2]			
The maximum deviation from rectangularity, in percent, related to the corresponding work sizes	± 0,5 %	± 0,3 %	ISO 10545-2
Surface flatness			
The maximum deviation from flatness, in percent:			
a) centre curvature, related to diagonal calculated from the work sizes;	+ 0,5 % − 0,3 %	+ 0,8 mm − 0,2 mm	ISO 10545-2
b) edge curvature, related to the corresponding work sizes;	+ 0,5 % − 0,3 %	+ 0,8 mm − 0,2 mm	ISO 10545-2
c) warpage, related to diagonal calculated from the work sizes.	± 0,5 %	0,5 mm for sizes ≤ 250 cm^2 0,75 mm for sizes > 250 cm^2	ISO 10545-2
Surface quality [3]	A minimum of 95 % of the tiles shall be free from visible defects that would impair the appearance of a major area of tiles		ISO 10545-2
Physical properties	**Requirements**		**Test**
Water absorption Percent by mass	Average > 10 %. When the average exceeds 20 %, this shall be indicated by the manufacturer Individual minimum value 9 %		ISO 10545-3
Breaking strength, in N [8]			
a) Thickness ≥ 7,5 mm	Not less than 600		ISO 10545-4
b) Thickness < 7,5 mm	Not less than 200		ISO 10545-4
Modulus of rupture, in N/mm² Not applicable to tiles with breaking strength ≥ 3 000 N.			
a) Thickness ≤ 7,5 mm	Minimum 15		ISO 10545-4
b) Thickness > 7,5 mm	Minimum 12		ISO 10545-4
Abrasion resistance			
Resistance to surface abrasion of glazed tiles intended for use on floors [4].	Report abrasion class and cycles passed		ISO 10545-7
Coefficient of linear thermal expansion [5]			
From ambient temperature to 100 °C.	Test method available		ISO 10545-8
Thermal shock resistance [5]	Test method available		ISO 10545-9
Crazing resistance: glazed tiles [6]	Required		ISO 10545-11
Frost resistance	Test method available		ISO 10545-12
Coefficient of friction			
Tiles intended for use on floors.	Manufacturer to state value and test method used		ISO 10545-17

Figure A12 Classification of ceramic tiles with respect to water absorption and shape

Table L.1 *(concluded)*

Physical properties	Requirements	Test
Moisture expansion, in mm/m 5)	Test method available	ISO 10545-10
Small colour differences 5)	Test method available	ISO 10545-16
Impact resistance 5)	Test method available	ISO 10545-5
Chemical properties	**Requirements**	**Test**
Resistance to staining		
a) Glazed tiles	Minimum Class 3	ISO 10545-14
b) Unglazed tiles 5)	Test method available	ISO 10545-14
Resistance to chemicals		
Resistance to low concentrations of acids and alkalis.	Test method available	ISO 10545-13
Resistance to high concentrations of acids and alkalis 5).	Test method available	ISO 10545-13
Resistance to household chemicals and swimming pool salts: glazed tiles.	Minimum GB	ISO 10545-13
Lead and cadmium release 5)	Test method available	ISO 10545-15

1) Similar joint widths may be used to apply to traditional systems based on non-metric sizes.
2) Not applicable for tiles having curved shapes.
3) Because of firing, slight variations from the standard colour are unavoidable. This does not apply to intentional irregularities of colour variation of the face of tiles (which can be unglazed, glazed or partly glazed) or to the colour variation over a tile area which is characteristic for this type of tile and desirable. Spots or coloured dots which are introduced for decorative purposes are not considered a defect.
4) Reference may be made to annex N of this International Standard for the abrasion resistance classification for all glazed tiles intended for use on floors.
5) Reference may be made to annex P of this International Standard for information regarding requirements which are non-compulsory but which are listed "test method available".
6) Certain decorative effects may have a tendency to craze. They shall be identified by the manufacturer, in which case the crazing test given in ISO 10545-11 is not applicable.
7) For tiles having one or more adjacent glazed edges.
8) Tiles with breaking strength less than 400 N are intended for use on walls only and this must be indicated by the manufacturer.

Figure A13 Classification of ceramic tiles with respect to water absorption and shape

Suranaree University of Technology

HORIBA Laser Scattering Particle Size Distribution Analyzer LA-950

Sample Name	:	A1
ID#	:	201409041125689
Data Name	:	201409041125689
Transmittance(R)	:	87.7(%)
Transmittance(B)	:	86.4(%)
Circulation Speed	:	5
Agitation Speed	:	10
Ultra Sonic	:	04:00 (7)
Form of Distribution	:	Auto
Distribution Base	:	Volume
Refractive Index (R)	:	Bentonite[Bentonite(1.560 - 0.000i),Water(1.333)]
Refractive Index (B)	:	Bentonite[Bentonite(1.560 - 0.000i),Water(1.333)]
Source	:	
Sensitivity Setting	:	Normal Sensitivity
Material	:	

Median Size	:	70.27379(µm)
Mean Size	:	69.73430(µm)
Std.Dev.	:	33.4800(µm)
Geo.Mean Size	:	57.8615(µm)
Geo.Std.Dev.	:	2.1038(µm)
Mode Size	:	73.0895(µm)
Span	:	1.2592
D(v,0.1)	:	17.01578(µm)
D(v,0.5)	:	70.27379(µm)
D(v,0.9)	:	105.50716(µm)

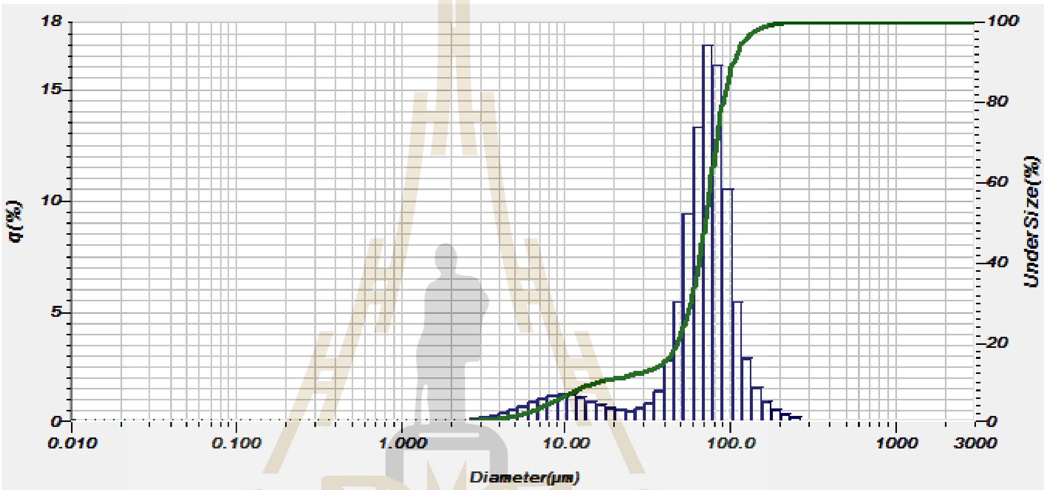

No.	Diameter(µm)	q(%)	UnderSize(%)
1	0.011	0.000	0.000
2	0.013	0.000	0.000
3	0.015	0.000	0.000
4	0.017	0.000	0.000
5	0.020	0.000	0.000
6	0.022	0.000	0.000
7	0.026	0.000	0.000
8	0.029	0.000	0.000
9	0.034	0.000	0.000
10	0.039	0.000	0.000
11	0.044	0.000	0.000
12	0.051	0.000	0.000
13	0.058	0.000	0.000
14	0.067	0.000	0.000
15	0.076	0.000	0.000
16	0.087	0.000	0.000
17	0.100	0.000	0.000
18	0.115	0.000	0.000
19	0.131	0.000	0.000
20	0.150	0.000	0.000
21	0.172	0.000	0.000
22	0.197	0.000	0.000
23	0.226	0.000	0.000
24	0.259	0.000	0.000
25	0.296	0.000	0.000

No.	Diameter(µm)	q(%)	UnderSize(%)
26	0.339	0.000	0.000
27	0.389	0.000	0.000
28	0.445	0.000	0.000
29	0.510	0.000	0.000
30	0.584	0.000	0.000
31	0.669	0.000	0.000
32	0.766	0.000	0.000
33	0.877	0.000	0.000
34	1.005	0.000	0.000
35	1.151	0.000	0.000
36	1.318	0.000	0.000
37	1.510	0.000	0.000
38	1.729	0.000	0.000
39	1.981	0.000	0.000
40	2.269	0.000	0.000
41	2.599	0.000	0.000
42	2.976	0.116	0.116
43	3.409	0.173	0.289
44	3.905	0.251	0.539
45	4.472	0.356	0.895
46	5.122	0.495	1.390
47	5.867	0.665	2.055
48	6.720	0.849	2.904
49	7.697	1.018	3.922
50	8.816	1.135	5.057

No.	Diameter(µm)	q(%)	UnderSize(%)
51	10.097	1.189	6.246
52	11.565	1.182	7.428
53	13.246	1.070	8.498
54	15.172	0.896	9.394
55	17.377	0.717	10.111
56	19.904	0.578	10.689
57	22.797	0.496	11.185
58	26.111	0.483	11.668
59	29.907	0.559	12.227
60	34.255	0.788	13.015
61	39.234	1.370	14.385
62	44.938	2.738	17.123
63	51.471	5.367	22.491
64	58.953	9.323	31.814
65	67.523	13.216	45.030
66	77.339	16.898	61.927
67	88.583	16.041	77.968
68	101.460	10.476	88.444
69	116.210	5.401	93.844
70	133.103	2.797	96.642
71	152.453	1.513	98.155
72	174.616	0.850	99.005
73	200.000	0.499	99.504
74	229.075	0.304	99.808
75	262.376	0.192	100.000

No.	Diameter(µm)	q(%)	UnderSize(%)
76	300.518	0.000	100.000
77	344.206	0.000	100.000
78	394.244	0.000	100.000
79	451.556	0.000	100.000
80	517.200	0.000	100.000
81	592.387	0.000	100.000
82	678.504	0.000	100.000
83	777.141	0.000	100.000
84	890.116	0.000	100.000
85	1019.515	0.000	100.000
86	1167.725	0.000	100.000
87	1337.481	0.000	100.000
88	1531.914	0.000	100.000
89	1754.613	0.000	100.000
90	2009.687	0.000	100.000
91	2301.841	0.000	100.000
92	2636.467	0.000	100.000
93	3000.000	0.000	100.000

Figure A14 Particle size analysis by particle size analyzerof sample C_1

2014.09.04 11:43:25

Suranaree University of Technology

HORIBA Laser Scattering Particle Size Distribution Analyzer LA-950

Sample Name	: A2		Median Size	: 64.49066(µm)
ID#	: 201409041138691		Mean Size	: 66.29677(µm)
Data Name	: 201409041138691		Std.Dev.	: 19.3989(µm)
Transmittance(R)	: 88.8(%)		Geo.Mean Size	: 63.3747(µm)
Transmittance(B)	: 91.5(%)		Geo.Std.Dev.	: 1.3676(µm)
Circulation Speed	: 5		Mode Size	: 63.6960(µm)
Agitation Speed	: 10		Span	: 0.6950
Ultra Sonic	: 02:00 (7)		D(v,0.1)	: 44.95798(µm)
Form of Distribution	: Auto		D(v,0.5)	: 64.49066(µm)
Distribution Base	: Volume		D(v,0.9)	: 89.77908(µm)
Refractive Index (R)	: Bentonite[Bentonite(1.560 - 0.000i),Water(1.333)]			
Refractive Index (B)	: Bentonite[Bentonite(1.560 - 0.000i),Water(1.333)]			
Source	:			
Sensitivity Setting	: Normal Sensitivity			
Material	:			

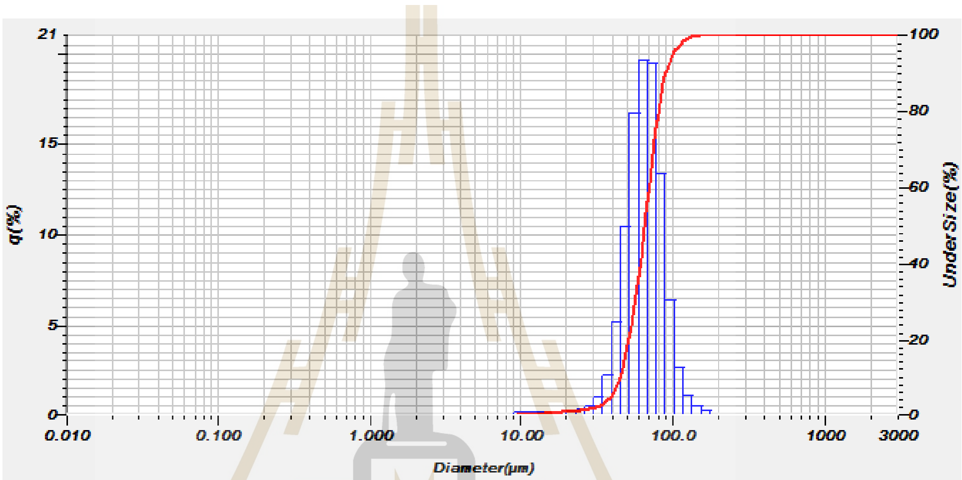

No.	Diameter(µm)	q(%)	UnderSize(%)	No.	Diameter(µm)	q(%)	UnderSize(%)	No.	Diameter(µm)	q(%)	UnderSize(%)	No.	Diameter(µm)	q(%)	UnderSize(%)
1	0.011	0.000	0.000	26	0.339	0.000	0.000	51	10.097	0.108	0.108	76	300.518	0.000	100.000
2	0.013	0.000	0.000	27	0.389	0.000	0.000	52	11.565	0.121	0.229	77	344.206	0.000	100.000
3	0.015	0.000	0.000	28	0.445	0.000	0.000	53	13.246	0.129	0.358	78	394.244	0.000	100.000
4	0.017	0.000	0.000	29	0.510	0.000	0.000	54	15.172	0.135	0.492	79	451.556	0.000	100.000
5	0.020	0.000	0.000	30	0.584	0.000	0.000	55	17.377	0.142	0.635	80	517.200	0.000	100.000
6	0.022	0.000	0.000	31	0.669	0.000	0.000	56	19.904	0.158	0.793	81	592.387	0.000	100.000
7	0.026	0.000	0.000	32	0.766	0.000	0.000	57	22.797	0.194	0.987	82	678.504	0.000	100.000
8	0.029	0.000	0.000	33	0.877	0.000	0.000	58	26.111	0.275	1.262	83	777.141	0.000	100.000
9	0.034	0.000	0.000	34	1.005	0.000	0.000	59	29.907	0.464	1.726	84	890.116	0.000	100.000
10	0.039	0.000	0.000	35	1.151	0.000	0.000	60	34.255	0.935	2.661	85	1019.515	0.000	100.000
11	0.044	0.000	0.000	36	1.318	0.000	0.000	61	39.234	2.180	4.841	86	1167.725	0.000	100.000
12	0.051	0.000	0.000	37	1.510	0.000	0.000	62	44.938	5.125	9.966	87	1337.481	0.000	100.000
13	0.058	0.000	0.000	38	1.729	0.000	0.000	63	51.471	10.439	20.404	88	1531.914	0.000	100.000
14	0.067	0.000	0.000	39	1.981	0.000	0.000	64	58.953	16.636	37.040	89	1754.613	0.000	100.000
15	0.076	0.000	0.000	40	2.269	0.000	0.000	65	67.523	19.594	56.634	90	2009.687	0.000	100.000
16	0.087	0.000	0.000	41	2.599	0.000	0.000	66	77.339	19.382	76.016	91	2301.841	0.000	100.000
17	0.100	0.000	0.000	42	2.976	0.000	0.000	67	88.583	13.354	89.370	92	2636.467	0.000	100.000
18	0.115	0.000	0.000	43	3.409	0.000	0.000	68	101.460	6.377	95.746	93	3000.000	0.000	100.000
19	0.131	0.000	0.000	44	3.905	0.000	0.000	69	116.210	2.558	98.305				
20	0.150	0.000	0.000	45	4.472	0.000	0.000	70	133.103	1.043	99.348				
21	0.172	0.000	0.000	46	5.122	0.000	0.000	71	152.453	0.448	99.796				
22	0.197	0.000	0.000	47	5.867	0.000	0.000	72	174.616	0.204	100.000				
23	0.226	0.000	0.000	48	6.720	0.000	0.000	73	200.000	0.000	100.000				
24	0.259	0.000	0.000	49	7.697	0.000	0.000	74	229.075	0.000	100.000				
25	0.296	0.000	0.000	50	8.816	0.000	0.000	75	262.376	0.000	100.000				

Figure A15 Particle size analysis by particle size analyzerof sample C_2

2014.09.04 12:49:04

Suranaree University of Technology

HORIBA Laser Scattering Particle Size Distribution Analyzer LA-950

Sample Name	: A5	Median Size	: 66.23211(µm)
ID#	: 201409041156693	Mean Size	: 67.69480(µm)
Data Name	: 201409041156693	Std.Dev.	: 23.1591(µm)
Transmittance(R)	: 86.1(%)	Geo.Mean Size	: 63.0481(µm)
Transmittance(B)	: 89.4(%)	Geo.Std.Dev.	: 1.5193(µm)
Circulation Speed	: 5	Mode Size	: 71.5334(µm)
Agitation Speed	: 10	Span	: 0.8044
Ultra Sonic	: 02:00 (7)	D(v,0.1)	: 42.32658(µm)
Form of Distribution	: Auto	D(v,0.5)	: 66.23211(µm)
Distribution Base	: Volume	D(v,0.9)	: 95.60126(µm)
Refractive Index (R)	: Bentonite[Bentonite(1.560 - 0.000i),Water(1.333)]		
Refractive Index (B)	: Bentonite[Bentonite(1.560 - 0.000i),Water(1.333)]		
Source	:		
Sensitivity Setting	: Normal Sensitivity		
Material	:		

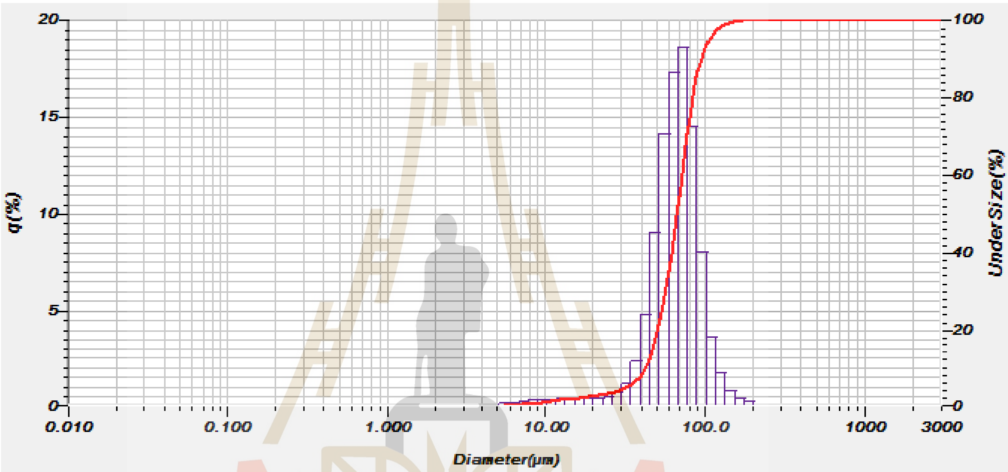

No.	Diameter(µm)	q(%)	UnderSize(%)	No.	Diameter(µm)	q(%)	UnderSize(%)	No.	Diameter(µm)	q(%)	UnderSize(%)	No.	Diameter(µm)	q(%)	UnderSize(%)
1	0.011	0.000	0.000	26	0.339	0.000	0.000	51	10.097	0.272	0.950	76	300.518	0.000	100.000
2	0.013	0.000	0.000	27	0.389	0.000	0.000	52	11.565	0.304	1.253	77	344.206	0.000	100.000
3	0.015	0.000	0.000	28	0.445	0.000	0.000	53	13.246	0.317	1.571	78	394.244	0.000	100.000
4	0.017	0.000	0.000	29	0.510	0.000	0.000	54	15.172	0.317	1.888	79	451.556	0.000	100.000
5	0.020	0.000	0.000	30	0.584	0.000	0.000	55	17.377	0.314	2.202	80	517.200	0.000	100.000
6	0.022	0.000	0.000	31	0.669	0.000	0.000	56	19.904	0.320	2.522	81	592.387	0.000	100.000
7	0.026	0.000	0.000	32	0.766	0.000	0.000	57	22.797	0.354	2.876	82	678.504	0.000	100.000
8	0.029	0.000	0.000	33	0.877	0.000	0.000	58	26.111	0.444	3.319	83	777.141	0.000	100.000
9	0.034	0.000	0.000	34	1.005	0.000	0.000	59	29.907	0.651	3.970	84	890.116	0.000	100.000
10	0.039	0.000	0.000	35	1.151	0.000	0.000	60	34.255	1.127	5.097	85	1019.515	0.000	100.000
11	0.044	0.000	0.000	36	1.318	0.000	0.000	61	39.234	2.260	7.358	86	1167.725	0.000	100.000
12	0.051	0.000	0.000	37	1.510	0.000	0.000	62	44.938	4.728	12.085	87	1337.481	0.000	100.000
13	0.058	0.000	0.000	38	1.729	0.000	0.000	63	51.471	8.978	21.063	88	1531.914	0.000	100.000
14	0.067	0.000	0.000	39	1.981	0.000	0.000	64	58.953	14.117	35.180	89	1754.613	0.000	100.000
15	0.076	0.000	0.000	40	2.269	0.000	0.000	65	67.523	17.278	52.458	90	2009.687	0.000	100.000
16	0.087	0.000	0.000	41	2.599	0.000	0.000	66	77.339	18.542	71.000	91	2301.841	0.000	100.000
17	0.100	0.000	0.000	42	2.976	0.000	0.000	67	88.583	14.498	85.498	92	2636.467	0.000	100.000
18	0.115	0.000	0.000	43	3.409	0.000	0.000	68	101.460	8.014	93.512	93	3000.000	0.000	100.000
19	0.131	0.000	0.000	44	3.905	0.000	0.000	69	116.210	3.629	97.141				
20	0.150	0.000	0.000	45	4.472	0.000	0.000	70	133.103	1.623	98.764				
21	0.172	0.000	0.000	46	5.122	0.000	0.000	71	152.453	0.736	99.500				
22	0.197	0.000	0.000	47	5.867	0.106	0.106	72	174.616	0.340	99.840				
23	0.226	0.000	0.000	48	6.720	0.147	0.252	73	200.000	0.160	100.000				
24	0.259	0.000	0.000	49	7.697	0.191	0.443	74	229.075	0.000	100.000				
25	0.296	0.000	0.000	50	8.816	0.234	0.677	75	262.376	0.000	100.000				

Figure A16 Particle size analysis by particle size analyzerof sample C_3

2014.09.04 13:04:22

Suranaree University of Technology

HORIBA Laser Scattering Particle Size Distribution Analyzer LA-950

Sample Name : A6-1
ID# : 201409041302700
Data Name : 201409041302700
Transmittance(R) : 86.4(%)
Transmittance(B) : 77.9(%)
Circulation Speed : 5
Agitation Speed : 10
Ultra Sonic : 02:00 (7)
Form of Distribution : Auto
Distribution Base : Volume
Refractive Index (R) : Bentonite[Bentonite(1.560 - 0.000i),Water(1.333)]
Refractive Index (B) : Bentonite[Bentonite(1.560 - 0.000i),Water(1.333)]
Source :
Sensitivity Setting : Normal Sensitivity
Material :

Median Size : 6.10568(µm)
Mean Size : 6.56342(µm)
Std.Dev. : 3.1095(µm)
Geo.Mean Size : 5.8413(µm)
Geo.Std.Dev. : 1.6506(µm)
Mode Size : 6.3062(µm)
Span : 1.2743
D(v,0.1) : 2.97774(µm)
D(v,0.5) : 6.10568(µm)
D(v,0.9) : 10.75797(µm)

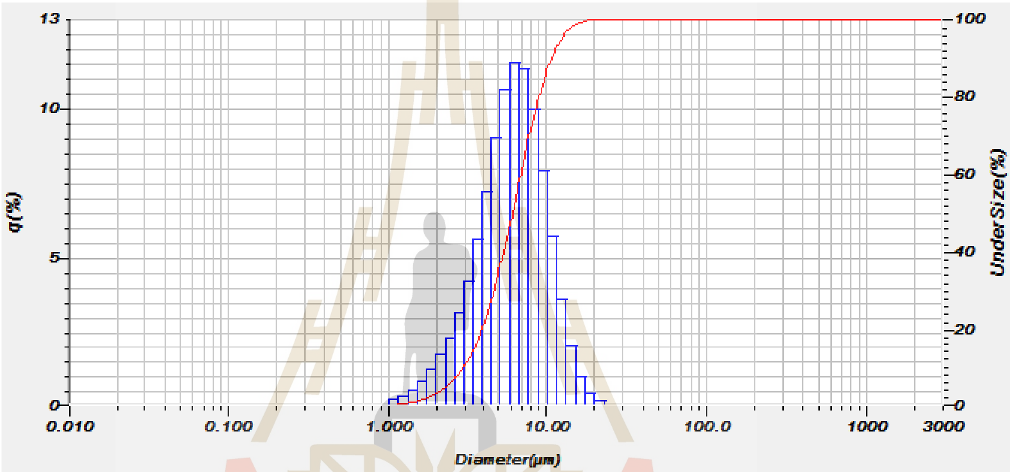

No.	Diameter(µm)	q(%)	UnderSize(%)	No.	Diameter(µm)	q(%)	UnderSize(%)	No.	Diameter(µm)	q(%)	UnderSize(%)	No.	Diameter(µm)	q(%)	UnderSize(%)
1	0.011	0.000	0.000	26	0.339	0.000	0.000	51	10.097	7.919	87.349	76	300.518	0.000	100.000
2	0.013	0.000	0.000	27	0.389	0.000	0.000	52	11.565	5.676	93.025	77	344.206	0.000	100.000
3	0.015	0.000	0.000	28	0.445	0.000	0.000	53	13.246	3.609	96.633	78	394.244	0.000	100.000
4	0.017	0.000	0.000	29	0.510	0.000	0.000	54	15.172	1.967	98.600	79	451.556	0.000	100.000
5	0.020	0.000	0.000	30	0.584	0.000	0.000	55	17.377	0.915	99.515	80	517.200	0.000	100.000
6	0.022	0.000	0.000	31	0.669	0.000	0.000	56	19.904	0.363	99.878	81	592.387	0.000	100.000
7	0.026	0.000	0.000	32	0.766	0.000	0.000	57	22.797	0.122	100.000	82	678.504	0.000	100.000
8	0.029	0.000	0.000	33	0.877	0.000	0.000	58	26.111	0.000	100.000	83	777.141	0.000	100.000
9	0.034	0.000	0.000	34	1.005	0.000	0.000	59	29.907	0.000	100.000	84	890.116	0.000	100.000
10	0.039	0.000	0.000	35	1.151	0.160	0.160	60	34.255	0.000	100.000	85	1019.515	0.000	100.000
11	0.044	0.000	0.000	36	1.318	0.293	0.453	61	39.234	0.000	100.000	86	1167.725	0.000	100.000
12	0.051	0.000	0.000	37	1.510	0.490	0.943	62	44.938	0.000	100.000	87	1337.481	0.000	100.000
13	0.058	0.000	0.000	38	1.729	0.781	1.725	63	51.471	0.000	100.000	88	1531.914	0.000	100.000
14	0.067	0.000	0.000	39	1.981	1.168	2.893	64	58.953	0.000	100.000	89	1754.613	0.000	100.000
15	0.076	0.000	0.000	40	2.269	1.664	4.557	65	67.523	0.000	100.000	90	2009.687	0.000	100.000
16	0.087	0.000	0.000	41	2.599	2.300	6.856	66	77.339	0.000	100.000	91	2301.841	0.000	100.000
17	0.100	0.000	0.000	42	2.976	3.128	9.985	67	88.583	0.000	100.000	92	2636.467	0.000	100.000
18	0.115	0.000	0.000	43	3.409	4.209	14.194	68	101.460	0.000	100.000	93	3000.000	0.000	100.000
19	0.131	0.000	0.000	44	3.905	5.581	19.775	69	116.210	0.000	100.000				
20	0.150	0.000	0.000	45	4.472	7.225	27.000	70	133.103	0.000	100.000				
21	0.172	0.000	0.000	46	5.122	9.005	36.005	71	152.453	0.000	100.000				
22	0.197	0.000	0.000	47	5.867	10.604	46.609	72	174.616	0.000	100.000				
23	0.226	0.000	0.000	48	6.720	11.539	58.147	73	200.000	0.000	100.000				
24	0.259	0.000	0.000	49	7.697	11.343	69.490	74	229.075	0.000	100.000				
25	0.296	0.000	0.000	50	8.816	9.940	79.430	75	262.376	0.000	100.000				

Figure A17 Particle size analysis by particle size analyzerof sample M

2014.09.04 13:32:17

Suranaree University of Technology

HORIBA Laser Scattering Particle Size Distribution Analyzer LA-950

Sample Name	: A7	Median Size	: 6.27225(µm)
ID#	: 201409041313703	Mean Size	: 6.64721(µm)
Data Name	: 201409041313703	Std.Dev.	: 2.6661(µm)
Transmittance(R)	: 85.4(%)	Geo.Mean Size	: 6.1295(µm)
Transmittance(B)	: 76.9(%)	Geo.Std.Dev.	: 1.5094(µm)
Circulation Speed	: 5	Mode Size	: 6.3078(µm)
Agitation Speed	: 10	Span	: 1.0579
Ultra Sonic	: 02:00 (7)	D(v,0.1)	: 3.55879(µm)
Form of Distribution	: Auto	D(v,0.5)	: 6.27225(µm)
Distribution Base	: Volume	D(v,0.9)	: 10.19445(µm)
Refractive Index (R)	: Bentonite[Bentonite(1.560 - 0.000i),Water(1.333)]		
Refractive Index (B)	: Bentonite[Bentonite(1.560 - 0.000i),Water(1.333)]		
Source	:		
Sensitivity Setting	: Normal Sensitivity		
Material	:		

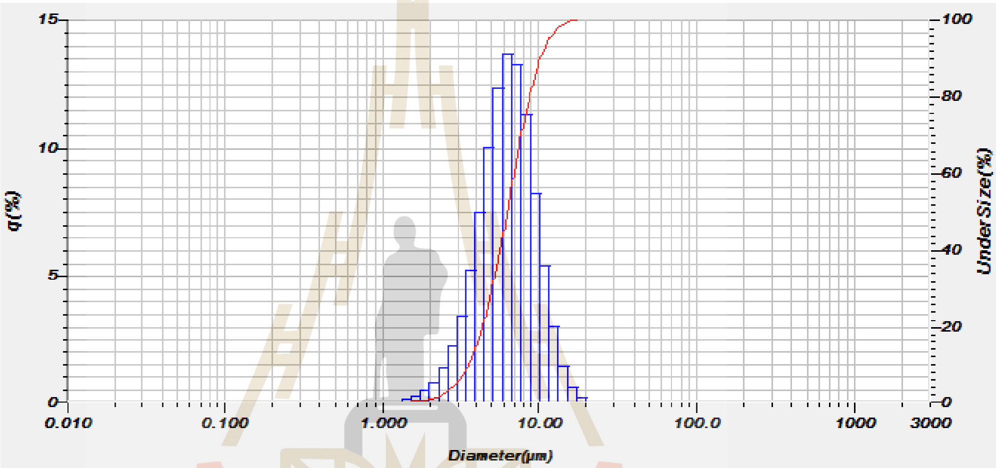

No.	Diameter(µm)	q(%)	UnderSize(%)
1	0.011	0.000	0.000
2	0.013	0.000	0.000
3	0.015	0.000	0.000
4	0.017	0.000	0.000
5	0.020	0.000	0.000
6	0.022	0.000	0.000
7	0.026	0.000	0.000
8	0.029	0.000	0.000
9	0.034	0.000	0.000
10	0.039	0.000	0.000
11	0.044	0.000	0.000
12	0.051	0.000	0.000
13	0.058	0.000	0.000
14	0.067	0.000	0.000
15	0.076	0.000	0.000
16	0.087	0.000	0.000
17	0.100	0.000	0.000
18	0.115	0.000	0.000
19	0.131	0.000	0.000
20	0.150	0.000	0.000
21	0.172	0.000	0.000
22	0.197	0.000	0.000
23	0.226	0.000	0.000
24	0.259	0.000	0.000
25	0.296	0.000	0.000
26	0.339	0.000	0.000
27	0.389	0.000	0.000
28	0.445	0.000	0.000
29	0.510	0.000	0.000
30	0.584	0.000	0.000
31	0.669	0.000	0.000
32	0.766	0.000	0.000
33	0.877	0.000	0.000
34	1.005	0.000	0.000
35	1.151	0.000	0.000
36	1.318	0.000	0.000
37	1.510	0.108	0.108
38	1.729	0.223	0.331
39	1.981	0.420	0.751
40	2.269	0.752	1.503
41	2.599	1.295	2.799
42	2.976	2.148	4.947
43	3.409	3.414	8.360
44	3.905	5.174	13.534
45	4.472	7.430	20.965
46	5.122	9.987	30.952
47	5.867	12.328	43.279
48	6.720	13.654	56.933
49	7.697	13.252	70.185
50	8.816	11.250	81.435
51	10.097	8.187	89.622
52	11.565	5.345	94.967
53	13.246	2.971	97.937
54	15.172	1.368	99.305
55	17.377	0.525	99.830
56	19.904	0.170	100.000
57	22.797	0.000	100.000
58	26.111	0.000	100.000
59	29.907	0.000	100.000
60	34.255	0.000	100.000
61	39.234	0.000	100.000
62	44.938	0.000	100.000
63	51.471	0.000	100.000
64	58.953	0.000	100.000
65	67.523	0.000	100.000
66	77.339	0.000	100.000
67	88.583	0.000	100.000
68	101.460	0.000	100.000
69	116.210	0.000	100.000
70	133.103	0.000	100.000
71	152.453	0.000	100.000
72	174.616	0.000	100.000
73	200.000	0.000	100.000
74	229.075	0.000	100.000
75	262.376	0.000	100.000
76	300.518	0.000	100.000
77	344.206	0.000	100.000
78	394.244	0.000	100.000
79	451.556	0.000	100.000
80	517.200	0.000	100.000
81	592.387	0.000	100.000
82	678.504	0.000	100.000
83	777.141	0.000	100.000
84	890.116	0.000	100.000
85	1019.515	0.000	100.000
86	1167.725	0.000	100.000
87	1337.481	0.000	100.000
88	1531.914	0.000	100.000
89	1754.613	0.000	100.000
90	2009.687	0.000	100.000
91	2301.841	0.000	100.000
92	2636.467	0.000	100.000
93	3000.000	0.000	100.000

Figure A18 Particle size analysis by particle size analyzerof sample P_1

2014.09.04 12:19:46

Suranaree University of Technology

HORIBA Laser Scattering Particle Size Distribution Analyzer LA-950

Sample Name	:	A3
ID#	:	201409041147692
Data Name	:	201409041147692
Transmittance(R)	:	86.7(%)
Transmittance(B)	:	80.6(%)
Circulation Speed	:	5
Agitation Speed	:	10
Ultra Sonic	:	02:00 (7)
Form of Distribution	:	Auto
Distribution Base	:	Volume
Refractive Index (R)	:	Bentonite[Bentonite(1.560 - 0.000i),Water(1.333)]
Refractive Index (B)	:	Bentonite[Bentonite(1.560 - 0.000i),Water(1.333)]
Source	:	
Sensitivity Setting	:	Normal Sensitivity
Material	:	

Median Size	:	6.14479(µm)
Mean Size	:	6.42071(µm)
Std.Dev.	:	2.2344(µm)
Geo.Mean Size	:	6.0417(µm)
Geo.Std.Dev.	:	1.4260(µm)
Mode Size	:	6.2835(µm)
Span	:	0.9137
D(v,0.1)	:	3.81051(µm)
D(v,0.5)	:	6.14479(µm)
D(v,0.9)	:	9.42512(µm)

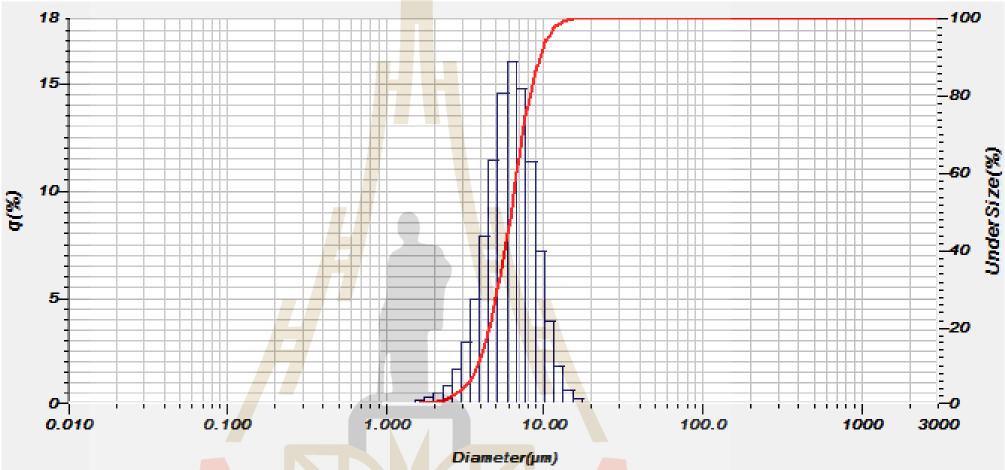

No.	Diameter(µm)	q(%)	UnderSize(%)
1	0.011	0.000	0.000
2	0.013	0.000	0.000
3	0.015	0.000	0.000
4	0.017	0.000	0.000
5	0.020	0.000	0.000
6	0.022	0.000	0.000
7	0.026	0.000	0.000
8	0.029	0.000	0.000
9	0.034	0.000	0.000
10	0.039	0.000	0.000
11	0.044	0.000	0.000
12	0.051	0.000	0.000
13	0.058	0.000	0.000
14	0.067	0.000	0.000
15	0.076	0.000	0.000
16	0.087	0.000	0.000
17	0.100	0.000	0.000
18	0.115	0.000	0.000
19	0.131	0.000	0.000
20	0.150	0.000	0.000
21	0.172	0.000	0.000
22	0.197	0.000	0.000
23	0.226	0.000	0.000
24	0.259	0.000	0.000
25	0.296	0.000	0.000
26	0.339	0.000	0.000
27	0.389	0.000	0.000
28	0.445	0.000	0.000
29	0.510	0.000	0.000
30	0.584	0.000	0.000
31	0.669	0.000	0.000
32	0.766	0.000	0.000
33	0.877	0.000	0.000
34	1.005	0.000	0.000
35	1.151	0.000	0.000
36	1.318	0.000	0.000
37	1.510	0.000	0.000
38	1.729	0.108	0.108
39	1.981	0.216	0.324
40	2.269	0.422	0.746
41	2.599	0.819	1.565
42	2.976	1.558	3.123
43	3.409	2.849	5.972
44	3.905	4.910	10.882
45	4.472	7.835	18.716
46	5.122	11.340	30.056
47	5.867	14.508	44.564
48	6.720	15.944	60.508
49	7.697	14.680	75.187
50	8.816	11.298	86.485
51	10.097	7.136	93.621
52	11.565	3.858	97.479
53	13.246	1.729	99.208
54	15.172	0.616	99.823
55	17.377	0.177	100.000
56	19.904	0.000	100.000
57	22.797	0.000	100.000
58	26.111	0.000	100.000
59	29.907	0.000	100.000
60	34.255	0.000	100.000
61	39.234	0.000	100.000
62	44.938	0.000	100.000
63	51.471	0.000	100.000
64	58.953	0.000	100.000
65	67.523	0.000	100.000
66	77.339	0.000	100.000
67	88.583	0.000	100.000
68	101.460	0.000	100.000
69	116.210	0.000	100.000
70	133.103	0.000	100.000
71	152.453	0.000	100.000
72	174.616	0.000	100.000
73	200.000	0.000	100.000
74	229.075	0.000	100.000
75	262.376	0.000	100.000
76	300.518	0.000	100.000
77	344.206	0.000	100.000
78	394.244	0.000	100.000
79	451.556	0.000	100.000
80	517.200	0.000	100.000
81	592.387	0.000	100.000
82	678.504	0.000	100.000
83	777.141	0.000	100.000
84	890.116	0.000	100.000
85	1019.515	0.000	100.000
86	1167.725	0.000	100.000
87	1337.481	0.000	100.000
88	1531.914	0.000	100.000
89	1754.613	0.000	100.000
90	2009.687	0.000	100.000
91	2301.841	0.000	100.000
92	2636.467	0.000	100.000
93	3000.000	0.000	100.000

Figure A19 Particle size analysis by particle size analyzerof sample P_2

2014.09.04 12:38:59

Suranaree University of Technology

HORIBA Laser Scattering Particle Size Distribution Analyzer LA-950

Sample Name	: A8		Median Size	: 8.87613(µm)
ID#	: 201409041238697		Mean Size	: 14.61286(µm)
Data Name	: 201409041238697		Std.Dev.	: 20.7347(µm)
Transmittance(R)	: 88.1(%)		Geo.Mean Size	: 9.4807(µm)
Transmittance(B)	: 81.3(%)		Geo.Std.Dev.	: 2.3087(µm)
Circulation Speed	: 5		Mode Size	: 9.4065(µm)
Agitation Speed	: 10		Span	: 2.7360
Ultra Sonic	: 02:00 (7)		D(v,0.1)	: 3.51815(µm)
Form of Distribution	: Auto		D(v,0.5)	: 8.87613(µm)
Distribution Base	: Volume		D(v,0.9)	: 27.80361(µm)
Refractive Index (R)	: Bentonite[Bentonite(1.560 - 0.000i),Water(1.333)]			
Refractive Index (B)	: Bentonite[Bentonite(1.560 - 0.000i),Water(1.333)]			
Source	:			
Sensitivity Setting	: Normal Sensitivity			
Material	:			

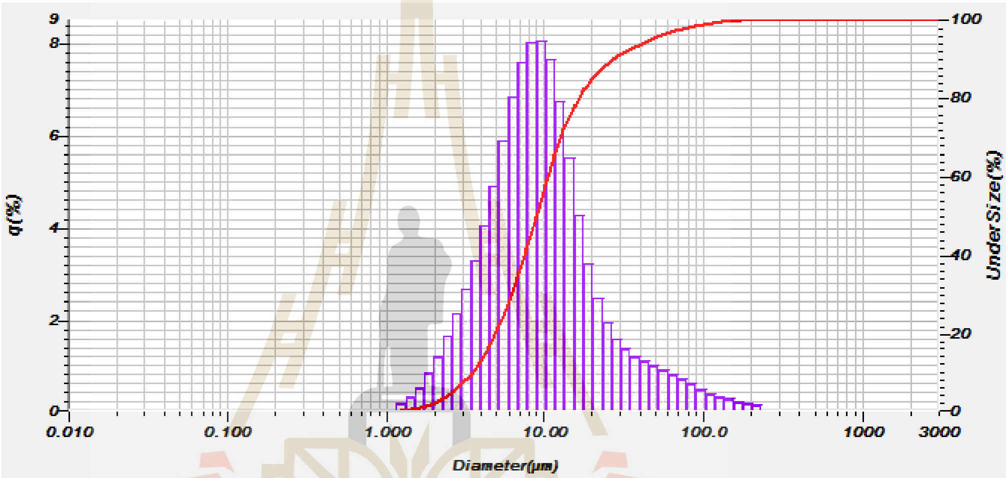

No.	Diameter(µm)	q(%)	UnderSize(%)	No.	Diameter(µm)	q(%)	UnderSize(%)	No.	Diameter(µm)	q(%)	UnderSize(%)	No.	Diameter(µm)	q(%)	UnderSize(%)
1	0.011	0.000	0.000	26	0.339	0.000	0.000	51	10.097	8.027	57.622	76	300.518	0.000	100.000
2	0.013	0.000	0.000	27	0.389	0.000	0.000	52	11.565	7.630	65.252	77	344.206	0.000	100.000
3	0.015	0.000	0.000	28	0.445	0.000	0.000	53	13.246	6.713	71.965	78	394.244	0.000	100.000
4	0.017	0.000	0.000	29	0.510	0.000	0.000	54	15.172	5.494	77.458	79	451.556	0.000	100.000
5	0.020	0.000	0.000	30	0.584	0.000	0.000	55	17.377	4.258	81.716	80	517.200	0.000	100.000
6	0.022	0.000	0.000	31	0.669	0.000	0.000	56	19.904	3.213	84.929	81	592.387	0.000	100.000
7	0.026	0.000	0.000	32	0.766	0.000	0.000	57	22.797	2.437	87.365	82	678.504	0.000	100.000
8	0.029	0.000	0.000	33	0.877	0.000	0.000	58	26.111	1.910	89.275	83	777.141	0.000	100.000
9	0.034	0.000	0.000	34	1.005	0.000	0.000	59	29.907	1.567	90.842	84	890.116	0.000	100.000
10	0.039	0.000	0.000	35	1.151	0.000	0.000	60	34.255	1.338	92.180	85	1019.515	0.000	100.000
11	0.044	0.000	0.000	36	1.318	0.152	0.152	61	39.234	1.181	93.361	86	1167.725	0.000	100.000
12	0.051	0.000	0.000	37	1.510	0.281	0.433	62	44.938	1.063	94.424	87	1337.481	0.000	100.000
13	0.058	0.000	0.000	38	1.729	0.489	0.922	63	51.471	0.959	95.383	88	1531.914	0.000	100.000
14	0.067	0.000	0.000	39	1.981	0.789	1.712	64	58.953	0.862	96.245	89	1754.613	0.000	100.000
15	0.076	0.000	0.000	40	2.269	1.171	2.883	65	67.523	0.765	97.010	90	2009.687	0.000	100.000
16	0.087	0.000	0.000	41	2.599	1.613	4.496	66	77.339	0.662	97.673	91	2301.841	0.000	100.000
17	0.100	0.000	0.000	42	2.976	2.101	6.597	67	88.583	0.562	98.234	92	2636.467	0.000	100.000
18	0.115	0.000	0.000	43	3.409	2.644	9.241	68	101.460	0.454	98.688	93	3000.000	0.000	100.000
19	0.131	0.000	0.000	44	3.905	3.269	12.509	69	116.210	0.337	99.026				
20	0.150	0.000	0.000	45	4.472	4.009	16.518	70	133.103	0.265	99.291				
21	0.172	0.000	0.000	46	5.122	4.879	21.398	71	152.453	0.231	99.522				
22	0.197	0.000	0.000	47	5.867	5.844	27.242	72	174.616	0.197	99.719				
23	0.226	0.000	0.000	48	6.720	6.798	34.041	73	200.000	0.160	99.879				
24	0.259	0.000	0.000	49	7.697	7.572	41.612	74	229.075	0.121	100.000				
25	0.296	0.000	0.000	50	8.816	7.983	49.595	75	262.376	0.000	100.000				

Figure A20 Particle size analysis by particle size analyzerof sample **L**

Volume shrinkage of ceramic tile sample

Table A1 Volume shrinkage of sample C_1firing varies temperature

Sample no	Temp. (°C)	Dried sample (cm)		Fired sample (cm)		Volume shrinkage		
		Diameter	Length	Diameter	Length	Dried (cm^3)	Fired (cm^3)	%
1	800	1.00	2.10	1.01	2.06	1.66	1.64	1.32
2		1.01	2.12	1.00	1.98	1.69	1.57	7.24
3		1.01	2.08	1.00	2.00	1.65	1.58	4.42
4		1.01	2.06	1.00	2.05	1.63	1.60	2.07
5		1.01	2.12	1.00	2.01	1.68	1.59	5.57
6	900	1.00	2.03	0.99	2.01	1.61	1.55	3.53
7		1.00	2.02	0.99	2.00	1.60	1.54	3.34
8		1.01	2.02	0.99	2.01	1.60	1.55	3.25
9		1.01	2.04	0.99	1.98	1.62	1.52	5.91
10		1.01	2.08	0.99	1.99	1.65	1.54	6.88
11	1,000	1.00	2.05	0.99	1.97	1.62	1.51	6.76
12		1.01	2.05	0.98	1.99	1.63	1.51	7.13
13		1.01	2.03	0.99	1.96	1.61	1.50	7.06
14		1.01	2.05	0.98	2.00	1.63	1.51	7.03
15		1.01	1.92	1.00	1.91	1.53	1.50	1.60
16	1,100	0.97	2.06	0.93	1.76	1.51	1.18	21.57
17		1.00	2.05	0.92	1.78	1.61	1.19	26.28
18		1.00	2.10	0.93	1.74	1.65	1.17	29.26
19		1.00	2.08	0.93	1.76	1.65	1.20	27.25
20		1.00	2.06	0.93	1.78	1.61	1.21	25.13
21	1,150	1.00	2.05	0.93	1.81	1.61	1.23	23.80
22		1.00	2.08	0.93	1.75	1.63	1.18	27.69
23		1.00	2.07	0.93	1.78	1.62	1.20	26.06
24		1.00	2.13	0.93	1.77	1.68	1.20	28.27
25		1.00	2.12	0.93	1.77	1.66	1.20	27.66
26	1,200	1.00	2.12	0.93	2.10	1.68	1.43	14.84
27		1.01	2.10	1.00	2.05	1.67	1.63	2.58
28		1.01	2.12	1.00	2.08	1.69	1.62	3.92
29		1.01	2.10	1.00	2.10	1.67	1.65	1.18
30		1.01	2.11	1.00	2.08	1.68	1.64	2.14

Table A2 Volume shrinkage of sample C_2 firing at varies temperature

sample no	Temp. (°C)	Dried sample (cm)		Fired sample (cm)		Volume shrinkage		
		Diameter	Length	Diameter	Length	Dried (cm^3)	Fired (cm^3)	%
1	800	1.008	1.954	1.006	1.950	1.56	1.55	0.60
2		1.008	2.002	1.004	2.000	1.60	1.58	0.89
3		1.008	2.020	1.004	1.880	1.61	1.49	7.67
4		1.004	1.996	0.998	1.990	1.58	1.56	1.49
5		1.006	2.024	1.000	2.017	1.61	1.58	1.53
6	900	1.006	1.962	0.992	1.920	1.56	1.48	4.85
7		1.006	1.976	0.992	1.934	1.57	1.49	4.83
8		1.005	1.972	0.996	1.934	1.56	1.51	3.68
9		1.006	1.924	0.994	1.892	1.53	1.47	4.00
10		1.005	1.998	0.996	1.946	1.58	1.52	4.34
11	1,000	1.004	1.982	0.990	1.932	1.57	1.49	5.22
12		1.006	1.898	0.988	1.842	1.51	1.41	6.39
13		1.006	1.984	0.988	1.932	1.58	1.48	6.07
14		1.006	1.998	0.984	1.916	1.59	1.46	8.25
15		1.006	1.966	0.990	1.900	1.56	1.46	6.41
16	1,100	1.008	1.931	0.992	1.878	1.54	1.45	5.81
17		1.004	1.952	0.890	1.752	1.54	1.09	29.47
18		0.998	1.980	0.891	1.748	1.55	1.09	29.63
19		1.002	1.996	0.890	1.760	1.57	1.09	30.43
20		1.006	1.956	0.887	1.756	1.55	1.08	30.21
21	1,150	1.000	2.048	0.889	1.740	1.61	1.08	32.85
22		1.012	2.038	0.894	1.716	1.64	1.08	34.29
23		1.004	2.045	0.879	1.732	1.62	1.05	35.08
24		1.002	2.020	0.889	1.722	1.59	1.07	32.90
25		1.010	2.060	0.889	1.740	1.65	1.08	34.56
26	1,200	1.006	2.048	1.002	1.950	1.63	1.54	5.54
27		1.008	2.038	1.010	2.000	1.63	1.60	1.47
28		1.008	2.045	1.006	1.880	1.63	1.49	8.43
29		1.004	2.020	1.011	1.990	1.60	1.60	0.11
30		1.006	2.060	1.007	2.017	1.64	1.61	1.89

Table A3 Volume shrinkage of sample C_3 firing at varies temperature

Sample no	Temp. (°C)	Dried sample (cm)		Fired sample (cm)		Volume shrinkage		
		Diameter	Length	Diameter	Length	Dried (cm^3)	Fired (cm^3)	%
1	800	1.01	2.13	1.00	2.04	1.69	1.59	5.74
2		1.01	2.09	0.99	2.03	1.66	1.57	5.46
3		1.01	2.12	1.00	2.06	1.68	1.61	4.45
4		1.01	2.10	1.00	2.05	1.67	1.59	4.31
5		1.01	2.08	1.00	2.06	1.65	1.62	2.04
6	900	1.01	2.05	0.99	1.99	1.64	1.54	5.79
7		1.01	2.07	0.99	1.98	1.64	1.53	6.72
8		1.01	2.10	1.00	1.97	1.67	1.54	7.40
9		1.01	2.03	0.99	1.99	1.61	1.55	4.01
10		1.01	2.03	0.99	2.02	1.61	1.56	3.15
11	1,000	1.01	2.06	0.98	1.98	1.63	1.48	9.21
12		1.01	2.05	0.98	1.97	1.63	1.48	9.08
13		1.01	2.06	0.98	1.97	1.65	1.48	10.06
14		1.01	2.06	0.98	1.97	1.64	1.47	10.34
15		1.01	2.06	0.97	2.05	1.64	1.51	7.96
16	1,100	1.00	2.07	0.90	1.84	1.62	1.16	28.18
17		1.00	2.10	0.90	1.81	1.66	1.14	31.29
18		1.01	2.03	0.90	1.83	1.62	1.16	28.06
19		1.00	2.03	0.90	1.81	1.60	1.15	28.24
20		1.00	2.06	0.89	1.83	1.63	1.14	29.73
21	1,150	1.00	2.05	0.89	1.82	1.61	1.13	30.06
22		1.00	2.06	0.89	1.80	1.61	1.11	31.11
23		1.00	2.06	0.89	1.80	1.62	1.11	31.46
24		1.00	2.10	0.89	1.81	1.64	1.11	32.08
25		1.00	2.03	0.89	1.82	1.59	1.12	29.65
26	1,200	1.01	2.03	0.90	1.98	1.61	1.25	22.53
27		1.01	2.06	0.95	1.97	1.63	1.40	14.29
28		1.01	2.06	0.90	1.99	1.64	1.27	22.76
29		1.00	2.06	0.95	2.02	1.61	1.44	11.04
30		1.00	2.05	0.95	1.98	1.61	1.39	13.15

Table A4 Volume shrinkage of sample P_1 firing at varies temperature

sample no	Temp. (°C)	Dried sample (cm)		Fired sample (cm)		Volume shrinkage		
		Diameter	Length	Diameter	Length	Dried (cm^3)	Fired (cm^3)	%
1	800	1.01	1.90	1.00	1.88	1.52	1.48	2.42
2		1.01	1.94	1.00	1.93	1.55	1.52	1.70
3		1.00	1.90	0.99	1.88	1.49	1.44	3.22
4		1.00	1.91	1.00	1.91	1.50	1.49	0.96
5		1.00	1.90	1.00	1.88	1.50	1.47	1.94
6	900	1.00	1.92	0.99	1.88	1.50	1.44	4.08
7		1.00	1.94	0.99	1.90	1.52	1.45	4.78
8		1.00	1.93	0.99	1.87	1.52	1.43	5.60
9		1.00	1.94	1.00	1.89	1.54	1.47	4.02
10		1.00	1.93	0.98	1.89	1.52	1.43	5.99
11	1,000	1.00	1.92	0.96	1.83	1.51	1.32	12.56
12		1.00	1.93	0.96	1.80	1.52	1.30	14.20
13		1.00	2.00	0.96	1.90	1.57	1.37	12.45
14		1.00	2.00	0.96	1.91	1.57	1.38	11.99
15		1.00	1.94	0.96	1.87	1.52	1.36	10.52
16	1,100	1.01	1.95	0.91	1.74	1.56	1.12	27.81
17		1.01	1.97	0.90	1.79	1.58	1.14	27.61
18		1.00	1.97	0.90	1.77	1.54	1.13	26.55
19		1.00	1.91	0.90	1.76	1.50	1.13	24.68
20		1.00	1.96	0.90	1.76	1.54	1.13	26.67
21	1,150	1.00	1.98	0.90	1.76	1.56	1.12	28.27
22		1.00	1.95	0.90	1.75	1.54	1.12	27.54
23		1.00	1.96	0.90	1.76	1.55	1.12	27.76
24		1.01	1.99	0.90	1.77	1.60	1.13	29.57
25		1.00	1.95	0.90	1.74	1.53	1.12	27.27
26	1,200	1.00	2.00	0.91	1.78	1.57	1.16	25.78
27		1.00	1.99	0.91	1.80	1.56	1.16	25.43
28		1.00	1.96	0.91	1.76	1.54	1.15	25.53
29		1.00	1.96	0.91	1.78	1.55	1.16	25.20
30		1.01	1.96	0.91	1.77	1.57	1.14	27.59

Table A5 Volume shrinkage of sample P_2 firing at varies temperature

sample no	Temp. (°C)	Dried sample (cm)		Fired sample (cm)		Volume shrinkage		
		Diameter	Length	Diameter	Length	Dried (cm^3)	Fired (cm^3)	%
1	800	1.003	1.880	0.998	1.746	1.485	1.365	8.05
2		1.001	1.930	0.998	1.765	1.518	1.380	9.10
3		1.001	1.880	0.998	1.843	1.479	1.441	2.55
4		1.002	1.907	0.998	1.809	1.503	1.414	5.89
5		1.000	1.880	0.998	1.795	1.476	1.403	4.90
6	900	0.998	1.883	0.987	1.758	1.472	1.344	8.69
7		0.998	1.904	0.985	1.785	1.489	1.360	8.68
8		0.998	1.874	0.983	1.724	1.465	1.308	10.75
9		0.996	1.894	0.985	1.775	1.475	1.352	8.34
10		0.998	1.885	0.980	1.694	1.474	1.277	13.35
11	1,000	0.996	1.827	0.956	1.707	1.423	1.225	13.92
12		0.996	1.804	0.956	1.688	1.405	1.211	13.79
13		0.998	1.904	0.959	1.701	1.489	1.228	17.51
14		1.004	1.910	0.955	1.830	1.511	1.310	13.31
15		0.998	1.870	0.958	1.675	1.462	1.207	17.46
16	1,100	0.998	1.885	0.930	1.638	1.474	1.112	24.54
17		1.000	1.827	0.927	1.659	1.434	1.119	21.97
18		0.998	1.804	0.912	1.672	1.410	1.092	22.60
19		0.998	1.904	0.925	1.645	1.489	1.105	25.78
20		0.998	1.910	0.936	1.660	1.493	1.142	23.55
21	1,150	0.996	1.880	0.926	1.652	1.464	1.112	24.05
22		1.001	1.883	0.929	1.669	1.481	1.131	23.66
23		1.002	1.904	0.923	1.647	1.501	1.101	26.60
24		0.999	1.874	0.926	1.640	1.468	1.104	24.81
25		1.001	1.894	0.928	1.642	1.490	1.110	25.49
26	1,200	1.002	1.874	0.985	1.737	1.477	1.323	10.43
27		1.000	1.894	0.986	1.741	1.487	1.329	10.63
28		0.998	1.885	0.981	1.732	1.474	1.308	11.22
29		0.998	1.827	0.991	1.730	1.428	1.334	6.63
30		0.996	1.804	0.984	1.785	1.405	1.357	3.42

Table A6 Volume shrinkage of sample L firing at varies temperature

sample no	Temp. (°C)	Dried sample (cm)		Fired sample (cm)		Volume shrinkage		
		Diameter	Length	Diameter	Length	Dried (cm^3)	Fired (cm^3)	%
1	800	1.01	1.99	1.00	1.98	1.587	1.568	1.19
2		1.01	2.02	1.00	2.01	1.608	1.586	1.38
3		1.00	2.00	1.00	2.00	1.583	1.573	0.60
4		1.01	1.97	1.00	1.96	1.565	1.553	0.75
5		1.00	2.04	1.00	2.04	1.616	1.607	0.54
6	900	1.00	2.05	0.99	1.99	1.616	1.542	4.57
7		1.00	2.00	0.99	1.95	1.570	1.506	4.10
8		1.00	2.09	1.00	1.92	1.654	1.497	9.50
9		1.01	2.01	1.00	1.93	1.597	1.501	6.03
10		1.00	2.02	1.00	1.92	1.586	1.494	5.81
11	1,000	1.01	2.04	0.98	1.97	1.627	1.484	8.81
12		1.01	2.02	1.00	1.80	1.605	1.413	11.95
13		1.01	2.01	1.01	1.83	1.597	1.456	8.79
14		1.00	2.04	1.00	1.80	1.610	1.424	11.55
15		1.00	2.08	1.00	1.83	1.642	1.440	12.32
16	1,100	1.00	2.02	0.91	1.72	1.588	1.117	29.67
17		1.00	2.03	0.92	1.70	1.590	1.130	28.93
18		1.00	2.01	0.93	1.68	1.590	1.139	28.37
19		1.01	2.00	0.95	1.73	1.589	1.228	22.70
20		1.00	2.04	0.95	1.78	1.614	1.246	22.83
21	1,150	1.00	2.03	0.92	1.69	1.594	1.131	29.01
22		1.00	2.00	0.93	1.71	1.564	1.154	26.22
23		1.00	2.06	0.94	1.71	1.607	1.184	26.29
24		1.00	1.98	0.92	1.75	1.554	1.166	25.00
25		1.00	2.00	0.92	1.72	1.570	1.139	27.42
26	1,200	1.01	2.00	0.96	1.88	1.597	1.354	15.24
27		1.00	2.01	0.96	1.87	1.584	1.339	15.49
28		1.00	2.05	0.94	1.85	1.622	1.294	20.26
29		1.00	1.99	0.96	1.89	1.564	1.363	12.87
30		1.01	2.03	0.95	1.86	1.609	1.323	17.79

Table A7 Volume shrinkage of sample L firing at varies temperature

sample no	Temp. (°C)	Dried sample (cm)		Fired sample (cm)		Volume shrinkage		
		Diameter	Length	Diameter	Length	Dried (cm^3)	Fired (cm^3)	%
1	800	1.01	2.10	1.00	2.09	1.675	1.639	2.14
2		1.01	2.12	1.01	2.11	1.701	1.681	1.15
3		1.02	2.14	1.01	2.10	1.748	1.695	3.03
4		1.02	2.08	1.01	2.07	1.697	1.661	2.14
5		1.02	2.06	1.01	2.03	1.682	1.628	3.24
6	900	1.02	2.12	1.01	2.05	1.730	1.638	5.28
7		1.03	2.11	1.03	2.10	1.757	1.730	1.53
8		1.01	2.15	1.00	2.12	1.706	1.665	2.45
9		1.02	2.12	1.00	2.11	1.733	1.659	4.26
10		1.03	2.09	1.02	2.05	1.739	1.680	3.39
11	1,000	1.00	2.05	1.00	1.82	1.625	1.426	12.29
12		1.00	2.05	1.00	1.82	1.622	1.426	12.12
13		1.01	2.11	0.95	1.83	1.688	1.309	22.46
14		1.00	2.05	0.96	1.83	1.622	1.316	18.89
15		1.00	2.09	0.95	1.82	1.638	1.299	20.68
16	1,100	1.00	2.10	0.96	1.85	1.662	1.326	20.21
17		1.00	2.06	0.92	1.84	1.619	1.223	24.47
18		1.00	2.05	0.93	1.83	1.621	1.237	23.66
19		1.00	2.10	0.92	1.85	1.652	1.236	25.19
20		1.00	2.08	0.92	1.86	1.639	1.244	24.12
21	1,150	1.00	2.06	0.93	1.99	1.630	1.348	17.29
22		1.00	2.05	0.93	1.93	1.622	1.301	19.78
23		1.00	2.08	0.92	1.93	1.646	1.273	22.68
24		1.01	2.07	0.93	1.92	1.643	1.293	21.29
25		1.01	2.13	0.93	1.94	1.697	1.319	22.31
26	1,200	1.01	2.12	0.97	2.06	1.683	1.504	10.64
27		1.00	2.12	0.97	2.06	1.678	1.507	10.18
28		1.01	2.10	0.96	2.04	1.668	1.480	11.31
29		1.00	2.12	0.97	2.07	1.666	1.520	8.73
30		1.00	2.10	0.97	2.06	1.662	1.504	9.47

Water absorption data of ceramic tile samples

Table A8 Ceramic tile samples of the drilling mud wastes from petroleum drill holes at Fang (sample C_1)

Sample	Temperature (°C)	Weight (g)			Water absorption (%)
		Dry	Suspended	Saturated	
C_{1-1}	800	2.685	1.597	3.289	22.495
C_{1-6}	900	2.661	1.570	3.213	20.744
C_{1-11}	1,000	2.586	1.489	3.010	16.396
C_{1-16}	1,100	2.573	1.433	2.698	4.858
C_{1-21}	1,150	2.552	1.403	2.605	2.077
C_{1-26}	1,200	2.540	1.392	2.580	1.595

Table A9 Ceramic tile samples of the drilling mud wastes from petroleum drill holes at Fang (sample C_2)

Sample	Temperature (°C)	Weight (g)			Water absorption (%)
		Dry	Suspended	Saturated	
C_{2-1}	800	2.610	1.513	3.216	23.218
C_{2-6}	900	2.562	1.480	3.105	21.194
C_{2-11}	1,000	2.555	1.441	2.986	16.869
C_{2-16}	1,100	2.543	1.405	2.691	5.820
C_{2-21}	1,150	2.538	1.398	2.580	1.655
C_{2-26}	1,200	2.534	1.391	2.565	1.223

Table A10 Ceramic tile samples of the drilling mud wastes from petroleum drill holes at Fang (sample C_3)

Sample	Temperature (°C)	Weight (g)			Water absorption (%)
		Dry	Suspended	Saturated	
C_{3-1}	800	2.600	1.609	3.230	24.231
C_{3-6}	900	2.558	1.560	3.062	19.703
C_{3-11}	1,000	2.551	1.526	2.961	16.072
C_{3-16}	1,100	2.540	1.456	2.740	7.895
C_{3-21}	1,150	2.535	1.415	2.610	2.959
C_{3-26}	1,200	2.535	1.398	2.580	1.795

Table A11 Ceramic tile samples of the drilling mud wastes from petroleum drill holes at Phitsanulok basin (sample P_1)

Sample	Temperature (°C)	Weight (g)			Water absorption (%)
		Dry	Suspended	Saturated	
P_{1-1}	800	2.650	1.604	3.100	16.963
P_{1-6}	900	2.638	1.579	3.041	15.277
P_{1-11}	1,000	2.624	1.561	2.936	11.890
P_{1-19}	1,100	2.615	1.530	2.723	4.138
P_{1-21}	1,150	2.608	1.522	2.678	2.684
P_{1-26}	1,200	2.620	1.510	2.648	1.069

Table A12 Ceramic tile samples of the drilling mud wastes from petroleum drill holes at Phitsanulok basin (sample P_2)

Sample	Temperature (°C)	Weight (g)			Water absorption (%)
		Dry	Suspended	Saturated	
P_{2-1}	800	2.619	1.665	3.013	15.044
P_{2-6}	900	2.609	1.631	2.948	12.993
P_{2-11}	1,000	2.598	1.598	2.834	9.084
P_{2-16}	1,100	2.595	1.540	2.710	4.432
P_{2-21}	1,150	2.582	1.501	2.659	2.998
P_{2-26}	1,200	2.558	1.446	2.590	1.251

Table A13 Ceramic tile samples of the drilling mud wastes from petroleum drill holes at Mae Thabasin(sample M)

Sample	Temperature (°C)	Weight (g)			Water absorption (%)
		Dry	Suspended	Saturated	
M_1	800	2.705	1.659	3.326	22.957
M_6	900	2.674	1.603	3.246	21.391
M_{11}	1,000	2.651	1.522	3.099	16.899
M_{16}	1,100	2.637	1.465	2.890	9.615
M_{21}	1,150	2.582	1.387	2.712	5.043
M26	1,200	2.575	1.380	2.624	1.903

Table A14 Ceramic tile samples of the drilling mud wastes from petroleum drill holes at Lampangbasin(sample L)

Sample	Temperature (°C)	Weight (g)			Water absorption (%)
		Dry	Suspended	Saturated	
L_1	800	2.564	1.540	3.080	20.125
L_6	900	2.548	1.508	3.031	18.956
L_{11}	1,000	2.528	1.469	2.906	14.953
L_{16}	1,100	2.504	1.306	2.607	4.113
L_{21}	1,150	2.488	1.268	2.540	2.090
L_{26}	1,200	2.477	1.250	2.506	1.187

Table A15 Building brick samples made from the drilling mud wastes of petroleum drill holes only of Phitsanulok basin fired temperature at 1,000°C.

Sample No.	Dry mass (g)	Saturation weight (g)	Water Absorption (%)
1	431.58	498.48	15.50
2	448.64	515.19	14.83
3	454.75	515.2	13.29
4	427.76	488.66	14.24
5	444.68	510.11	14.71
6	438.6	507.52	15.71
7	441.91	510.26	15.47
8	429.6	502.2	16.90
9	454.85	510.48	12.23
10	446.03	511.54	14.69
11	451.6	522.34	15.66
12	467.74	524.3	12.09
13	431.89	499.7	15.70
14	435.89	504.57	15.76
15	430.57	504.08	17.07
Average			12.98

Results of apparent porosity of ceramic tile samples

Table A16 Sample of the drilling mud wastes from petroleum drill holes fromFang basin (sample C_1)

Sample	Temp. (°C)	Dry Weight (g)	Suspended weight (g)	Saturation weight (g)	External volume (cm^3)	Apparent porosity (%)
C_{1-1}	800	2.685	1.597	3.289	1.692	35.697
C_{1-6}	900	2.661	1.570	3.213	1.643	33.597
C_{1-11}	1,000	2.586	1.489	3.010	1.521	27.876
C_{1-16}	1,100	2.573	1.433	2.698	1.265	9.881
C_{1-21}	1,150	2.552	1.403	2.605	1.202	4.409
C_{1-26}	1,200	2.540	1.392	2.580	1.188	3.409

Table A17 Sample of the drilling mud wastes from petroleum drill holes from Fang basin (sample C_2)

Sample	Temp. (°C)	Dry Weight (g)	Suspended weight (g)	Saturation weight (g)	External volume (cm^3)	Apparent porosity (%)
C_{2-1}	800	2.610	1.513	3.216	1.703	35.584
C_{2-6}	900	2.562	1.480	3.105	1.625	33.415
C_{2-11}	1,000	2.555	1.441	2.986	1.545	27.896
C_{2-16}	1,100	2.543	1.405	2.691	1.286	11.509
C_{2-21}	1,150	2.538	1.398	2.580	1.182	3.553
C_{2-26}	1,200	2.534	1.391	2.565	1.174	2.641

Table A18 Sample of the drilling mud wastes from petroleum drill holes from Fang basin (sample C_3)

Sample	Temp. (°C)	Dry Weight (g)	Suspended weight (g)	Saturation weight (g)	External volume (cm^3)	Apparent porosity (%)
C_{3-1}	800	2.600	1.609	3.230	1.621	38.865
C_{3-6}	900	2.558	1.560	3.062	1.502	33.555
C_{3-11}	1,000	2.551	1.526	2.961	1.435	28.571
C_{3-16}	1,100	2.540	1.456	2.740	1.284	15.615
C_{3-21}	1,150	2.535	1.415	2.610	1.195	6.276
C_{3-26}	1,200	2.535	1.398	2.580	1.182	3.849

Table A19 Sample of the drilling mud wastes from petroleum drill holes from Phitsanulok basin (sample P_1)

Sample	Temp. (°C)	Dry Weight (g)	Suspended weight (g)	Saturation weight (g)	External volume (cm^3)	Apparent porosity (%)
P_{1-1}	800	2.650	1.604	3.100	1.496	30.053
P_{1-6}	900	2.638	1.579	3.041	1.462	27.565
P_{1-11}	1,000	2.624	1.561	2.936	1.375	22.691
P_{1-19}	1,100	2.615	1.530	2.723	1.193	9.070
P_{1-21}	1,150	2.608	1.522	2.678	1.156	6.055
P_{1-26}	1,200	2.620	1.510	2.648	1.138	2.460

Table A20 Sample of the drilling mud wastes from petroleum drill holes from Phitsanulok basin (sample P_2)

Sample	Temp. (°C)	Dry Weight (g)	Suspended weight (g)	Saturation weight (g)	External volume (cm^3)	Apparent porosity (%)
$P_{2\text{-}1}$	800	2.619	1.665	3.013	1.348	29.228
$P_{2\text{-}6}$	900	2.609	1.631	2.948	1.317	25.740
$P_{2\text{-}11}$	1,000	2.598	1.598	2.834	1.236	19.094
$P_{2\text{-}16}$	1,100	2.595	1.540	2.710	1.170	9.829
$P_{2\text{-}21}$	1,150	2.582	1.501	2.659	1.158	6.684
$P_{2\text{-}26}$	1,200	2.558	1.446	2.590	1.144	2.797

Table A21 Sample of the drilling mud wastes from petroleum drill holes from Mae Tha basin (sample M)

Sample	Temp. (°C)	Dry Weight (g)	Suspended weight (g)	Saturation weight (g)	External volume (cm^3)	Apparent porosity (%)
M_1	800	2.705	1.659	3.3	1.667	37.253
M_6	900	2.674	1.603	3.246	1.643	34.814
M_{11}	1,000	2.651	1.522	3.099	1.577	28.408
M_{16}	1,100	2.637	1.465	2.890	1.425	17.789
M_{21}	1,150	2.582	1.387	2.712	1.325	9.826
M_{26}	1,200	2.575	1.380	2.624	1.244	3.939

Table A22 Ceramic tile samples of the drilling mud wastes from petroleum drill holes from Lampang basin (sample L)

Sample	Temp. (°C)	Dry Weight (g)	Suspended weight (g)	Saturation weight (g)	External volume (cm^3)	Apparent porosity (%)
L_1	800	2.564	1.540	3.080	1.540	33.506
L_6	900	2.548	1.508	3.031	1.523	31.714
L_{11}	1,000	2.528	1.469	2.906	1.437	26.305
L_{16}	1,100	2.504	1.306	2.607	1.301	7.917
L_{21}	1,150	2.488	1.268	2.540	1.272	4.088
L_{26}	1,200	2.477	1.250	2.506	1.256	2.341

Results of apparent relative density

Table A23 Ceramic tile samples of the drilling mud wastes from Fang basin (sample C_1)

Sample	Temperature (°C)	Dry Weight (g)	Suspended weight(g)	After boiled weight(g)	Apparent relative density (g/cm^3)
C_{1-1}	800	2.685	1.597	3.289	2.468
C_{1-6}	900	2.661	1.570	3.213	2.439
C_{1-11}	1,000	2.586	1.489	3.010	2.357
C_{1-16}	1,100	2.573	1.433	2.698	2.257
C_{1-21}	1,150	2.552	1.403	2.605	2.221
C_{1-26}	1,200	2.540	1.392	2.580	2.213

Table A24 Ceramic tile samples made of the drilling mud wastes from Fang basin (sample C_2)

Sample	Temperature (°C)	Dry Weight (g)	Suspended weight (g)	After boiled weight (g)	Apparent relative density (g/cm^3)
$C_{2\text{-}1}$	800	2.610	1.513	3.216	2.379
$C_{2\text{-}6}$	900	2.562	1.480	3.105	2.368
$C_{2\text{-}11}$	1,000	2.555	1.441	2.986	2.294
$C_{2\text{-}16}$	1,100	2.543	1.405	2.691	2.235
$C_{2\text{-}21}$	1,150	2.538	1.398	2.580	2.226
$C_{2\text{-}26}$	1,200	2.534	1.391	2.565	2.217

Table A25 Ceramic tile samples of the drilling mud wastes from Fang basin (sample C_3)

Sample	Temperature (°C)	Dry Weight (g)	Suspended weight (g)	After boiled weight (g)	Apparent relative density (g/cm^3)
$C_{3\text{-}1}$	800	2.600	1.609	3.230	2.624
$C_{3\text{-}6}$	900	2.558	1.560	3.062	2.563
$C_{3\text{-}11}$	1,000	2.551	1.526	2.961	2.489
$C_{3\text{-}16}$	1,100	2.540	1.456	2.740	2.344
$C_{3\text{-}21}$	1,150	2.535	1.415	2.610	2.263
$C_{3\text{-}26}$	1,200	2.535	1.398	2.580	2.230

Table A26 Ceramic tile samples of the drilling mud wastes from Phitsanulok basin (sample P_1)

Sample	Temperature (°C)	Dry Weight (g)	Suspended weight (g)	After boiled weight (g)	Apparent relative density (g/cm^3)
P_{1-1}	800	2.650	1.604	3.100	2.533
P_{1-6}	900	2.638	1.579	3.041	2.491
P_{1-11}	1,000	2.624	1.561	2.936	2.468
P_{1-19}	1,100	2.615	1.530	2.723	2.410
P_{1-21}	1,150	2.608	1.522	2.678	2.401
P_{1-26}	1,200	2.620	1.510	2.648	2.360

Table A27 Ceramic tile samples of the drilling mud wastes from Phitsanulok basin (sample P_2)

Sample	Temperature (°C)	Dry Weight (g)	Suspended weight (g)	After boiled weight (g)	Apparent relative density (g/cm^3)
P_{2-1}	800	2.619	1.665	3.013	2.745
P_{2-6}	900	2.609	1.631	2.948	2.668
P_{2-11}	1,000	2.598	1.598	2.834	2.598
P_{2-16}	1,100	2.595	1.540	2.710	2.460
P_{2-21}	1,150	2.582	1.501	2.659	2.389
P_{2-26}	1,200	2.558	1.446	2.590	2.300

Table A28 Ceramic tile samples made of the drilling mud wastes from Mae Tha basin (Sample M)

Sample	Temperature (°C)	Dry Weight (g)	Suspended weight (g)	After boiled weight (g)	Apparent relative density (g/cm^3)
M_1	800	2.705	1.659	3.326	2.586
M_6	900	2.674	1.603	3.246	2.497
M_{11}	1,000	2.651	1.522	3.099	2.348
M_{16}	1,100	2.637	1.465	2.890	2.251
M_{21}	1,150	2.582	1.387	2.712	2.161
M_{26}	1,200	2.575	1.380	2.624	2.155

Table A29 Ceramic tile samples of the drilling mud wastes from Lampang basin (Sample L)

Sample	Temperature (°C)	Dry Weight (g)	Suspended weight (g)	After boiled weight (g)	Apparent relative density (g/cm^3)
L_1	800	2.564	1.540	3.080	2.504
L_6	900	2.548	1.508	3.031	2.450
L_{11}	1,000	2.528	1.469	2.906	2.387
L_{16}	1,100	2.504	1.306	2.607	2.090
L_{21}	1,150	2.488	1.268	2.540	2.039
L_{26}	1,200	2.477	1.250	2.506	2.019

Results of bulk density of ceramic tile samples

Table A30 Drilling mud wastes from Fang basin (sample C_1)

Sample	Temp. (°C)	Dry Weight(g)	Suspended weight (g)	After boiled weight (g)	Bulk density (g/cm^3)
C_{1-1}	800	2.685	1.597	3.289	1.587
C_{1-6}	900	2.661	1.570	3.213	1.620
C_{1-11}	1,000	2.586	1.489	3.010	1.700
C_{1-16}	1,100	2.573	1.433	2.698	2.034
C_{1-21}	1,150	2.552	1.403	2.605	2.123
C_{1-26}	1,200	2.540	1.392	2.580	2.138

Table A31 Drilling mud wastes from Fang basin (sample C_2)

Sample	Temp.(°C)	Dry Weight(g)	Suspended weight(g)	After boiled weight(g)	Bulk density (g/cm^3)
C_{2-1}	800	2.610	1.513	3.216	1.533
C_{2-6}	900	2.562	1.480	3.105	1.577
C_{2-11}	1,000	2.555	1.441	2.986	1.654
C_{2-16}	1,100	2.543	1.405	2.691	1.977
C_{2-21}	1,150	2.538	1.398	2.580	2.147
C_{2-26}	1,200	2.534	1.391	2.565	2.158

Table A32 Drilling mud wastes from Fang basin (sample C_3)

Sample	Temp.(°C)	Dry Weight(g)	Suspended weight(g)	After boiled weight(g)	Bulk density (g/cm^3)
$C_{3\text{-}1}$	800	2.600	1.609	3.230	1.604
$C_{3\text{-}6}$	900	2.558	1.560	3.062	1.703
$C_{3\text{-}11}$	1,000	2.551	1.526	2.961	1.778
$C_{3\text{-}16}$	1,100	2.540	1.456	2.740	1.978
$C_{3\text{-}21}$	1,150	2.535	1.415	2.610	2.121
$C_{3\text{-}26}$	1,200	2.535	1.398	2.580	2.144

Table A33 Drilling mud wastes from Phitsanulok basin (sample P_1)

Sample	Temp. (°C)	Dry Weight(g)	Suspended weight(g)	After boiled weight(g)	Bulk density (g/cm^3)
$P_{1\text{-}1}$	800	2.650	1.604	3.100	1.772
$P_{1\text{-}6}$	900	2.638	1.579	3.041	1.804
P1-11	1,000	2.624	1.561	2.936	1.908
P1-19	1,100	2.615	1.530	2.723	2.192
P1-21	1,150	2.608	1.522	2.678	2.256
P1-26	1,200	2.620	1.510	2.648	2.302

Table A34 Drilling mud wastes from Phitsanulok basin (sample P_2)

Sample	Temp. (°C)	Dry Weight (g)	Suspended weight (g)	After boiled weight (g)	Bulk density (g/cm^3)
P_{2-1}	800	2.619	1.665	3.013	1.943
P_{2-6}	900	2.609	1.631	2.948	1.981
P_{2-11}	1,000	2.598	1.598	2.834	2.102
P_{2-16}	1,100	2.595	1.540	2.710	2.218
P_{2-21}	1,150	2.582	1.501	2.659	2.229
P_{2-26}	1,200	2.558	1.446	2.590	2.236

Table A35 Drilling mud wastes from Mae tha basin (sample M)

Sample	Temp. (°C)	Dry Weight (g)	Suspended weight (g)	After boiled weight (g)	Bulk density (g/cm^3)
M_1	800	2.705	1.659	3.326	1.623
M_6	900	2.674	1.603	3.246	1.628
M_{11}	1,000	2.651	1.522	3.099	1.681
M_{16}	1,100	2.637	1.465	2.890	1.850
M_{21}	1,150	2.582	1.387	2.712	1.949
M_{26}	1,200	2.575	1.380	2.624	2.070

Table A36 Bulk density of drilling mud wastes from Lampang basin (sample L)

Sample	Temp. (°C)	Dry Weight(g)	Suspended weight(g)	After boiled weight(g)	Bulk density (g/cm^3)
L_1	800	2.564	1.540	3.080	1.665
L_6	900	2.548	1.508	3.031	1.673
L_{11}	1,000	2.528	1.469	2.906	1.759
L_{16}	1,100	2.504	1.306	2.607	1.925
L_{21}	1,150	2.488	1.268	2.540	1.956
L_{26}	1,200	2.477	1.250	2.506	1.972

Results of compressive strength measurement of ceramic tile samples

Table A37 Compressive strength of ceramic tile samples from Fang basin (C_1)

Sample	Temperature (°C)	Cross-section area (cm^2)	Max Load (kg_f)	Compressive Strength	
				(kg_f/cm^2)	(MPa)
C_{1-1}	800	0.7933	72.86	91.84	9.01
C_{1-2}	800	0.7901	117.26	148.41	14.55
C_{1-3}	800	0.7933	96.01	121.02	11.87
C_{1-4}	800	0.8252	72.38	87.71	8.6
C_{1-5}	800	0.8091	100.15	123.77	12.14
C_{1-7}	900	0.7729	232.06	300.24	29.44
C_{1-8}	900	0.7729	207.89	268.97	26.38
C_{1-9}	900	0.7698	280.21	364.01	35.7
C_{1-10}	900	0.7729	267.62	346.25	33.96
C_{1-12}	1,000	0.7605	349.53	459.61	45.07
C_{1-13}	1,000	0.7636	459.49	601.74	59.01
C_{1-14}	1,000	0.7574	295.26	389.83	38.23
C_{1-15}	1,000	0.7854	181.56	231.17	22.67
C_{1-16}	1,100	0.6504	833.14	1280.97	125.62
C_{1-17}	1,100	0.6362	409.08	643.01	63.06
C_{1-18}	1,100	0.6604	510.26	772.66	75.77
C_{1-19}	1,100	0.649	1023.96	1577.75	154.73
C_{1-20}	1,100	0.65468	695.82	1062.84	104.23
C_{1-21}	1,150	0.6447	650.18	1008.5	98.9
C_{1-22}	1,150	0.6533	751.77	1150.73	112.86
C_{1-23}	1,150	0.6461	648.38	1003.53	98.41

Table A37 Compressive strength of ceramic tile samples from Fang basin (C_1) (continued)

Sample	Temperature (°C)	Cross-section area (cm^2)	Max Load (kg_f)	Compressive Strength	
				(kg_f/cm^2)	(MPa)
C_{1-24}	1,150	0.6561	627.1	955.81	93.73
C_{1-25}	1,150	0.6533	774.83	1186.03	116.32
C_{1-26}	1,200	0.7605	103.27	135.8	13.32
C_{1-27}	1,200	0.7528	117.75	156.41	15.34
C_{1-28}	1,200	0.7528	165.03	219.22	21.5
C_{1-29}	1,200	0.7451	200.77	269.46	26.43
C_{1-30}	1,200	0.762	149.64	196.38	19.26

Table A38 Compressive strength of ceramic tile samples from Fang basin (C_2)

Sample	Temperature (°C)	Cross-section area (cm^2)	Max Load (kg_f)	Compressive Strength	
				(kg_f/cm^2)	(MPa)
C_{2-1}	800	0.7543	129.06	171.10	16.78
C_{2-2}	800	0.7854	96.74	123.17	12.08
C_{2-3}	800	0.7682	141.14	183.73	18.02
C_{2-4}	800	0.798	92.70	116.16	11.39
C_{2-5}	800	0.7964	69.46	87.22	8.55
C_{2-8}	900	0.7729	265.26	343.20	33.66
C_{2-9}	900	0.7791	236.76	303.89	29.80
C_{2-10}	900	0.776	313.44	403.92	39.61
C_{2-12}	1,000	0.7791	307.76	395.01	38.74
C_{2-13}	1,000	0.7667	263.16	343.24	33.66

Table A38 Compressive strength of ceramic tile samples from Fang basin (C_2) (continued)

Sample	Temperature (°C)	Cross-section area (cm^2)	Max Load (kg_f)	Compressive Strength	
				(kg_f/cm^2)	(MPa)
C_{2-14}	1,000	0.7667	228.67	298.25	29.25
C_{2-15}	1,000	0.7605	288.51	379.37	37.21
C_{2-16}	1,100	0.6221	597.23	960.03	94.14
C_{2-17}	1,100	0.5648	743.49	1316.37	129.10
C_{2-18}	1,100	0.6291	1055.35	1677.55	164.51
C_{2-19}	1,100	0.6179	957.01	1548.80	151.88
C_{2-20}	1,100	0.6362	1087.79	1709.82	167.68
C_{2-21}	1,150	0.6263	568.32	907.42	88.99
C_{2-22}	1,150	0.6348	823.45	1297.18	127.22
C_{2-23}	1,150	0.6319	1139.35	1803.05	176.81
C_{2-24}	1,150	0.6221	988.90	1589.62	155.89
C_{2-25}	1,150	0.6277	414.38	660.16	64.74
C_{2-26}	1,200	0.7729	124.62	161.23	15.81
C_{2-27}	1,200	0.776	106.49	137.23	13.46
C_{2-28}	1,200	0.7791	116.51	149.54	14.66
C_{2-29}	1,200	0.7667	148.93	194.25	19.05
C_{2-30}	1,200	0.7823	116.24	148.59	14.57

Table A39 Compressive strength of ceramic tile samples from Fang basin (C_3)

Sample	Temperature (°C)	Cross-section area (cm^2)	Max Load (kg$_f$)	Compressive Strength	
				(kg$_f$/cm^2)	(MPa)
C_{3-2}	800	0.8139	81.27	99.85	9.79
C_{3-3}	800	0.8155	49.29	60.44	5.93
C_{3-4}	800	0.7932	67.23	84.76	8.31
C_{3-5}	800	0.7901	72.01	91.14	8.94
C_{3-7}	900	0.7698	297.73	386.77	37.93
C_{3-8}	900	0.7732	295.34	381.97	37.46
C_{3-9}	900	0.7823	284.91	364.19	35.72
C_{3-10}	900	0.776	230.99	297.67	29.19
C_{3-11}	1,000	0.7682	244.68	318.52	31.24
C_{3-12}	1,000	0.7436	258.86	348.12	34.14
C_{3-13}	1,000	0.7451	283.11	379.96	37.26
C_{3-14}	1,000	0.739	218.30	295.39	28.97
C_{3-15}	1,000	0.8044	232.04	288.46	28.29
C_{3-16}	1,100	0.6221	415.32	667.61	65.47
C_{3-17}	1,100	0.6277	1035.85	1650.23	161.83
C_{3-18}	1,100	0.639	747.50	1169.80	114.72
C_{3-19}	1,100	0.6447	747.50	1159.46	113.71
C_{3-20}	1,100	0.5568	583.51	1047.97	102.77
C_{3-21}	1,150	0.6235	696.11	1116.45	109.48
C_{3-22}	1,150	0.611	289.23	473.37	46.42
C_{3-23}	1,150	0.589	399.63	678.49	66.54

Table A39 Compressive strength of ceramic tile samples from Fang basin (C_3)(continued)

Sample	**Temperature (°C)**	**Cross-section area (cm^2)**	**Max Load (kg_f)**	**Compressive Strength**	
				(kg_f/cm^2)	**(MPa)**
C_{3-24}	1,150	0.5931	468.97	790.71	77.54
C_{3-25}	1,150	0.6138	670.32	1092.08	107.10
C_{3-26}	1,200	0.7088	204.02	287.84	28.23
C_{3-27}	1,200	0.7238	267.92	370.16	36.30
C_{3-28}	1,200	0.7118	291.15	409.04	40.11
C_{3-29}	1,200	0.7299	160.37	219.71	21.55
C_{3-30}	1,200	0.7103	138.79	195.40	19.16

Table A40 Compressive strength of ceramic tile samples from Fang basin (P_1)

Sample	**Temperature (°C)**	**Cross-section area (cm^2)**	**Max Load (kg_f)**	**Compressive Strength**	
				(kg_f/cm^2)	**(MPa)**
P_{1-1}	800	0.787	100.61	127.84	12.54
P_{1-2}	800	0.7885	122.34	155.15	15.21
P_{1-3}	800	0.7807	141.14	180.79	17.73
P_{1-4}	800	0.7807	128.79	164.96	16.18
P_{1-5}	800	0.7823	150.87	192.85	18.91
P_{1-6}	900	0.7651	185.70	242.71	23.80
P_{1-7}	900	0.7651	140.56	183.72	18.02

Table A40 Compressive strength of ceramic tile samples from Fang basin (P_1)(continued)

Sample	Temperature (°C)	Cross-section area (cm^2)	Max Load (kg_f)	Compressive Strength	
				(kg_f/cm^2)	(MPa)
P_{1-8}	900	0.762	240.54	315.67	30.96
P_{1-9}	900	0.7791	216.30	277.62	27.23
P_{1-10}	900	0.7605	226.15	297.37	29.16
P_{1-11}	1,000	0.7253	253.39	349.36	34.26
P_{1-12}	1,000	0.7223	323.87	448.38	43.97
P_{1-14}	1,000	0.7238	205.30	283.64	27.82
P_{1-15}	1,000	0.7299	254.52	348.70	34.20
P_{1-16}	1,100	0.6461	475.92	736.60	72.24
P_{1-17}	1,100	0.6404	518.85	810.20	79.45
P_{1-18}	1,100	0.6418	287.32	447.68	43.90
P_{1-20}	1,100	0.6404	313.36	489.33	47.99
P_{1-21}	1,150	0.6348	485.87	765.39	75.06
P_{1-22}	1,150	0.6376	254.35	398.93	39.12
P_{1-23}	1,150	0.6376	466.98	732.40	71.82
P_{1-24}	1,150	0.6362	263.08	413.53	40.55
P_{1-25}	1,150	0.6418	485.30	756.15	74.15
P_{1-26}	1,200	0.6533	435.29	666.30	65.34
P_{1-27}	1,200	0.649	139.47	214.90	21.07
P_{1-28}	1,200	0.6518	235.46	361.25	35.43
P_{1-29}	1,200	0.6518	273.57	419.71	41.16
P_{1-30}	1,200	0.6461	440.96	682.50	66.93

Table A41 Compressive strength of ceramic tile samples from Fang basin (P_2)

Sample	Temperature (°C)	Cross-section area (cm^2)	Max Load (kg_f)	Compressive Strength	
				(kg_f/cm^2)	(MPa)
P_{2-1}	800	0.7901	416.19	526.75	51.66
P_{2-2}	800	0.787	318.16	404.27	39.65
P_{2-3}	800	0.787	292.60	371.79	36.46
P_{2-4}	800	0.7885	236.93	300.48	29.47
P_{2-5}	800	0.7838	244.71	312.21	30.62
P_{2-7}	900	0.762	463.48	608.24	59.65
P_{2-8}	900	0.7589	325.09	428.38	42.01
P_{2-9}	900	0.762	495.28	649.97	63.74
P_{2-10}	900	0.7543	687.43	911.35	89.37
P_{2-11}	1,000	0.7178	570.54	794.85	77.95
P_{2-12}	1,000	0.7178	931.30	1297.44	127.24
P_{2-13}	1,000	0.7223	753.92	1043.78	102.36
P_{2-14}	1,000	0.7163	686.30	958.11	93.96
P_{2-15}	1,000	0.7208	591.16	820.15	80.43
P_{2-16}	1,100	0.6793	334.00	491.69	48.22
P_{2-17}	1,100	0.6749	160.60	237.97	23.34
P_{2-18}	1,100	0.6533	569.88	872.32	85.55
P_{2-19}	1,100	0.672	311.82	464.01	45.50
P_{2-20}	1,100	0.6881	1162.25	1689.08	165.65
P_{2-21}	1,150	0.6735	1164.04	1728.35	169.50
P_{2-22}	1,150	0.6778	1059.47	1563.10	153.28

Table A41 Compressive strength of ceramic tile samples from Fang basin (P_2) (continued)

Sample	Temperature (°C)	Cross-section area (cm^2)	Max Load (kg_f)	Compressive Strength	
				(kg_f/cm^2)	(MPa)
$P_{2\text{-}23}$	1,150	0.6691	964.82	1441.96	141.41
$P_{2\text{-}24}$	1,150	0.6735	880.61	1307.52	128.23
$P_{2\text{-}25}$	1,150	0.6764	1212.00	1791.84	175.73
$P_{2\text{-}26}$	1,200	0.762	1066.28	1399.32	137.22
$P_{2\text{-}27}$	1,200	0.7636	986.09	1291.37	126.65
$P_{2\text{-}28}$	1,200	0.7558	935.85	1238.23	121.42
$P_{2\text{-}29}$	1,200	0.7713	934.65	1211.78	118.83
$P_{2\text{-}30}$	1,200	0.7605	751.73	988.47	96.94

Table A42 Compressive strength of ceramic tile samples from Fang basin (M)

Sample	Temperature (°C)	Cross-section area (cm^2)	Max Load (kg_f)	Compressive Strength	
				(kg_f/cm^2)	(MPa)
M_2	800	0.798	12.57	15.75	1.54
M3	800	0.806	11.88	14.74	1.45
M4	800	0.8012	20.80	25.97	2.55
M5	800	0.8012	23.29	29.07	2.85
M7	900	0.8252	18.78	22.76	2.23
M8	900	0.8028	12.61	15.70	1.54
M9	900	0.8028	11.93	14.86	1.46
M10	900	0.8187	25.75	31.45	3.08

Table A42 Compressive strength of ceramic tile samples from Fang basin (M) (continued)

Sample	Temperature (°C)	Cross-section area (cm^2)	Max Load (kg$_f$)	Compressive Strength	
				(kg$_f$/cm^2)	(MPa)
M_{11}	1,000	0.7854	224.88	286.33	28.08
M_{12}	1,000	0.7148	492.27	688.68	67.54
M_{13}	1,000	0.7178	450.15	627.13	61.50
M_{14}	1,000	0.7148	347.85	486.65	47.72
M_{15}	1,000	0.7178	484.51	674.99	66.19
M_{16}	1,100	0.6793	421.88	621.05	60.90
M_{17}	1,100	0.6648	621.81	935.34	91.73
M_{18}	1,100	0.6749	519.01	769.02	75.41
M_{19}	1,100	0.6691	569.96	851.84	83.54
M_{20}	1,100	0.6691	663.18	991.15	97.20
M_{21}	1,150	0.6778	444.04	655.11	64.24
M_{22}	1,150	0.6764	390.05	576.66	56.55
M_{23}	1,150	0.6604	521.09	789.06	77.38
M_{24}	1,150	0.6749	396.67	587.75	57.64
M_{25}	1,150	0.6808	259.23	380.77	37.34
M_{26}	1,200	0.7314	312.77	427.63	41.94
M_{27}	1,200	0.7329	263.36	359.34	35.24
M_{28}	1,200	0.7253	409.37	564.42	55.35
M_{29}	1,200	0.7359	237.00	322.05	31.58
M_{30}	1,200	0.7314	236.22	322.97	31.67

Table A43 Compressive strength of ceramic tile samples from Fang basin (L)

Sample	Temperature (°C)	Cross-section area (cm^2)	Max Load (kg_f)	Compressive Strength	
				(kg_f/cm^2)	(MPa)
L_1	800	-	-	-	-
L_2	800	0.7964	99.19	124.55	12.21
L_3	800	0.8012	100.87	125.90	12.35
L_4	800	0.798	124.29	155.76	15.27
L_5	800	0.7996	65.30	81.67	8.01
L_6	900	0.7744	233.42	301.42	29.56
L_7	900	0.7729	263.90	341.44	33.48
L_8	900	0.7791	255.48	327.91	32.16
L_9	900	0.7791	269.10	345.39	33.87
L_{10}	900	0.7791	258.42	331.69	32.53
L_{11}	1,000	0.7543	310.43	411.54	40.36
L_{12}	1,000	0.7917	210.00	265.25	26.01
L_{14}	1,000	0.7917	210.01	265.27	26.01
L_{15}	1,000	0.7854	220.09	280.23	27.48
L_{17}	1,100	0.6633	97.15	146.47	14.36
L_{18}	1,100	0.6793	147.28	216.81	21.26
L_{19}	1,100	0.7103	151.88	213.83	20.97
L_{20}	1,100	0.7014	164.76	234.91	23.04
L_{21}	1,150	0.6706	665.40	992.25	97.31
L 22	1,150	0.6735	674.38	1001.30	98.20
L 23	1,150	0.6925	655.03	945.89	92.76

Table A43 Compressive strength of ceramic tile samples from Fang basin (L) (continued)

Sample	Temperature (°C)	Cross-section area (cm^2)	Max Load (kg_f)	Compressive Strength	
				(kg_f/cm^2)	(MPa)
L_{24}	1,150	0.6677	618.99	927.05	90.92
L_{25}	1,150	0.6648	176.18	265.01	25.99
L_{26}	1,200	0.7193	128.51	178.66	17.52
L_{27}	1,200	0.7178	223.30	311.09	30.51
L_{28}	1,200	0.6984	130.47	186.81	18.32
L_{29}	1,200	0.7223	246.89	341.81	33.52
L_{30}	1,200	0.7118	108.95	153.06	15.01

Table A45 Results of compressive strength measurement of building brick samples firing at 1,000°C.

Sample No.	Mass	Dimensions of specimen (cm)			Density	Section area	Load	Compressive strength	
	gram	Width	Length	Height	g/cm^3	cm^2	kg$_f$	kg$_f$/cm^2	MPa
1	429.24	6.32	13.68	3.85	1.29	86.46	18890	218.49	21.43
2	440.85	6.25	13.82	3.87	1.32	86.38	18360	212.56	20.85
3	444.66	6.35	13.66	3.86	1.33	86.74	18190	209.70	20.56
4	443.30	6.31	13.55	3.88	1.34	85.50	18720	218.95	21.47
5	438.31	6.31	13.55	3.84	1.34	85.50	18550	216.96	21.28
Average								**215.33**	**21.12**

BIOGRAPHY

Miss Chompunut Sawaengpol was born on the 15th of December 1988 in Amnat Charoen province. She earned her Bachelor's Degree in the School of Geotechnology, from Suranaree University of Technology (SUT) in 2011. After graduation, she continued with her master's degree in the School of Geotechnology, Institute of Engineering at SUT with the major in Petroleum Engineering. During 2011-2016, she was a teaching assistant and research assistant at SUT. Her expertise is in the areas of engineering which are drilling engineering, production operation and others.